

Resource-optimal quantum mode parameter estimation with multimode Gaussian states

Maximilian Reichert,^{1,2,*} Mikel Sanz,^{1,2,3} and Nicolas Fabre^{4,†}

¹*Department of Physical Chemistry, University of the Basque Country UPV/EHU, Apartado 644, 48080 Bilbao, Spain*

²*EHU Quantum Center, University of the Basque Country UPV/EHU, Apartado 644, 48080 Bilbao, Spain*

³*Basque Center for Applied Mathematics (BCAM), Alameda de Mazarredo 14, 48009 Bilbao, Spain*

⁴*Telecom Paris, Institut Polytechnique de Paris, 19 Place Marguerite Perey, 91120 Palaiseau, France*

(Dated: March 27, 2026)

Quantum mode parameter estimation addresses the problem of determining parameters that govern the shape of electromagnetic modes occupied by a quantum state of radiation. Canonical examples — estimating time delays and frequency shifts — underpin technologies such as radar, lidar, and optical clocks. A comprehensive framework for this class of problems was recently established, revealing that a broad family of quantum state designs can attain the Heisenberg limit and thereby surpass the precision of any classical strategy. This naturally raises the fundamental question: among all quantum-enhanced strategies, which is truly optimal? Answering this question requires identifying the physically meaningful resources that govern a given mode parameter estimation task, so that quantum states can be compared on equal footing. We show that these resources are intimately connected to the eigenmode basis of the generator of the relevant mode transformation. For time-shift estimation, whose generator is diagonal in the frequency domain, the pertinent resources are the mean frequency and bandwidth of the quantum state; analogous quantities emerge for other transformations. Crucially, our framework unifies two perspectives that have historically been treated separately: the particle-number (photon-counting) aspect and the mode-structure perspective of quantum light, providing a single coherent picture of quantum-enhanced sensing with multimode radiation. Within this unified framework, we derive a tight upper bound on the quantum Fisher information for Gaussian states, expressed in terms of these natural resources, and analytically identify the optimal Gaussian states saturating it. Strikingly, these optimal states take a particularly transparent form when expressed in the eigenbasis of the generator, which is a structural simplicity that reflects the deep connection between the geometry of the mode transformation and the architecture of the optimal probe. We further demonstrate that multimode homodyne detection constitutes the optimal measurement, achieving the quantum Fisher information bound and thus, completing the end-to-end characterization of optimal quantum metrology strategies for mode parameter estimation.

I. INTRODUCTION

Quantum light carrying information of interest – whether in coherent, squeezed, thermal, or Fock states – is characterized not only by its particle-number statistics but also by the specific electromagnetic modes involved. When used as a probe for parameter estimation, both degrees of freedom jointly determine the achievable precision. Modes are orthonormal solutions of Maxwell’s equations [1], and the parameters that characterize their shape – such as central frequency, bandwidth, temporal duration, or spatial profile – are called mode parameters. Canonical examples arise throughout science and technology: the time delay of a returned pulse in lidar or radar, the frequency shift induced by the Doppler effect, and the transverse displacement of a beam in quantum microscopy. The natural framework for comparing classical and quantum strategies in such tasks is quantum metrology [2, 3], which establishes the ultimate precision limits of any parameter estimation protocol regardless of the measurement performed. These limits are set by the quantum Cramér–Rao bound (QCRB), a fundamental lower bound on the variance of any unbiased estimator expressed in terms of the quantum Fisher information (QFI) of the probe state, and asymptotically saturable in the limit of many identical repetitions. A central theoretical goal is then

to identify the optimal quantum probe states, that is, the best combination of mode engineering and particle-number statistics that minimizes the QCRB for a given estimation task, and to determine the measurement that saturates it.

A broad consensus in the literature is to quantify resources by the mean photon number N_S , comparing only protocols that share the same value of this resource, while other state parameters such as bandwidth are often treated as classical resources. Within this framework, classical strategies are limited by the standard quantum limit (SQL), with estimator variance scaling as N_S^{-1} , whereas quantum-enhanced protocols attain the Heisenberg limit, with variance scaling as N_S^{-2} . This paradigm has been demonstrated across a wide range of mode-parameter estimation problems: squeezed states in gravitational-wave interferometry [4, 5], NOON-state phase estimation [6, 7] — experimentally demanding in both photonic and atomic platforms —, nonlinear interferometers based on stimulated emission of squeezed light [8], which offer greater robustness to losses, time-frequency cluster states for time estimation [9], and phase measurements using vibrational modes of trapped ions [10, 11] or spin-squeezed states [12, 13]. In all these cases, however, decoherence and losses ultimately prevent reaching the full Heisenberg limit at large photon number [7, 9]. Using quantum resources are not only about beating the SQL: quantum metrology framework allows to highlight other quantum advantages in the low photon-number regime such as same resolution over the measurement of a given parameter using an entangled photon pair and low-classical field with phase stabilization, a higher

* maximilian.reichert@ehu.eus

† nicolas.fabre@telecom-paris.fr

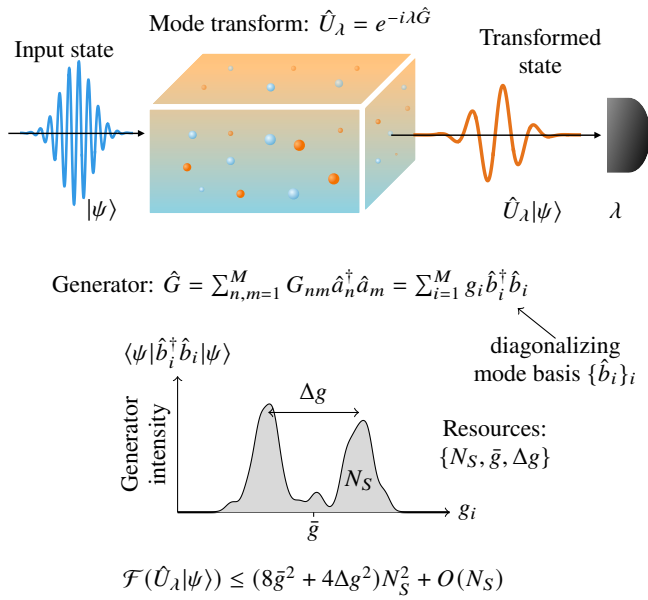


FIG. 1. (Top) General mode parameter estimation protocol. An input state $|\psi\rangle$ passes through an optical medium that induces a unitary mode transformation \hat{U}_λ , encoding the parameter of interest λ into the state. M being the number of modes. (Bottom) The relevant resources for the mode parameter estimation task are the signal photon number N_S , and the two modal resource parameters \bar{g} and Δg , corresponding to the mean and variance of the normalized generator intensity distribution, as defined in the main text.

signal-to-noise ratio with quantum states, that has impact on scanning fragile samples such as biological ones [14–18].

More recently, Ref. [19] developed a unified framework for mode-parameter estimation, providing a general recipe for designing quantum states that surpass the SQL and showing that populating at least two modes is generally required. This work led to the identification of a broad class of quantum states that beat the classical limit, including coherent states with added squeezing, multimode squeezed vacuum states, and Fock states. Quantum advantage arises not only from particle-number statistics of the probe but also from the modal structure of the field [9], as illustrated for instance by the interplay between time and energy [20]. Another important class of mode parameter estimation problems arises in lidar and radar [21–23], whose main tasks are to estimate the distance and velocity of a remote target by transmitting electromagnetic radiation and measuring the reflected echo. The distance is determined by measuring the time delay between the emitted and received signals, while the velocity is inferred from the Doppler-induced frequency shift. Various quantum protocols have been proposed for these tasks [24–29], some of which demonstrate that quantum enhancement beyond the SQL is achievable.

In this manuscript, we study arbitrary mode parameter estimation protocols for a single unknown parameter λ , as represented in Fig. 1. We first consider estimation with a finite set of bosonic modes, and show that the ultimate accuracy

limit depends on the signal photon number N_S and two modal resource parameters, \bar{g} and Δg , which quantify characteristic features of the intensity distribution associated with a mode basis naturally induced by the mode transformation, for pure Gaussian quantum states. We derive an upper bound on the QFI of multimode pure Gaussian states expressed as a simple function of these three resources, exhibiting Heisenberg-limited scaling, and identify an optimal squeezed-vacuum state — constructed as a product of two single-mode squeezers in the mode basis induced by the transformation — whose QFI saturates this bound. This yields a resource-normalized framework in which quantum states sharing the same values of \bar{g} , Δg , and N_S can be compared directly, with their QFIs serving as a benchmark for how effectively each state exploits the available resources. In particular, we show that differently spectrally engineered quantum states exhibit varying degrees of resolution enhancement through increased prefactors, while achieving Heisenberg scaling. We further show that multimode homodyne detection on these two modes constitutes an optimal measurement for achieving this bound. In the case of parameter shifts transformations, the two modal resources play physically distinct roles: achieving the precision associated with \bar{g} requires phase-sensitive interferometric measurements that rely on prior knowledge of the parameter, whereas the precision enabled by Δg can be attained with phase-insensitive measurements requiring no such prior knowledge.

We then apply our general framework to several concrete estimation scenarios, including time delays and frequency shifts [9, 17] as well as beam displacement and beam tilt [30–32]. This requires starting from a continuous, infinite set of modes [33] — the setting that arises naturally in the estimation of time delays and frequency shifts — which is subsequently discretized and truncated to make contact with the finite-mode results established in the first part. In these cases, the modal resource parameters \bar{g} and Δg reduce to familiar physical quantities: for time-shift (resp. frequency-shift) estimation, they correspond respectively to the mean frequency (mean time) and the spectral bandwidth (time duration) of the probe state. This distinction between phase-sensitive and phase-insensitive measurements has direct implications for the practical implementation of optimal protocols across the scenarios we consider. The framework applies broadly, encompassing superresolution imaging protocols as well as lidar and radar scenarios, and provides a unified basis for identifying and comparing optimal quantum strategies across these diverse applications. We also discuss realistic experimental implementations of the optimal protocols identified throughout this work.

The article is organized as follows. In Sec. II, we introduce the necessary background on mode transformations, Gaussian states, and quantum estimation theory. Sec. III presents the general expression for the QFI of a Gaussian state undergoing a mode transformation. There, we also derive a tight upper bound, identify a state that saturates it, and show that homodyne detection constitutes an optimal measurement. In Sec. IV and Sec. V, we apply our framework to several representative mode-parameter estimation problems, time and frequency parameters as well as beam-displacement and beam-tilt estimation, illustrating the practical relevance and usefulness of our

results. Finally, in Sec. VI, we will conclude and open new perspectives.

II. PRELIMINARIES

A. Mode transforms

Let us introduce the modes and mode transformations that encode a parameter λ into the field, where more details are given in Appendix A. We introduce the set $\{\hat{a}_n\}_{n=1}^M$ of bosonic annihilation operators satisfying the commutation relations $[\hat{a}_n, \hat{a}_m^\dagger] = \delta_{nm}$. For now, the number of modes M is taken to be finite; in Sections IV and V we show that our results extend to the case of infinitely many modes. We note that our results apply to any physical system described by bosonic mode operators, but here we focus on quantum light. The positive-frequency part of the electromagnetic field in a given quantization volume \mathcal{V} can be decomposed as [1, 34]

$$\hat{\mathbf{E}}^{(+)}(\mathbf{r}, t) = \sum_{n=1}^M \mathcal{E}_n \mathbf{v}_n(\mathbf{r}, t) \hat{a}_n, \quad (1)$$

where \mathcal{E}_n is the electric field per photon and $\{\mathbf{v}_n(\mathbf{r}, t)\}_{n=1}^M$ is a set of M mode functions that are solutions of Maxwell's equations, orthonormal under the scalar product $\int_{\mathcal{V}} d^3r \mathbf{v}_n^*(\mathbf{r}, t) \mathbf{v}_m(\mathbf{r}, t) / \mathcal{V} = \delta_{nm}$. The mode set can be chosen arbitrarily, though in many cases a preferred choice exists, adapted to the problem at hand. Here, \hat{a}_n (\hat{a}_n^\dagger) is the annihilation (creation) operator associated with the mode $\mathbf{v}_n(\mathbf{r}, t)$. A mode transformation

$$\hat{U}_\lambda = \exp\left(-i\lambda \sum_{n,m=1}^M G_{nm} \hat{a}_n^\dagger \hat{a}_m\right) \quad (2)$$

is a unitary transformation generated by the Hermitian operator $\hat{G} = \sum_{n,m=1}^M G_{nm} \hat{a}_n^\dagger \hat{a}_m$, where G_{nm} are the elements of the Hermitian $M \times M$ generator matrix G . One could consider more general transformations with a parameter-dependent generator $G_{nm}(\lambda)$. However, in local parameter estimation, this effectively reduces to our case given sufficiently accurate prior knowledge. For clarity, we therefore focus on this setting. The action of \hat{U}_λ on the mode operators is

$$\hat{a}_n(-\lambda) := \hat{U}_\lambda^\dagger \hat{a}_n \hat{U}_\lambda = \sum_{i=1}^M U_{ni}(\lambda) \hat{a}_i, \quad (3)$$

where $U_{ni}(\lambda) = (e^{-i\lambda G})_{ni}$ are the elements of a unitary $M \times M$ matrix, and one verifies that $[\hat{a}_n(\lambda), \hat{a}_m^\dagger(\lambda)] = \delta_{nm}$. This induces the following transformation of the electromagnetic field in the Heisenberg picture:

$$\hat{\mathbf{E}}^{(+)}(\mathbf{r}, t; \lambda) = \sum_{n=1}^M \mathcal{E}_n \mathbf{v}_n(\mathbf{r}, t) \hat{a}_n(-\lambda) = \sum_{i=1}^M \mathcal{E}_i \mathbf{v}_i(\mathbf{r}, t; \lambda) \hat{a}_i, \quad (4)$$

where $\mathbf{v}_i(\mathbf{r}, t; \lambda) = \sum_{n=1}^M U_{ni}(\lambda) \mathbf{v}_n(\mathbf{r}, t)$ is a new set of parameter-dependent orthonormal modes. The modes discussed above are cavity modes. In Sec. IV and V we will also introduce spectro-temporal and spatial-momentum transverse modes.

B. Gaussian states

The quantum states of radiation we primarily consider in this paper are pure Gaussian states. In a given mode basis $\{\hat{a}_n\}_n$, any pure Gaussian state can be written as [35]:

$$|\psi\rangle = \exp\left(\sum_{n=1}^M \beta_n \hat{a}_n^\dagger - \text{h.c.}\right) \times \exp\left(\frac{1}{2} \sum_{n,m=1}^M f_{nm} \hat{a}_n^\dagger \hat{a}_m^\dagger - \text{h.c.}\right) |0\rangle. \quad (5)$$

Here, $|0\rangle$ is the vacuum state satisfying $\hat{a}_n|0\rangle = 0$ for all n , $\beta_n \in \mathbb{C}$ is the displacement amplitude in mode \hat{a}_n , and f_{nm} are the elements of the complex $M \times M$ squeezing matrix f in the basis $\{\hat{a}_n\}_n$. Without loss of generality, f can be taken to be symmetric, since its antisymmetric part cancels identically. The displacement vector $\beta = (\beta_1, \dots, \beta_M)^T$ and the squeezing matrix f thus fully characterize the state. These quantities are straightforwardly related to the more commonly used mean vector and covariance matrix, as shown in Appendix A 3.

By applying the Takagi factorization of the squeezing matrix, which is analogous to the Bloch–Messiah decomposition of the covariance matrix; see Appendix A 2, any pure Gaussian state can be brought into a product form of independent single-mode displacement and squeezing operations:

$$|\psi\rangle = \hat{V} \left[\bigotimes_{n=1}^M \hat{D}_{\hat{a}_n}(\alpha_n) \hat{S}_{\hat{a}_n}(r_n) \right] |0\rangle. \quad (6)$$

Here, $\hat{D}_{\hat{a}_n}(\alpha_n) = \exp(\alpha_n \hat{a}_n^\dagger - \alpha_n^* \hat{a}_n)$ is the single-mode displacement operator with $\alpha_n \in \mathbb{C}$, and $\hat{S}_{\hat{a}_n}(r_n) = \exp\left(\frac{r_n}{2} (\hat{a}_n^{\dagger 2} - \hat{a}_n^2)\right)$ is the single-mode squeezing operator with $r_n \geq 0$. The operator \hat{V} is a mode transformation of the same form as \hat{U}_λ , mixing the modes linearly as $\hat{V}^\dagger \hat{a}_n \hat{V} = \sum_{i=1}^M V_{ni} \hat{a}_i$, where V_{ni} are the elements of a unitary $M \times M$ matrix.

The Eq. (6) represents the same state as Eq. (5), but expressed in the mode basis $\{\hat{c}_n\}_n$ defined by $\hat{c}_n = \hat{V} \hat{a}_n \hat{V}^\dagger$, in which the state takes the disentangled form

$$|\psi\rangle = \bigotimes_{n=1}^M \hat{D}_{\hat{c}_n}(\alpha_n) \hat{S}_{\hat{c}_n}(r_n) |0\rangle, \quad (7)$$

where we have used the identity $\hat{V} e^{\hat{A}} \hat{V}^\dagger = e^{\hat{V} \hat{A} \hat{V}^\dagger}$. In this basis, the displacement and squeezing parameters transform as $\alpha_n = \sum_{i=1}^M (V^{-1})_{ni} \beta_i$ and $\text{diag}(r_1, \dots, r_M) = V^{-1} f V^{-1}$, so that the squeezing matrix — and correspondingly the covariance matrix (see Appendix A 3) — becomes diagonal.

Now, the Gaussian state transforms under the mode transform in the Schrödinger picture as

$$|\psi_\lambda\rangle = \hat{U}_\lambda|\psi\rangle = \hat{U}_\lambda\hat{V}\hat{D}\hat{S}|0\rangle, \quad (8)$$

where we defined $\hat{D} = \otimes_{n=1}^M \hat{D}_{\hat{a}_n}(\alpha_n)$ and $\hat{S} = \otimes_{n=1}^M \hat{S}_{\hat{a}_n}(r_n)$. As the mode transform \hat{U}_λ is a passive Gaussian unitary, the parameter-imprinted state $|\psi_\lambda\rangle$ remains Gaussian after the interaction.

C. Quantum estimation theory

To determine the ultimate accuracy limit for unbiased estimation of λ encoded in the state $|\psi_\lambda\rangle$ for a particular positive-operator valued measure (POVM) $\{\hat{\Pi}_u\}_u$ with $\sum_u \hat{\Pi}_u = \mathbb{1}$, we introduce the Cramér-Rao bound (CRB) [36]

$$\text{Var}[\lambda_{\text{est}}] \geq \frac{1}{F(|\psi_\lambda\rangle, \{\hat{\Pi}_u\}_u)}, \quad (9)$$

which is a lower bound on the variance for any unbiased estimator λ_{est} , given by the inverse of the Fisher information (FI)

$$F(|\psi_\lambda\rangle, \{\hat{\Pi}_u\}_u) = \sum_u \frac{(\partial_\lambda p(u|\lambda))^2}{p(u|\lambda)}, \quad (10)$$

where $p(u|\lambda) = \langle \psi_\lambda | \hat{\Pi}_u | \psi_\lambda \rangle$ is the probability of measurement outcomes indexed as u .

By optimizing over all possible measurements, we obtain the quantum Cramér-Rao bound (QCRB)[36]

$$\text{Var}[\lambda_{\text{est}}] \geq \frac{1}{\max_{\{\Pi_u\}_u} F(|\psi_\lambda\rangle, \{\hat{\Pi}_u\}_u)} = \frac{1}{\mathcal{F}(|\psi_\lambda\rangle)}, \quad (11)$$

where the quantum Fisher information (QFI) for pure states is given by

$$\mathcal{F}(|\psi_\lambda\rangle) = 4 \left[\langle \partial_\lambda \psi_\lambda | \partial_\lambda \psi_\lambda \rangle - |\langle \partial_\lambda \psi_\lambda | \psi_\lambda \rangle|^2 \right]. \quad (12)$$

As the QFI determines the ultimate accuracy limit for unbiased estimation, we use it as a metric to compare the performance of different quantum states.

III. MODE PARAMETER ESTIMATION FOR GAUSSIAN STATES

In this section, we present a resource-normalized framework applicable to any physical system described by a finite number of bosonic modes. The corresponding quantum circuit for mode parameter estimation is shown in Fig. 2.

A. QFI for mode parameter estimation with Gaussian states

We now determine the ultimate accuracy limits for mode parameter estimation with Gaussian quantum states. First, let

us note that the derivative of the parameter imprinted state can be written as [37]:

$$|\partial_\lambda \psi_\lambda\rangle = -i\hat{U}_\lambda \sum_{n,m=1}^M G_{nm} \hat{a}_n^\dagger \hat{a}_m |\psi\rangle. \quad (13)$$

With this and the transformation rules $\hat{V}^\dagger a_m \hat{V} = \sum_j V_{mj} \hat{a}_j$, $\hat{D}^\dagger \hat{a}_j \hat{D} = \hat{a}_j + \alpha_j$, $\hat{S}^\dagger \hat{a}_j \hat{S} = c_j \hat{a}_j + s_j \hat{a}_j^\dagger$, we obtain, as shown in Appendix B 1, for the derivative state

$$\begin{aligned} |\partial_\lambda \psi_\lambda\rangle &= -i\hat{U}_\lambda \hat{V} \hat{D} \hat{S} \sum_{i,j=1}^M \tilde{G}_{ij} \left[c_i s_j \hat{a}_i^\dagger \hat{a}_j^\dagger |0\rangle \right. \\ &\quad \left. + (s_j \alpha_i^* \hat{a}_j^\dagger + c_i \alpha_j \hat{a}_i^\dagger) |0\rangle + (s_i s_j \delta_{ij} + \alpha_i^* \alpha_j) |0\rangle \right] \\ &=: |\partial_\lambda \psi\rangle_2 + |\partial_\lambda \psi\rangle_1 + |\partial_\lambda \psi\rangle_0, \end{aligned} \quad (14)$$

where we denote $\tilde{G} := V^\dagger G V$ and $c_j := \cosh(r_j)$ and $s_j := \sinh(r_j)$. Note that $\langle \partial_\lambda \psi | \partial_\lambda \psi \rangle = {}_2 \langle \partial_\lambda \psi | \partial_\lambda \psi \rangle_2 + {}_1 \langle \partial_\lambda \psi | \partial_\lambda \psi \rangle_1 + {}_0 \langle \partial_\lambda \psi | \partial_\lambda \psi \rangle_0$. Putting the pieces together, we arrive at the mode parameter QFI for Gaussian states

$$\begin{aligned} \mathcal{F}(|\psi_\lambda\rangle) &= 4 \sum_{i,j=1}^M \tilde{G}_{ij} c_j s_j \tilde{G}_{ji}^* c_i s_i + 4 \sum_{i,j=1}^M \tilde{G}_{ij} s_j s_j \tilde{G}_{ji} c_i c_i \\ &\quad + \sum_{i,i',j=1}^M 4 \left[\tilde{G}_{ij} s_j s_j \tilde{G}_{j i'} \alpha_{i'}^* \alpha_i^* + \tilde{G}_{i' j} c_j c_j \tilde{G}_{ji} \alpha_i \alpha_{i'} \right. \\ &\quad \left. + \tilde{G}_{i' j} c_j s_j \tilde{G}_{ji}^* \alpha_i^* \alpha_{i'}^* + \tilde{G}_{i' j}^* s_j c_j \tilde{G}_{ji} \alpha_i \alpha_{i'} \right]. \end{aligned} \quad (17)$$

We refer to Appendix B 1 for the detailed calculation. This formula is rather cumbersome and we can put it into a more convenient form

$$\begin{aligned} \mathcal{F}(|\psi_\lambda\rangle) &= 4 \left(\text{Tr}[\tilde{G} C S \tilde{G}^* C S] + \text{Tr}[\tilde{G} S^2 \tilde{G} C^2] \right. \\ &\quad \left. + \text{Tr}[\tilde{G} (S^2 + C^2) \tilde{G} \mathcal{A}] + 2 \text{Re} [\text{Tr}[\tilde{G}^* S C \tilde{G} \mathcal{B}]] \right), \end{aligned} \quad (18)$$

where $C = \text{diag}(c_1, \dots, c_M)$, $S = \text{diag}(s_1, \dots, s_M)$, and \mathcal{A} and \mathcal{B} are matrices with components $\mathcal{A}_{ij} = \alpha_i \alpha_j^*$ and $\mathcal{B}_{ij} = \alpha_i \alpha_j$.

B. Resources and optimality for coherent states

As the general expression for the QFI for Gaussian states is quite complicated, let us first build some intuition by considering the subclass of coherent states, which are often considered to be classical states of radiation.

The coherent states are of the form $|\psi^{\text{coh}}\rangle = \hat{V} \hat{D} |0\rangle$, which implies no squeezing, *i.e.*, $r_i = 0$. The QFI in this case takes the simple form

$$\mathcal{F}(|\psi^{\text{coh}}\rangle) = 4 \sum_{i,i',j=1}^M \alpha_i^* \tilde{G}_{i' j} \tilde{G}_{ji} \alpha_i = 4 \alpha^\dagger \tilde{G}^2 \alpha. \quad (20)$$

This is already a much simpler expression than the general case. To gain even deeper insight, let us rewrite the above expression. For that, note that $\tilde{G} = V^\dagger G V$ is Hermitian, so that it can be diagonalized by a unitary W , i.e., $W\tilde{G}W^\dagger = D = \text{diag}(g_1, \dots, g_M)$, where $\{g_n\}_n$ are the real eigenvalues of the generator matrix. We assume throughout the paper that $g_1 \leq g_2 \leq \dots \leq g_M$. We find in Appendix B 2

$$\mathcal{F}(|\psi^{\text{coh}}\rangle) = 4\alpha^\dagger W^\dagger D^2 W \alpha = \sum_{n=1}^M g_n^2 \langle \psi^{\text{coh}} | \hat{b}_n^\dagger \hat{b}_n | \psi^{\text{coh}} \rangle. \quad (21)$$

The bosonic operators $\hat{b}_n = \sum_i (B^\dagger)_{ni} \hat{a}_i$ with unitary $M \times M$ matrix $B^\dagger = W V^\dagger$ and $[\hat{b}_n, \hat{b}_m^\dagger] = \delta_{nm}$ here correspond to the special mode basis in which the generator appears diagonal, that is,

$$\hat{G} = \sum_{i,j=1}^M G_{ij} \hat{a}_i^\dagger \hat{a}_j = \sum_{n=1}^M g_n \hat{b}_n^\dagger \hat{b}_n. \quad (22)$$

Let us seek the optimal coherent state that maximizes the QFI. We see that by, for example, letting the photon number of some mode j with $g_j \neq 0$ grow without bound, i.e., $\langle \psi^{\text{coh}} | \hat{b}_j^\dagger \hat{b}_j | \psi^{\text{coh}} \rangle \rightarrow \infty$, we have $\mathcal{F}(|\psi^{\text{coh}}\rangle) \rightarrow \infty$. Hence, an unbounded increase in photon number leads to an arbitrarily large QFI. In this naive sense, the ‘‘optimal’’ coherent state would correspond to one with an infinite photon number. However, in practice, one has only access to a finite amount of photons, and thus it makes sense to consider the number of photons a (constraint) resource. With this in mind, one can seek the optimal coherent state that maximizes the QFI for a constrained amount of photons.

In many physical settings, the number of modes is infinite, $M = \infty$, and the generator matrix G may likewise be unbounded. For mathematical clarity, we treat M as finite but arbitrarily large, interpreting it as a truncation cutoff, and allow the generator eigenvalues $\{g_1, \dots, g_M\}$ to grow without bound as M increases. This situation arises in the examples considered in Secs. IV and V. In this regime, Eq. (21) shows that the QFI can grow without bound even at fixed photon number, which underscores the necessity of introducing additional resource parameters associated with the modal distribution of the state.

We introduce two additional resources \bar{g} and Δg related to how the photon intensity is distributed among the modes $\{\hat{b}_n\}_n$ that diagonalize the generator $\hat{G} = \sum_n g_n \hat{b}_n^\dagger \hat{b}_n$. We define the normalized generator intensity distribution as

$$I_n = \frac{\langle \psi^{\text{coh}} | \hat{b}_n^\dagger \hat{b}_n | \psi^{\text{coh}} \rangle}{N_S}, \quad (23)$$

where

$$N_S = \sum_{n \in \mathcal{I}_S} \langle \psi^{\text{coh}} | \hat{b}_n^\dagger \hat{b}_n | \psi^{\text{coh}} \rangle \quad (24)$$

is the signal photon number. The sum runs over all indices in $\mathcal{I}_S := \{i = 1, \dots, M \mid g_i \neq 0\}$. The modes that belong to \mathcal{I}_S

are referred to the signal modes. The complement $\mathcal{I}_I := \{i = 1, \dots, M \mid g_i = 0\}$ of \mathcal{I}_S is the set of idler modes, as these modes are unaffected by the action of the mode transform \hat{U}_λ . We further define

$$\bar{g} = \sum_{n=1}^M g_n I_n \quad (25)$$

as the mean value of the normalized generator intensity and

$$\Delta g^2 = \sum_{n=1}^M (g_n - \bar{g})^2 I_n \quad (26)$$

as the variance. With this, we see that the QFI takes the form

$$\mathcal{F}(|\psi^{\text{coh}}\rangle) = 4 \left(\bar{g}^2 + \Delta g^2 \right) N_S. \quad (27)$$

In this form, it is clear that $\{N_S, \bar{g}, \Delta g\}$ play the role of resource parameters: increasing any one of them raises the QFI and thus improves metrological performance. Notably, any two coherent states sharing the same values of these parameters yield identical QFI, regardless of the detailed structure of the underlying modal intensity distribution. The metrological performance is therefore determined entirely by the first two moments \bar{g} and Δg of that distribution, together with the signal photon number N_S . As we show below, the full modal photon distribution becomes relevant once squeezing is introduced.

C. Resources for Gaussian states

Let us now generalize the insights from the previous section for coherent states to general pure Gaussian states. The parameters $\{\bar{g}, \Delta g, N_S\}$ defined in Eqs.(24)-(26) can be straightforwardly generalized by using

$$I_n = \frac{\langle \psi | \hat{b}_n^\dagger \hat{b}_n | \psi \rangle}{N_S}, \quad (28)$$

now taking the expectation value of the photon number operator with respect to a general Gaussian state $|\psi\rangle$. Note that $\bar{g} = \langle \psi | \hat{G} | \psi \rangle$, but importantly $\Delta g^2 \neq \langle \psi | \hat{G}^2 | \psi \rangle - \langle \psi | \hat{G} | \psi \rangle^2$. The variance Δg^2 is not a variance with respect to a quantum state, but a variance of the normalized generator intensity distribution I_n . We can also write the resource parameters in a basis-independent way

$$N_S = \text{Tr}[\tilde{P}_S (S^2 + \mathcal{A})] \quad (29)$$

$$\bar{g} = \frac{\text{Tr}[\tilde{G} (S^2 + \mathcal{A})]}{N_S} \quad (30)$$

$$\Delta g^2 = \frac{\text{Tr}[\tilde{G}^2 (S^2 + \mathcal{A})]}{N_S} - \bar{g}^2 \quad (31)$$

as we show in Appendix C. Here, $\tilde{P}_S = V^\dagger P_S V$, where P_S is the projector onto the support of G , that is, onto the subspace spanned by eigenvectors of G associated with all non-zero eigenvalues. One of the central findings of this work is:

Theorem III.1. *The QFI $\mathcal{F}(|\psi_\lambda\rangle)$ of a general pure Gaussian quantum state $|\psi_\lambda\rangle = \hat{U}_\lambda|\psi\rangle$ subject to a mode transform given in Eq. (2) is upper bounded by*

$$\mathcal{F}(|\psi_\lambda\rangle) \leq \mathcal{F}^{\text{UB}} = \left(8\bar{g}^2 + 4\Delta g^2\right) N_S^2 + O(N_S), \quad (32)$$

where $\{N_S, \bar{g}, \Delta g\}$ are the resource parameters as defined in Eqs. (29)–(31) of the input state $|\psi\rangle$.

The proof is provided in Appendix D. Establishing the above bound and demonstrating that it can be saturated confirms that the quantities $\{N_S, \bar{g}, \Delta g\}$ defined in Eqs. (29)–(31) are genuine resources for mode parameter estimation: larger values of any one of them raise the ultimate precision limit and thus directly enhance the ultimate metrological performance.

Let us give some context to interpret this result. In the following, we focus on the regime $N_S \gg 1$ and primarily consider the N_S^2 contributions, which exhibit HL scaling. In many cases of interest, the QFI of a Gaussian state takes the form

$$\mathcal{F}(|\psi_\lambda\rangle) = (c_{\bar{g}}\bar{g}^2 + c_{\Delta g}\Delta g^2)N_S^2 + O(N_S), \quad (33)$$

where $c_{\bar{g}} \geq 0$ and $c_{\Delta g} \geq 0$ are dimensionless constants. Provided $c_{\bar{g}}, c_{\Delta g} > 0$, it is clear that for large enough N_S , such states will always outperform any coherent state whose QFI only scales as $\sim N_S$. For this reason, one often focuses only on the scaling with N_S , rather than on the prefactors. The latter become important when comparing two Gaussian states whose QFIs both scale as N_S^2 . Traditionally, Gaussian states with the same photon number N_S have been compared by examining their total QFI values. However, such comparisons can be misleading because the QFI also depends on the modal resource parameters \bar{g} and Δg : a state with larger \bar{g} may appear superior even if it exploits its resources less efficiently. Our approach overcomes this limitation by introducing a resource-normalized framework in which Gaussian states can be compared on equal footing. Fixing the three resources $\{N_S, \bar{g}, \Delta g\}$, the coefficients $c_{\bar{g}}$ and $c_{\Delta g}$ encapsulate how the modal distribution of squeezing and displacement in a given Gaussian state affects its metrological performance, providing a direct and physically meaningful figure of merit for comparing competing strategies. Within this framework, the optimal states — those saturating the upper bound in the large-photon-number regime $N_S \gg 1$ — are characterized by $c_{\bar{g}} = 8$ and $c_{\Delta g} = 4$.

D. Optimal states

We now turn to the discussion of states that achieve different forms of optimality as defined by Eq. (32). As we demonstrate in Secs. IV and V, the two modal resources \bar{g} and Δg play physically distinct roles in the concrete estimation scenarios we consider. The quantity \bar{g} is associated with interferometric sensitivity: achieving the corresponding QFI scaling $\sim \bar{g}^2 N_S^2$ requires a phase-sensitive measurement, which typically performs best when substantial prior knowledge of the parameter is available. In contrast, the contribution $\sim \Delta g^2 N_S^2$ is accessible through phase-insensitive measurements, making

Δg the operationally relevant resource when such prior knowledge is unavailable. The relative importance of \bar{g} and Δg therefore depends on both the measurement strategy employed and the degree of prior information about the parameter.

We classify quantum states according to the type of optimality they achieve in the asymptotic scaling of the quantum Fisher information (QFI).

Definition III.2 (Optimality classes of states). Let $c_{\bar{g}}$ and $c_{\Delta g}$ be the coefficients appearing in the asymptotic expansion of the QFI in Eq. (33).

- A state is said to be optimal if $c_{\bar{g}} = 8$ and $c_{\Delta g} = 4$.
- A state is said to be mean optimal if $c_{\bar{g}} = 8$ and $c_{\Delta g} < 4$.
- A state is said to be variance optimal if $c_{\bar{g}} < 8$ and $c_{\Delta g} = 4$.

Optimal states simultaneously achieve the maximal asymptotic scaling associated with both the \bar{g} and the Δg contributions. Mean-optimal (variance-optimal) states saturate only the former (latter) contribution.

1. Optimal state

Let us now present an optimal state. It is a two-mode state and takes on a simple form in the $\{\hat{b}_n\}_n$ mode basis, which is the mode basis that diagonalizes the generator, i.e., $\hat{G} = \sum_n g_n \hat{b}_n^\dagger \hat{b}_n$. It takes the form

$$|\psi\rangle = \hat{S}_{e^{-i\phi_i/2}\hat{b}_i}(r_i) \hat{S}_{e^{-i\phi_j/2}\hat{b}_j}(r_j) |0\rangle, \quad (34)$$

where $i \neq j$ are some fixed mode indices, r_i, r_j are the squeezing strengths and ϕ_n and ϕ_m are freely adjustable squeezing angles. The different mode basis are represented in Fig. 2.

For desired mean and variance resource parameters \bar{g} and Δg , respectively, we choose the squeezing parameters r_i, r_j , such that

$$s_i^2 = \frac{N_S}{2} \left(1 - \frac{\bar{g}}{\sqrt{\bar{g}^2 + \Delta g^2}} \right) \quad (35)$$

$$s_j^2 = \frac{N_S}{2} \left(1 + \frac{\bar{g}}{\sqrt{\bar{g}^2 + \Delta g^2}} \right) \quad (36)$$

holds. We find that this state achieves an optimal QFI of

$$\mathcal{F}(|\psi_\lambda\rangle) = (8\bar{g}^2 + 4\Delta g^2)N_S^2 + \underbrace{8(\bar{g}^2 + \Delta g^2)N_S}_{=O(N_S)} \quad (37)$$

for arbitrary squeezing angles ϕ_i, ϕ_j , if we can find suitable modes with indices i, j , such that the corresponding generator eigenvalues g_i, g_j (with $g_i < g_j$ without loss of generality)

satisfy

$$g_i = \bar{g} - \Delta g \sqrt{\frac{s_j^2}{s_i^2}} \quad (38)$$

$$g_j = \bar{g} + \Delta g \sqrt{\frac{s_i^2}{s_j^2}}, \quad (39)$$

and note that $\Delta g > 0$.

For given resource parameters $\{\bar{g}, \Delta g, N_S\}$ and a given generator \hat{G} whose generator matrix has spectrum $\{g_1, \dots, g_M\}$, it may not always be possible to find indices i, j such that the corresponding eigenvalues g_i, g_j satisfy Eqs. (38) and (39). In such cases, a strictly optimal state may not exist. However, in many physically relevant situations — including those discussed in Secs. IV and V — the number of modes is large, $M \gg 1$, and the generator eigenvalues are densely, and possibly uniformly, distributed or even form a continuum. In such cases, indices i, j can always be found for which g_i and g_j satisfy Eqs. (38) and (39) to an excellent approximation, and the resulting state is therefore essentially optimal.

We also note that a state similar to Eq. (34) that makes use of two additional idler modes is also optimal as we discuss in Appendix E 4. Additional optimal states may exist beyond those discussed here; however, we are not aware of any others.

2. Variance-optimal state

Let us now present the two variance-optimal states we found. The first variance-optimal state has the same form as the fully optimal state in Eq. (34), but employs the squeezing equally in both modes, *i.e.*, $r_i = r_j$. We calculate the QFI in Appendix E 2 a and find

$$\mathcal{F}(|\psi_\lambda\rangle) = 4(\bar{g}^2 + \Delta g^2)N_S^2 + \underbrace{8(\bar{g}^2 + \Delta g^2)N_S}_{=O(N_S)}. \quad (40)$$

We see that the prefactor of the variance term $\Delta g^2 N_S^2$ takes on its maximum value 4, and thus the state is variance optimal. The prefactor of the mean term $\bar{g}^2 N_S^2$ is 4, only one half of its maximum value. Note that the state is optimal for arbitrary squeezing angles ϕ_i, ϕ_j . Also note that even in the limit $N_S \ll 1$, the state outperforms the coherent state by a factor of 2.

We also identify another two-mode state, similar to the one discussed in Ref. [38], in which half of the available energy is used to displace one mode while the other half is used to squeeze the second mode. Interestingly, these modes are not related to the mode basis $\{\hat{b}_i\}_i$. Under certain conditions, this state can be variance optimal. The detailed QFI calculation and the corresponding conditions are presented in Appendix E 2 b. In Sec. IV C 4 we demonstrate for the example of time shift estimation that the conditions can be satisfied and that such a state can be variance-optimal.

3. Mean-optimal state

Let us now present a mean-optimal state according to our definition above. We consider a single-mode squeezed state

$$|\psi\rangle = \hat{V}\hat{S}_{\hat{a}_j}(r_j)|0\rangle = \hat{S}_{\hat{V}\hat{a}_j\hat{V}^\dagger}(r_j)|0\rangle, \quad (41)$$

that is squeezed in a completely arbitrary mode $\hat{V}\hat{a}_j\hat{V}^\dagger$ with $j \in \{1, \dots, M\}$, where $\{\hat{a}_n\}_n$ are the operators corresponding to some initial mode basis. It is straightforward to show that

$$\mathcal{F}(|\psi_\lambda\rangle) = (8\bar{g}^2 + 0 \cdot \Delta g^2)N_S^2 + \underbrace{4(\bar{g}^2 + \Delta g^2)N_S}_{=O(N_S)}. \quad (42)$$

The state is therefore mean optimal according to the definition given above. Interestingly, the detailed shape of the squeezed mode $\hat{V}\hat{a}_j\hat{V}^\dagger$ (with arbitrary \hat{V}) becomes unimportant—similar to the coherent state case discussed in Sec. III B—whereas for the optimal and variance-optimal states, the squeezed modes must correspond to the specific modes \hat{b}_i, \hat{b}_j . Note that the prefactor of the variance term is $c_{\Delta g} = 0$; consequently, single-mode squeezing cannot be fully optimal when $\Delta g > 0$. Note that the fully optimal state presented in Sec. III D 1 reduces to a single-mode squeezed state in the regime $\bar{g}^2 \gg \Delta g^2$.

E. Optimal measurements

Let us now discuss two classes of optimal measurement strategies, that is represented at the right of the quantum circuit in Fig. 2.

Definition III.3 (Optimal measurements). Let $c_{\bar{g}}$ and $c_{\Delta g}$ be the coefficients appearing in the asymptotic expansion of the QFI in Eq. (33).

- A measurement $\{\hat{\Pi}_a\}_a$ is said to be optimal for a particular state $\hat{U}_\lambda|\psi\rangle$, if $F(\hat{U}_\lambda|\psi\rangle, \{\hat{\Pi}_a\}_a) = \mathcal{F}(\hat{U}_\lambda|\psi\rangle)$.
- A measurement $\{\hat{\Pi}_a\}_a$ is said to be variance optimal for a particular state $\hat{U}_\lambda|\psi\rangle$ whose QFI can be expressed as in Eq. (33), if $F(\hat{U}_\lambda|\psi\rangle, \{\hat{\Pi}_a\}_a) = c_{\Delta g}\Delta g^2 N_S^2 + c'_{\bar{g}}\bar{g}^2 N_S^2 + O(N_S)$, where $c'_{\bar{g}} \geq 0$ with $c'_{\bar{g}} \leq c_{\bar{g}}$.

1. Phase-sensitive optimal measurements

We refer to multimode homodyne detection as a phase-sensitive measurement, since the detection scheme depends on adjustable phase parameters that can significantly affect its performance.

For the optimal and variance-optimal two-mode squeezed states presented in Secs. III D 1 and III D 2, we consider homodyne detection on both populated modes i and j , corresponding to measuring the quadrature operators $\hat{b}_i e^{-i\varphi_i} + \hat{b}_i^\dagger e^{+i\varphi_i}$ and $\hat{b}_j e^{-i\varphi_j} + \hat{b}_j^\dagger e^{+i\varphi_j}$. Optimizing the measurement phases φ_i, φ_j

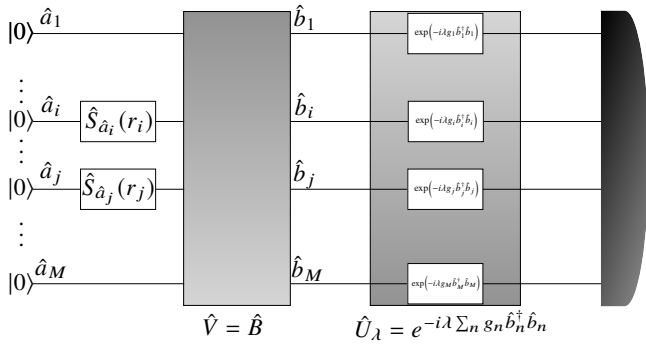


FIG. 2. Quantum circuit representing the optimal mode parameter estimation protocol. Two single-mode squeezed states are prepared in modes \hat{a}_i, \hat{a}_j with squeezing angles $\phi_i = \phi_j = 0$ (for illustrative clarity) after which the passive Gaussian unitary $\hat{V} = \hat{B}$ transfers this squeezing to modes \hat{b}_i, \hat{b}_j . In that mode basis, the mode parameter transform \hat{U}_λ acts as a simple phase shift on each individual mode. After crossing the sample, the state is measured, with either phase-sensitive or insensitive detection.

— to be distinguished from the squeezing angles ϕ_i, ϕ_j — for the optimal state of Sec. III D 1 yields the maximal Fisher information

$$\max_{\varphi_i, \varphi_j} F_{\text{hom}}(|\psi_\lambda\rangle) = (8\bar{g}^2 + 4\Delta g^2)N_S^2 + O(N_S), \quad (43)$$

as derived in Appendix F 1. For the variance-optimal state, the optimization gives $\max_{\varphi_i, \varphi_j} F_{\text{hom}}(|\psi_\lambda\rangle) = 4(\bar{g}^2 + \Delta g^2)N_S^2 + O(N_S)$. In both cases, two-mode homodyne detection is therefore an optimal measurement.

The optimal phase settings $\varphi_i^{\text{opt}}(\lambda)$ and $\varphi_j^{\text{opt}}(\lambda)$ depend on the parameter λ to be estimated, so that achieving near-optimal performance in practice requires sufficiently accurate prior knowledge of λ , in the form of a prior estimate λ_{prior} . When such prior information is unavailable, a phase-insensitive measurement strategy, as discussed in Sec. III E 2, is preferable.

In Appendix F 2, we consider the effect of photon loss and detector inefficiency, modeled by beam splitters of transmissivity η_i, η_j placed immediately before the detectors. To obtain a compact result, we assume $\eta := \eta_i = \eta_j$ and work in the limit $s_i^2, s_j^2 \gg 1$, yielding

$$\max_{\varphi_i, \varphi_j} F_{\text{hom}}(|\psi_\lambda\rangle) \approx \frac{2\eta}{1-\eta} [\bar{g}^2 + \Delta g^2] N_S. \quad (44)$$

This exceeds the QFI of a coherent state, $4\eta [\bar{\omega}^2 + \Delta\omega^2] N_S$, for transmissivities $\eta > 1/2$. We further show in Appendix F 3 that, for the mean-optimal state presented in Sec. III D 3, single-mode homodyne detection is an optimal measurement; this analysis is restricted to the lossless case $\eta = 1$.

2. Phase-insensitive variance-optimal measurements

We now turn to mode- and photon-number-resolved photon counting, a measurement that is phase-insensitive in the sense

that it requires no phase control, in contrast to homodyne detection. For the time and frequency estimation examples of Sec. IV, as well as the beam displacement and tilt estimation of Sec. V, the generators share the property that their eigenvalues $\{g_n\}_n$ are equally spaced. For these cases, we show that photon-number-resolved photon counting in a suitably chosen mode basis — the Fourier-dual of the generator eigenbasis $\{\hat{b}_i\}_i$ — constitutes a variance-optimal measurement in the sense of Definition III.3, provided the input state satisfies the conditions of Lemma K.1.

Such phase-insensitive measurements are of significant practical value in low-information scenarios, such as lidar-based range (time) and velocity (frequency) estimation. In realistic lidar settings, the precision associated with the mean contribution \bar{g}^2 is generally unattainable due to phase ambiguity [22], leaving only the variance contribution Δg^2 accessible. Identifying robust, phase-insensitive measurement strategies that are variance-optimal is therefore essential for such protocols.

F. Previous works on optimal metrology and optimal mode parameter estimation

Let us first review optimal quantum metrology for systems in a finite-dimensional Hilbert space. Firstly in Ref. [39], it was shown that for estimating a parameter λ encoded by a unitary $\hat{U}_\lambda = e^{-i\lambda\hat{G}}$ with a finite-dimensional generator $\hat{G} = \sum_{n \in \{n_{\min}, \dots, n_{\max}\}} g_n |n\rangle\langle n|$, the optimal state takes the form $(|n_{\min}\rangle + |n_{\max}\rangle)/\sqrt{2}$, where n_{\min} and n_{\max} are the indices corresponding to the minimal and maximal eigenvalues g_{\min} and g_{\max} of the generator. This result does not directly apply to our mode parameter estimation task, since each mode is associated with an infinite-dimensional Fock space. If one truncates the Fock space of each mode at a finite photon number N_{cut} , the optimal state according to Ref. [39] takes the form $\sim [(\hat{a}_{n_{\min}}^\dagger)^{N_{\text{cut}}} + (\hat{a}_{n_{\max}}^\dagger)^{N_{\text{cut}}}]|0\rangle$. This state achieves a QFI of $4\Delta g^2 N_S^2$, as shown in Appendix G. It is therefore variance-optimal, but lacks the mean contribution $\bar{g}^2 N_S^2$, rendering it suboptimal within our framework. Our approach thus offers a genuine advantage: by avoiding any truncation of the infinite Fock space, it yields the true ultimate precision limit for Gaussian states.

Secondly, we discuss Ref. [40] on optimal Gaussian metrology for generic multimode interferometric circuits. This work is relevant because an interferometric circuit can be interpreted as a mode transformation. The authors maximize the QFI for a fixed interferometric circuit under a constraint on the average photon number. Their analysis yields an optimal QFI of $8g_{\max}^2 N_S^2 + O(N_S)$, where g_{\max} is the largest eigenvalue of the generator matrix. This performance is achieved with a single-mode squeezed state and is consistent with our results. Unlike the previously discussed Ref. [39], this approach accommodates the infinite-dimensional Fock spaces associated with each bosonic mode. However, in many mode-parameter-estimation tasks, such as time and frequency estimation (Sec. IV) or beam-displacement and beam-tilt esti-

mation (Sec. V), one must consider infinitely many modes. The method of Ref. [40] requires truncating the mode space, which leads to optimal states that depend on the chosen cutoff, as can be seen in Ref. [41]. Such cutoff dependence is undesirable. By contrast, our approach yields optimal states that are independent of any mode-space truncation. Combined with our resource-based interpretation, our framework constitutes a clear advantage.

Third, we review the literature that explicitly addresses mode-parameter-estimation tasks. Ref. [19, 42] presents a general framework for designing quantum-enhanced protocols in this setting. The authors demonstrate that achieving Heisenberg scaling requires populating an initial mode together with an additional mode that has nonzero overlap with the derivative of the initial mode. While there exist many quantum-enhanced probe states that provide a quantum advantage over classical strategies through superior photon-number scaling, Ref. [19] leaves open the question of how to meaningfully compare different quantum-enhanced states with one another and what is the optimal state. In this work, we resolve this question for the subclass of pure Gaussian states by introducing the resource parameters \bar{g} and Δg .

Finally, Ref. [38] investigates optimal Gaussian probe states for mode-parameter estimation in the regime where most signal photons are allocated to the displacement of a single mode $\hat{a}(\lambda)$. A small amount of squeezing, satisfying $\sinh^2(r) \ll |\alpha|^2$, is distributed between this mode and its derivative mode $\partial_\lambda \hat{a}(\lambda)$. When the squeezing is equally distributed, the resulting state achieves a QFI of $\mathcal{F} = 4e^{2r}(\bar{g}^2 + \Delta g^2)N_S$. The QFI thus scales linearly with N_S (*i.e.*, SQL scaling), but with a constant prefactor enhancement $e^{2r} \ll N_S$ over a purely coherent-state strategy. This state is therefore suboptimal within our framework. However, as discussed in Sec. III D 2 and demonstrated in Sec. IV C 4, when half of the signal photons are allocated to squeezing the derivative mode, the state of Ref. [38] can be variance-optimal, provided certain conditions are satisfied, as we show in Appendix E 2 b. To achieve full optimality, however, the only state we are aware of is the one in Eq. (34), which allocates the entire signal photon budget to squeezing. We note that Ref. [38] neither introduced \bar{g} and Δg as resource parameters nor considered general Gaussian states, focusing instead on a specific subclass. Our framework applies to arbitrary Gaussian states and, consistent with their findings, confirms that two modes are generally required to achieve optimal performance.

IV. FIRST APPLICATION OF OPTIMAL MODE ESTIMATION: TIME-FREQUENCY SHIFT ESTIMATION

In the previous section, we focused on a general estimation protocol involving a finite, discrete set of bosonic modes. We now turn to intrinsically continuous modes—such as time–frequency and transverse position–momentum—which are first decomposed into an infinite set of discrete modes and then truncated so that the results of the previous section can be applied.

A. The model and the generators

We now consider the estimation of time and frequency shifts of quantum light. These two paradigmatic examples will be analyzed in detail in order to clearly demonstrate the capabilities and versatility of our framework. Note that we work exclusively within the framework of single-parameter estimation.

The estimation of time and frequency shifts is of central importance across a wide range of applications. For instance, in radar and lidar systems, a time delay encodes information about the distance to a target, while a Doppler-induced frequency shift provides access to the target's velocity.

In Sec. II A, we introduced so-called cavity modes whose extent is the entire quantization volume. Here, we consider spatio-temporal modes that are defined in the xy plane at $z = 0$ for some time interval (in our case we assume this interval to be infinite). Under the paraxial and quasi-monochromatic approximation [43] a single spatial mode of the positive-part of the EM field in the xy plane at $z = 0$ may be written as

$$\hat{E}(t) = \frac{1}{\sqrt{2\pi}} \int_{-\infty}^{\infty} d\omega e^{-i\omega t} \hat{A}(\omega), \quad (45)$$

where $[\hat{E}(t), \hat{E}(t')] = \delta(t - t')$ and $[\hat{A}(\omega), \hat{A}^\dagger(\omega')] = \delta(\omega - \omega')$ are the commutation relations of continuous mode operators $\hat{E}(t)$ and $\hat{A}(\omega)$. $\hat{E}^\dagger(t)$ may be interpreted as the creation operator for a photon localized at time t in the $z = 0$ plane, whereas $\hat{A}^\dagger(\omega)$ creates a photon of frequency ω that is not localized in time. Although negative frequency is not physical, we have extended the integration range to minus infinity. In practice, every considered quantum state will have a compact spectrum far away the zero frequency, typically in the GHz or THz range.

Now, the mode transforms $\hat{U}_\tau = e^{-i\tau\hat{G}_\tau}$ and $\hat{U}_\nu = e^{-i\nu\hat{G}_\nu}$ with generators

$$\hat{G}_\tau = \int_{-\infty}^{\infty} d\omega \omega \hat{A}^\dagger(\omega) \hat{A}(\omega) \quad (46)$$

$$\hat{G}_\nu = \int_{-\infty}^{\infty} dt t \hat{E}^\dagger(t) \hat{E}(t) \quad (47)$$

induce a time shift τ and a frequency shift ν in the input state $|\psi\rangle$. Note that both of the generators are written in their continuous diagonal basis. Such generators have been called time and frequency operators [44]. Such generators are often referred to as time and frequency operators [44]. Both possess a continuous spectrum, with $\omega, t \in \mathbb{R}$, as reflected by the presence of integrals rather than discrete sums. Consequently, this system corresponds to one with infinitely many modes. However, our formalism for optimal mode parameter estimation was developed for a finite number M of discrete modes. To bridge this gap, we discretize the continuous degrees of freedom and approximate the system as finite-dimensional by introducing mode truncations.

As we show in Appendix H 1, this procedure leads to the

discretized generators of finitely many modes

$$\hat{G}_\tau \approx \sum_{n=1}^M \omega_n \hat{a}_n^\dagger \hat{a}_n \quad (48)$$

$$\hat{G}_\nu \approx \sum_{n=1}^M t_n \hat{e}_n^\dagger \hat{e}_n, \quad (49)$$

where \hat{e}_n and \hat{a}_n are discretized versions of $\hat{E}(t)$ and $\hat{A}(\omega)$ with $[\hat{a}_n, \hat{a}_m^\dagger] = [\hat{e}_n, \hat{e}_m^\dagger] = \delta_{nm}$. Here, $\omega_n = \omega_{\min} + (n-1)\delta\omega$ and $t_n = t_{\min} + (n-1)\delta t$ are the eigenvalues of the discretized generator, where $\delta\omega$ and δt are the bin widths in the discretized frequency and time domain. This discretization constitutes a good approximation as long as the states we consider can be well approximated using this discrete mode basis. This can always be achieved (at least theoretically) by simply choosing the binning small enough and choosing the intervals $[\omega_{\min}, \omega_{\max}]$ and $[t_{\min}, t_{\max}]$ large enough, where $\omega_{\max} = \omega_M$ and $t_{\max} = t_M$.

Knowing that we can comfortably switch from a continuous to a discrete description, we will present the following results in the continuous description.

B. Resources for time and frequency estimation

Now, according to the formalism in Sec. III C, for a general input state, the resource signal photon number is given by

$$N_S = \int_{-\infty}^{\infty} dt \langle \psi | \hat{E}^\dagger(t) \hat{E}(t) | \psi \rangle = \int_{-\infty}^{\infty} d\omega \langle \psi | \hat{A}^\dagger(\omega) \hat{A}(\omega) | \psi \rangle \quad (50)$$

and the resources for time estimation are mean frequency $\bar{\omega}$ and bandwidth $\Delta\omega^2$ of the input state:

$$\bar{\omega} = \int_{-\infty}^{\infty} d\omega \omega \frac{\langle \psi | \hat{A}^\dagger(\omega) \hat{A}(\omega) | \psi \rangle}{N_S}, \quad (51)$$

$$\Delta\omega^2 = \int_{-\infty}^{\infty} d\omega (\omega - \bar{\omega})^2 \frac{\langle \psi | \hat{A}^\dagger(\omega) \hat{A}(\omega) | \psi \rangle}{N_S}. \quad (52)$$

They are the mean and variance of the normalized spectral intensity $\langle \psi | \hat{A}^\dagger(\omega) \hat{A}(\omega) | \psi \rangle / N_S$. The resources for frequency estimation are central time \bar{t} and time duration Δt , defined by

$$\bar{t} = \int_{-\infty}^{\infty} dt t \frac{\langle \psi | \hat{E}^\dagger(t) \hat{E}(t) | \psi \rangle}{N_S} \quad (53)$$

$$\Delta t^2 = \int_{-\infty}^{\infty} dt (t - \bar{t})^2 \frac{\langle \psi | \hat{E}^\dagger(t) \hat{E}(t) | \psi \rangle}{N_S}. \quad (54)$$

They are the mean and variance of the normalized temporal intensity $\langle \psi | \hat{E}^\dagger(t) \hat{E}(t) | \psi \rangle / N_S$.

C. Multimode Gaussian states for time and frequency estimation

1. Coherent states for time and frequency estimation

Let us first consider the bosonic coherent state [33, 45, 46], which is the quantum state describing by a phase-stabilized laser that can be written both in the time and frequency domains

$$|\psi^{\text{coh}}\rangle = \exp\left(+\alpha \int_{-\infty}^{\infty} dt \Psi(t) \hat{E}^\dagger(t) - h.c.\right) |0\rangle \quad (55)$$

$$= \exp\left(+\alpha \int_{-\infty}^{\infty} d\omega \tilde{\Psi}(\omega) \hat{A}^\dagger(\omega) - h.c.\right) |0\rangle \quad (56)$$

with eigenvalue relation $\hat{E}(t)|\psi^{\text{coh}}\rangle = \Psi(t)|\psi^{\text{coh}}\rangle$ and $\hat{A}(\omega)|\psi^{\text{coh}}\rangle = \tilde{\Psi}(\omega)|\psi^{\text{coh}}\rangle$. Recall that multi-mode displaced states can always be written as single-mode displaced states in an appropriate mode basis [1], and here, the creation operator of that single displaced mode is $\int_{-\infty}^{\infty} dt \Psi(t) \hat{E}^\dagger(t) = \int_{-\infty}^{\infty} d\omega \tilde{\Psi}(\omega) \hat{A}^\dagger(\omega)$, where $\Psi(t)$ is an arbitrary normalized complex function. The complex α is the displacement parameter. We can easily verify that $\hat{U}_\tau |\psi^{\text{coh}}\rangle$ shifts the signal in time $\Psi(t) \rightarrow \Psi(t + \tau)$ and $\hat{U}_\nu |\psi^{\text{coh}}\rangle$ causes a frequency shift $\tilde{\Psi}(\omega) \rightarrow \tilde{\Psi}(\omega - \nu)$.

To make this more concrete, consider a Gaussian mode function $\Psi(t) = \left(\frac{1}{2\sigma_t^2\pi}\right)^{1/4} e^{-\frac{1}{2}\left(\frac{t-t_0}{\sigma_t}\right)^2} e^{-i\omega_0(t-t_0)}$, plotted in Fig. 3. The Gaussian is characterized by the parameters t_0 , ω_0 , and σ_t , which are directly related to the resource parameters via $\bar{t} = t_0$, $\bar{\omega} = \omega_0$, $\Delta t^2 = \sigma_t^2$, and $\Delta\omega^2 = \sigma_\omega^2 = 1/(4\sigma_t^2)$. Furthermore, we have $N_S = |\alpha|^2$.

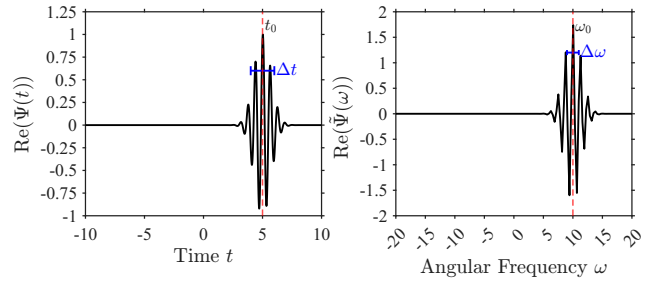


FIG. 3. Real part of the coherent states signal $\Psi(t) = e^{-(t-t_0)^2/2\sigma_t^2} e^{i\omega_0 t}$ (left) and its Fourier transform $\tilde{\Psi}(\omega)$ (right). This figure illustrates a convenient representation of the time and frequency resources for classical and coherent states. The resources are the temporal and spectral bandwidths σ_t and σ_ω , and the central frequency and mean arrival time ω_0 and t_0 , here shown for a Fourier-limited pulse.

Using Eq. (27), we find the expression of the QFI for bosonic coherent states:

$$\mathcal{F}(|\psi_\tau^{\text{coh}}\rangle) = 4(\bar{\omega}^2 + \Delta\omega^2)N_S \quad (57)$$

$$\mathcal{F}(|\psi_\nu^{\text{coh}}\rangle) = 4(\bar{t}^2 + \Delta t^2)N_S \quad (58)$$

which recovers well-known results from classical radar and lidar literature [22], and are also presented in [9].

In the radar and lidar literature, the quantities $\bar{\omega}$, $\Delta\omega$ and \bar{t} , Δt are well-established as the fundamental resources governing the estimation of time delay and Doppler frequency shift, respectively [22, 47]. This decomposition traces back to Woodward’s foundational analysis of the radar ambiguity function [21], which showed that the mean and spread of a waveform’s time-frequency support jointly determine the limits of range and velocity discrimination. In the quantum setting, these quantities enter the quantum Fisher information (QFI) as two structurally distinct contributions: a mean term ($4\bar{\omega}^2 N_S$ for time estimation, $4\bar{t}^2 N_S$ for frequency estimation) and a variance term ($4\Delta\omega^2 N_S$ for time estimation, $4\Delta t^2 N_S$ for frequency estimation) [48, 49]. These two terms are of different significance.

Consider time estimation, *i.e.*, target ranging. In any realistic narrowband waveform, the carrier frequency dominates the spectral spread: $\bar{\omega} \gg \Delta\omega$. Consequently, the mean term $4\bar{\omega}^2 N_S$ overwhelmingly dominates the total QFI. In principle, the Cramér–Rao bound associated with this term is achievable, but only via a phase-sensitive measurement, such as homodyne detection with a phase-locked local oscillator. Attaining this bound requires prior knowledge of the time delay τ to within a phase cycle of the carrier, $|\tau - \tau_{\text{prior}}| \lesssim 1/\bar{\omega}$, imposing sub-wavelength accuracy on the prior. Such knowledge is unavailable in typical uncooperative-target scenarios and is only achievable in highly controlled interferometric setups.

By contrast, the variance term $4\Delta\omega^2 N_S$ is governed by the root-mean-square bandwidth $\Delta\omega$ and is accessible through incoherent or envelope-based measurements—precisely the time-of-flight paradigm underlying most practical ranging systems [47]. Direct intensity detection, matched filtering of the envelope, or photon counting all respond to the pulse shape rather than its absolute carrier phase, and therefore require no phase prior. The Cramér–Rao bound associated with $4\Delta\omega^2 N_S$ is achievable with these prior-free measurements and in radar waveform design the use of high time-bandwidth product waveforms is motivated precisely by the need to maximize $\Delta\omega$ without access to a phase reference [21].

Similar conclusions can be drawn for general Gaussian states. This observation highlights that the mean parameter \bar{g} and the variance parameter Δg play fundamentally different roles, motivating their treatment as distinct resources.

2. Gaussian states with product structure in the Hermite-Gauss mode basis

Before discussing optimal states, let us examine some states that are commonly discussed in the literature — states that appear in product form in the Hermite–Gauss mode basis.

An arbitrary multimode squeezed vacuum state takes the

form

$$|\psi^{\text{sq}}\rangle = \exp\left(\frac{1}{2} \iint dt dt' f(t, t') \hat{E}^\dagger(t) \hat{E}^\dagger(t') - \text{h.c.}\right) |0\rangle \quad (59)$$

$$= \exp\left(\frac{1}{2} \iint d\omega d\omega' \tilde{f}(\omega, \omega') \hat{A}^\dagger(\omega) \hat{A}^\dagger(\omega') - \text{h.c.}\right) |0\rangle, \quad (60)$$

in the time and frequency domains, respectively. Here, $f(t, t')$ and $\tilde{f}(\omega, \omega')$ are the continuous analogues of the squeezing matrix in the time-domain and frequency-domain mode bases, respectively, and are known as the joint temporal amplitude (JTA) and joint spectral amplitude (JSA). Their modulus squares are known as the joint temporal intensity (JTI) and joint spectral intensity (JSI), respectively.

Now, similarly to the coherent state case, we can find a mode basis $\{\Psi_n\}_n$ in which the squeezed state takes on a simple (disentangled) form.

Since $f(t, t')$ is symmetric, it admits the expansion

$$f(t, t') = \sum_{n=0}^{\infty} r_n \Psi_n(t) \Psi_n(t'),$$

where $r_n \geq 0$. Interpreting $f(t, t')$ as a bipartite wavefunction, this expansion corresponds to its Schmidt decomposition [50]. In finite dimensions, the analogous decomposition of a complex symmetric matrix is given by the Takagi factorization, see Appendix A 2. Note that in the frequency domain the Schmidt decomposition is $\tilde{f}(\omega, \omega') = \sum_{n=0}^{\infty} r_n \tilde{\Psi}_n(\omega) \tilde{\Psi}_n(\omega')$ with $\tilde{\Psi}_n(\omega) = \int dt \Psi_n(t) e^{+i\omega t} / \sqrt{2\pi}$.

In this basis $\{\Psi_n\}_n$, we can write

$$|\psi^{\text{sq}}\rangle = [\otimes_{n=1}^M \hat{S}_{\hat{c}_n}(r_n)] |0\rangle. \quad (61)$$

with $\hat{c}_n^\dagger = \int dt \Psi_n(t) \hat{E}^\dagger(t)$ being the mode basis in which the state appears disentangled. We refer to $\{\hat{c}_n\}_n$ as the Schmidt basis.

To make it concrete, we consider the set of squeezed states that appear disentangled in the Hermite-Gauss (HG) mode basis

$$\begin{aligned} \Psi_n(t) = \Phi_n(t; t_0, \omega_0, \sigma_t, \theta) &= \left(\frac{1}{2\sigma^2\pi}\right)^{1/4} \sqrt{\frac{2^{-n}}{n!}} \\ &\times H_n\left(\frac{t-t_0}{\sqrt{2}\sigma_t}\right) e^{-\frac{1}{2}\left(\frac{t-t_0}{\sqrt{2}\sigma_t}\right)^2} e^{-i\omega_0(t-t_0)} e^{-i\theta}. \end{aligned} \quad (62)$$

where $H_n(t) = (-1)^n e^{t^2} \frac{d^n}{dt^n} e^{-t^2}$ are the physicist’s Hermite polynomials. The mode functions are centered around t_0 in the time domain and centered around ω_0 in the frequency domain. Their width is characterized by σ_t in the time domain and by $\sigma_\omega^2 = 1/(4\sigma_t^2)$ in the frequency domain. θ is a phase that will not impact what follows.

Let us now consider the QFI for time estimation of a state $|\psi^{\text{sq}}\rangle = \otimes_n \hat{S}_{\hat{c}_n} e^{-i\phi_n/2}(r_n) |0\rangle$, where we additionally introduced mode dependent squeezing angles ϕ_n . Let us assume the first two modes are equally populated, *i.e.*, $r_0 = r_1$ and $r_n = 0$ for

$n \geq 2$ and that the squeezing angles satisfy $\phi_1 - \phi_0 = \pi$. With this, we find in Appendix H 3 the QFI for time estimation τ :

$$\mathcal{F}(\hat{U}_\tau |\psi^{\text{sq}}\rangle) = (4\bar{\omega}^2 + 2\Delta\omega^2)N_S^2 + O(N_S). \quad (63)$$

It is evident that this specific state is suboptimal, as indicated by the prefactors of 4 and 2 preceding the mean and variance terms, respectively. Notably, both prefactors are only half of their maximal possible values. Since the Hermite–Gaussian modes are eigenfunctions of the Fourier transform, analogous results hold for frequency estimation.

3. Optimal states for time and frequency estimation

We now turn to the problem of optimal multimode Gaussian states for time and frequency estimation. As before, we consider multimode squeezed vacuum states of the form given in Eq. (59), or equivalently in Eq. (60). In Sec. III D, we derived the optimal states analytically under the assumption that the generator possesses a quasi-continuous spectrum. Since this condition is satisfied for the discretized versions of the generators \hat{G}_τ and \hat{G}_ν in Eqs. (48) and (49), the general results of Sec. III D apply directly to the specific tasks of time and frequency estimation. As shown in Sec. III D, the optimal states take a particularly simple form in the basis $\{\hat{b}_n\}$ that diagonalizes the generator, $\hat{G} = \sum_n g_n \hat{b}_n^\dagger \hat{b}_n$, in which the squeezing matrix f is diagonal.

Let us focus on time estimation; the analysis for frequency estimation is entirely analogous by Fourier duality.

By analogy with the discrete case, we expect the squeezing matrix to be diagonal in the generator eigenbasis $\{\hat{A}(\omega)\}$, recalling that $\hat{G}_\tau = \int d\omega \omega \hat{A}^\dagger(\omega) \hat{A}(\omega)$. Accordingly, we make the following Ansatz for the squeezing function in the frequency domain:

$$\tilde{f}(\omega, \omega') = \sum_{n \in \{i, j\}} r_n \delta(\omega - \omega_n) \delta(\omega' - \omega_n), \quad (64)$$

for some fixed modes $i, j \in \{1, 2, \dots, M\}$. However, this state is unphysical (non-normalizable) due to the presence of the Dirac delta functions. To obtain a physical state, we regularize the Dirac deltas by replacing them with Gaussians: $\delta(\omega - \omega_n) \rightarrow \tilde{\Phi}_0(\omega; t_n, \omega_n, \sigma_t, \theta)$, where $\tilde{\Phi}_0$ is the Fourier transform of the zeroth HG mode defined in Eq. (62), which is a Gaussian in both the time and frequency domains.

We thus propose the following physical Ansatz, with squeezing matrix

$$\tilde{f}(\omega, \omega') = \sum_{n \in \{i, j\}} r_n \tilde{\Phi}_0(\omega; t_n, \omega_n, \sigma_\omega, \theta) \tilde{\Phi}_0(\omega'; t_n, \omega_n, \sigma_\omega, \theta). \quad (65)$$

To achieve a good regularization, the width σ_ω of the Gaussians in the frequency domain should be much smaller than the separation between the two Gaussians, *i.e.*, $\sigma_\omega \ll |\omega_j - \omega_i|$. The remaining parameters r_n, ω_n , and t_n with $n \in \{i, j\}$ are to be chosen according to the type of optimality one wishes to attain.

Let us first consider a fully optimal state (see Sec. III D for the definition). In such a case, we have to choose the squeezing parameters r_i, r_j and the central frequencies ω_i, ω_j according to Eqs. (35)–(39). The QFI of the corresponding state can be calculated by using the Schmidt decomposition of $\tilde{f}(\omega, \omega')$ given in Eq. (65). We show in Appendix I that the first two populated Schmidt modes $\tilde{f}(\omega, \omega')$ are approximately equal to $\tilde{\Phi}_0(\omega; t_i, \omega_i, \sigma_t, \theta)$ and $\tilde{\Phi}_0(\omega; t_j, \omega_j, \sigma_t, \theta)$. The QFI for temporal estimation can then be calculated, and we find

$$\mathcal{F}(|\psi_\tau\rangle) = 8\bar{\omega}^2 N_S^2 + 4(\Delta\omega^2 - \sigma_\omega^2) N_S^2 + O(N_S) \quad (66)$$

which is optimal in the good regularization limit of $\sigma_\omega \ll |\omega_j - \omega_i| \sim \Delta\omega$. Note that when estimating a time parameter, we can freely choose t_i, t_j while ω_i, ω_j have to be chosen according to Eqs. (35)–(39). This freedom may be exploited for having a variance optimal state for the estimation of τ and ν , as we later discuss in the next section.

4. Variance-optimal state for time and frequency estimation

We now focus on finding the variance optimal state. Let us consider first a time-shift estimation scenario. If we only strive for variance optimality, we choose an equal weighting of the squeezing parameters, *i.e.*, $r_i = r_j$, and the Gaussian centers in the frequency domain are chosen such that $|\omega_j - \omega_i| \gg \sigma_\omega$. This choice yields $\frac{|\omega_j - \omega_i|^2}{2} = \Delta\omega^2 - \sigma_\omega^2 \approx \Delta\omega^2$ and $\frac{\omega_i + \omega_j}{2} = \bar{\omega}$. The state's QFI is

$$\mathcal{F}(|\psi_\tau\rangle) = 4\bar{\omega}^2 N_S^2 + (\Delta\omega^2 - \sigma_\omega^2) N_S^2 + O(N_S), \quad (67)$$

and thus the state is variance optimal in the good regularization limit $\Delta\omega^2 - \sigma_\omega^2 \approx \Delta\omega^2$. As in the case discussed in the previous paragraph, the parameters t_i, t_j can be freely chosen, and is not detrimental for temporal estimation. In the case of $t_i = t_j$, the state can only be optimal for time estimation, but not for frequency estimation, as the squeezing matrix takes on diagonal structure only in the frequency domain and not the time domain. Similar observations for time-frequency shifts estimation with two-photon states were made in [17]. The JSI and JTI of the variance optimal state is represented in Fig. 4, when $t_i = t_j$, and $|\omega_j - \omega_i| \gg \sigma_\omega$. If $|t_j - t_i| \gg \sigma_t$, the squeezing function takes on a diagonal structure also in the temporal domain (JTI) and the state's QFI with respect to frequency estimation is

$$\mathcal{F}(|\psi_\nu\rangle) = 4\bar{t}^2 N_S^2 + (\Delta t^2 - \sigma_t^2) N_S^2 + O(N_S) \quad (68)$$

and thus the state is variance optimal in the good regularization limit $\Delta t^2 - \sigma_t^2 \approx \Delta t^2$. Thus, the state can be variance optimal for both time and frequency estimation. However, we are not aware of a measurement scheme that can jointly estimate both parameters. We also point out that for specific resource parameter configurations it is possible to find states that are fully optimal for both time and frequency estimation.

The above states are two-mode squeezed states that do not make use of displacement. In Sec. III D 2 we have discussed that under certain conditions given in Appendix E 2 b,

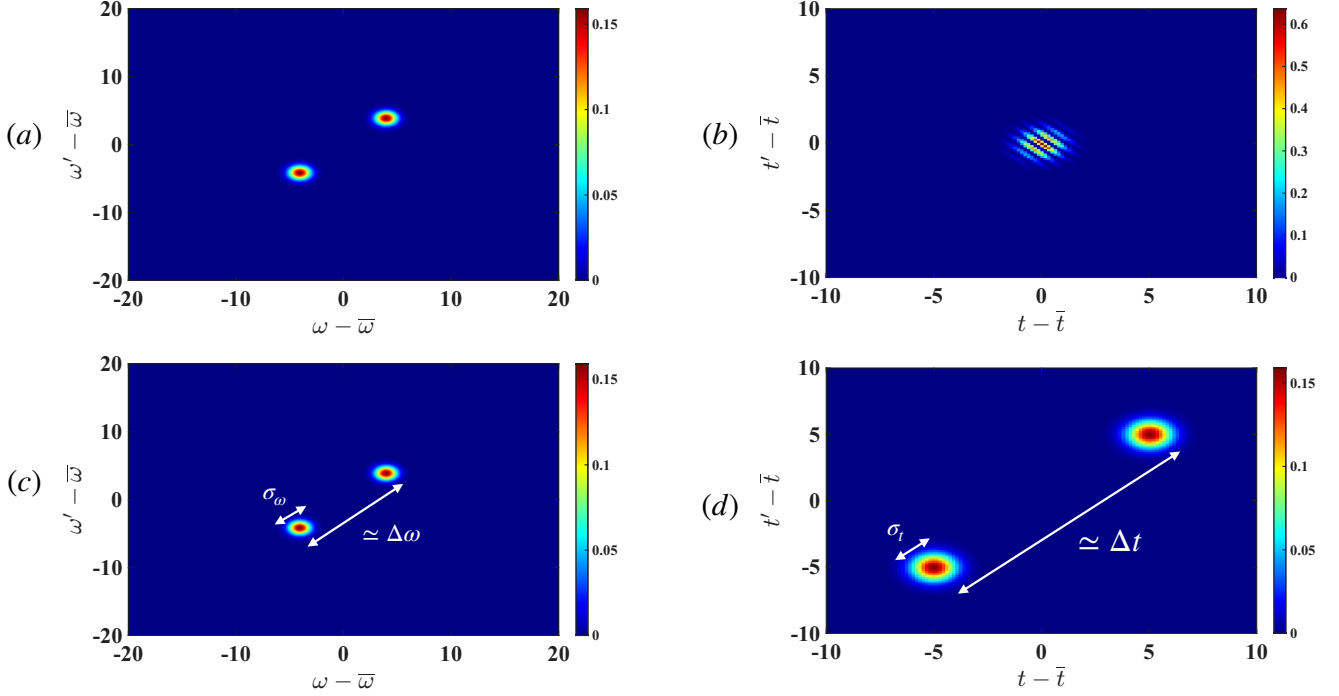


FIG. 4. (a), (b) JSI and JTI for variance optimal states for time estimation, with equal squeezing parameters $r_i = r_j$, central time-of-arrival $t_i = t_j$, and central frequency such as $|\omega_j - \omega_i| \gg \sigma_\omega$. We remind that the resource $\Delta\omega$ is related to other parameters such as $\frac{|\omega_j - \omega_i|^2}{2} = \Delta\omega^2 - \sigma_\omega^2 \approx \Delta\omega^2$. (c), (d) JSI and JTI for simultaneous variance optimal state for time and frequency estimation, that corresponds to the parameters: equal squeezing parameter $r_i = r_j$, with $|t_i - t_j| \gg \sigma_t$, and $|\omega_j - \omega_i| \gg \sigma_\omega$. We have chosen arbitrary central frequency and time $\bar{\omega}, \bar{t}$ for the two distributions.

it is possible to find variance-optimal states that use half of their energy for displacement. The first step is to find a pair of orthonormal modes $\{\hat{u}_0, \hat{u}_1\}$ that satisfies $\partial_\tau \hat{c}_0^\dagger(\tau) = -iG_{00}\hat{c}_0^\dagger(\tau) - iG_{10}\hat{c}_1^\dagger(\tau)$, i.e., the mode $\partial_\tau \hat{c}_0^\dagger(\tau)$ has only overlap with itself and one other mode $\hat{c}_1(\tau)$. This condition is satisfied for HG modes $\{\hat{c}_0, \hat{c}_1\}$ as can be seen in Appendix H 2. The second condition is $G_{00} = G_{11}$, which is also satisfied for the HG modes H 2. We therefore construct the state

$$|\psi\rangle = \hat{D}_{\hat{c}_0 e^{-i\phi_0/2}}(\alpha_0) \hat{S}_{\hat{c}_1 e^{-i\phi_1/2}}(r_1) |0\rangle \quad (69)$$

with $|\alpha_0|^2 = \sinh^2(r_1) = N_S/2$ and an appropriate choice for ϕ_0, ϕ_1 . According to E 2 b, we find that such a state is variance-optimal:

$$\mathcal{F}(|\psi_\tau\rangle) = (2\bar{\omega}^2 + 4\Delta\omega^2)N_S^2 + O(N_S). \quad (70)$$

Remarkably, unlike our other optimal and variance optimal states, this state is not prepared in the generator mode basis $\{\hat{b}_i\}_i$. It can be shown that homodyne detection of the single mode $\hat{c}_1(\tau)$ is a variance optimal measurement for this state. Since the HG modes are eigenfunctions of the Fourier transform, one can find analogous results for frequency estimation. Note that such states with $|\alpha_0|^2 \gg \sinh^2(r_1)$ have been frequently discussed in the literature [19, 31, 38, 51].

D. Optimal measurements for time and frequency estimation

Let us discuss the measurements that can be deployed for time and frequency estimation using the optimal (or variance-optimal) regularized state with squeezing matrix given in Eq. (65). We focus on time estimation, from which the frequency estimation case follows directly by analogy.

1. Phase-sensitive detection

From Sec. III E and Appendix F 1, phase-sensitive homodyne measurements in the mode basis in which the generator appears diagonally are optimal. In the case of a regularized state, the same analysis as in Appendix F 1 can be used to show that homodyning the regularized modes $\Phi_0(t + \tau_{\text{pr}}; t_i, \omega_i, \sigma_t, \theta)$ and $\Phi_0(t + \tau_{\text{pr}}; t_j, \omega_j, \sigma_t, \theta)$ is optimal for time estimation. The local oscillator (LO) modes must be shaped to match those of the two-mode squeezed vacuum state under investigation. For two-mode states with a significant frequency separation, a bichromatic local oscillator (BLO) — composed of two frequency components that match the signal modes — provides a critical practical advantage. This technique translates the two-mode squeezing information to a single, lower electronic frequency band, circumventing the need for high-bandwidth shot-noise-limited electronics and enabling the use

of more sensitive, low-frequency detection systems. [52]. Other schemes employ multipixel [53] or multiplexed [54] homodyne detection which necessitate shaping the temporal or spectral profile of a monochromatic LO to match an arbitrary mode can be achieved using a programmable waveshaper, as it was achieved for quantum frequency comb [55].

Finally, although phase-sensitive homodyne detection is fully optimal in principle for pure states, its implementation requires a substantial amount of prior information, owing to the need for precise tuning of the measurement apparatus and the presence of phase ambiguities. For instance, in gravitational wave interferometry, while the wave distorts spacetime transversally, optimal filtering and signal extraction depend critically on prior assumptions about source parameters to define the template bank and analysis bandwidth.

As discussed in Sec. IV C 1, these practical lack of knowledge about the prior information often render the contribution to the QFI arising from the mean term, scaling as $\sim \bar{g}^2 N_S^2$, effectively inaccessible. By contrast, for time-of-flight estimation in lidar systems, the contribution associated with the variance term, scaling as $\sim \Delta g^2 N_S^2$, is not subject to these constraints. Consequently, without a prior estimate τ_{pr} sufficiently close to τ , one must choose a relative phase of the homodyne detection ϕ suboptimally, leading to a direct and severe reduction in estimation precision.

2. Phase-insensitive detection

We now aim to identify variance-optimal measurements according to Definition III.3, namely measurements whose FI attains the contribution $\sim \Delta g^2 N_S^2$ of the QFI optimally, without necessarily achieving the mean contribution $\bar{g}^2 N_S^2$ optimally. We identify a phase-insensitive measurement scheme, or direct detection, that is variance optimal if the state under consideration satisfies the variance-optimal measurement condition given in Appendix K 1. Specifically, we propose time-resolved and frequency-resolved photon counting as phase-insensitive measurements for time and frequency estimation, respectively. Mathematically, these measurements correspond to projections onto the states $(K!)^{-1/2} \bigotimes_{n=1}^K \hat{E}^\dagger(t_n)|0\rangle$ and $(K!)^{-1/2} \bigotimes_{n=1}^K \hat{A}^\dagger(\omega_n)|0\rangle$, respectively. We will focus on the sensitivity achievable with time-resolved photon counting for time estimation, but the discussion is similar for frequency estimation with frequency resolved photon counting.

In Appendix K 2 b, we show that, for the variance-optimal state with squeezing matrix given in Eq. (65) and parameters satisfying $r_i = r_j$, $\sigma_\omega \ll |\omega_j - \omega_i|$, time-resolved photon counting yields a FI for time estimation of

$$F_{\text{direct}}(|\psi_\tau\rangle) = 4\Delta\omega^2 N_S^2 + O(N_S) \quad (71)$$

when $t_i = t_j$. The condition of the Gaussian centers in the time domain being equal, *i.e.*, $t_i = t_j$, is needed so that the variance-optimal state satisfies the variance-optimal measurement condition given in Appendix K 1. Notably, the mean

contribution $\sim \bar{\omega}^2 N_S^2$ is absent, and only the variance term contributes. While this may appear to represent a substantial reduction in precision, in many realistic scenarios the precision associated to the variance term is the only component that can be robustly achieved, as we have mentioned in Sec. IV C 1.

Furthermore, we show in Appendix K 2 that the state of the form given in Eq. (61), whose squeezing matrix appears diagonally in the HG mode basis, satisfies the variance-optimal measurement condition in Appendix K 1, and thus, time-resolved photon counting attains an FI of $2\Delta\omega^2 N_S^2 + O(N_S)$. This establishes time-resolved photon counting as a variance-optimal measurement for a broad class of pure Gaussian quantum states.

In practice, this detection scheme relies on the implementation of photon counters. Photon-number-resolving (PNR) detectors directly measure the photon-count distribution of the optical field incident upon them, giving access to the full statistics of the probe state at the detection stage. The practical construction of PNR detectors has followed two main routes, both achieving photon-number resolution of up to 100 photons: multiplexing multiple SNSPD detectors so that simultaneous arrival events are spatially or temporally separated [56], or employing transition-edge sensors (TES) [57], which exhibit a timing jitter of order nanoseconds. By contrast, the sub-picosecond timing jitter achieved by optimised single-pixel SNSPDs—demonstrated at 2.6 ps system jitter in [58]. Therefore, the use of two-mode squeezed states of light as probes for measuring time and frequency shifts—combined with photon-number-resolving detectors with a resolution of 100 photons and low timing jitter—enables performance beyond the shot-noise scaling and is accessible with current technology.

E. Literature on time-frequency parameter estimation

A substantial body of literature is dedicated to quantum-enhanced estimation of time delays and frequency shifts, exploiting non-classical states of light including two-photon and squeezed states. These protocols are of particular relevance to quantum sensing applications such as radar and lidar. In these contexts, an estimated temporal delay directly corresponds to the range of a target, while a measured frequency shift, induced by the Doppler effect, provides information about its relative velocity.

1. Two-photon states for time and frequency shifts estimation

Two-photon states, which are non-Gaussian and typically exhibit very low squeezing, offer valuable insights into the spectral and temporal engineering required for quantum metrological protocols. Two-photon states provide a clear advantage for probing sensitive samples [14, 59]. The measurement of time delays, classically performed using Optical Coherence Tomography—a Michelson interferometer—found its quantum counterpart in the Hong-Ou-Mandel (HOM) experiment. The HOM interferometer demonstrated the

ability to measure sub-picosecond time intervals [60], laying the foundation for Quantum Optical Coherence Tomography [61]. In [15] formally applied quantum metrology tools to the HOM interferometer, demonstrating ten of attosecond-scale resolution with entangled photon pairs. Subsequent spectral engineering of the biphoton state further enhanced precision. For instance, using a two-mode frequency-entangled state led to a factor-of-two improvement in resolution [16] for a fixed total bandwidth. Theoretical work then showed that engineered time-frequency grid states could push resolution to the sub-attosecond regime [17]. The estimation of frequency shifts has been proposed in [17] using generalized HOM interferometry with spectrally engineered two-photon states. The framework was further generalized by [62], who established the ultimate bounds for estimating a broader class of time-frequency parameters, such as shear and rotation in chronocyclic phase space.

These results connect naturally to the findings of the present manuscript. In particular, the factor-of-four improvement in time-delay resolution achieved with a two-color frequency-entangled biphoton state [16, 17] has a direct analogue in our framework: the same enhancement arises for two-mode squeezed vacuum states with the same spectral separation. This highlights that spectral engineering yields consistent metrological gains across different photon-number statistics — whether in the low-flux two-photon regime or the bright squeezed-light regime.

2. Multimode squeezed states for time-frequency estimation

The time or frequency accuracy enhancement achieved through spectral engineering of two-photon states, for a fixed amount of resources, is also demonstrably attainable using multimode squeezed states, as shown in this manuscript. This could be understood as two-mode squeezed state as a "Gaussification" of two-photon (two-mode) states, but such an explicit transformation will be left for further work. Let us now exhibit related works, and additional challenges to implement our idea.

The Gaussian state considered in Ref. [63], for example, is similar to the one discussed in Sec. IV C 2 and is suboptimal: its variance-term prefactor is only "1" for both time and frequency estimation, which is below the maximal value of "4". Ref. [23] studied an idler-assisted state with a Gaussian-shaped squeezing function, whose performance depends strongly on the specific form of the squeezing function and is likewise suboptimal in all cases.

Strong coherent states with a small amount of squeezing in the derivative mode, that were shown to be optimal in the limit $|\alpha| \gg \sinh^2(r)$ Ref. [38], were also considered theoretically for time estimation [51] and experimentally for frequency estimation [64]. According to our framework, these approaches are suboptimal due to the linear scaling with signal photon number, but can be made variance optimal as shown in Sec. IV C 4 by allocating half of the energy to squeezing.

We should precise finally that achieving a resolution en-

hancement with squeezed states, as compared to classical states, requires a substantial degree of squeezing. In practice, this is challenging to realize due to multiple sources of noise, including injection losses, thermal effects, and other decoherence mechanisms. These factors, particularly photon losses over extended distances, rapidly degrade squeezing and induce thermalization, thereby limiting the feasibility of our current proposal for long-range applications such as radar and lidar.

We now provide a simple estimate of the sensing distance. In such experimental settings, the total homodyne detection efficiency—accounting for photodiode quantum efficiencies, mode imbalance, optical losses, and equivalent electronic noise—can reach values as high as approximately 90% (see for instance [65]). Using a channel transmission under the form $\eta = 10^{-\alpha L/10}$ where L is the propagation length, and $\alpha \sim 0.2$ dB/km in optical fibers at telecom wavelength 1550nm, the total transmission is limited to ~ 12 km (equivalent to $\eta > 1/2$) for beating coherent states estimation for instance (see Eq. (44)).

V. SECOND APPLICATION OF OPTIMAL MODE ESTIMATION: BEAM DISPLACEMENT AND TILT ESTIMATION

A further illustrative example is the estimation of beam displacement and tilt, as represented in Fig. 5. Although its mathematical formulation is essentially equivalent to that of time and frequency estimation — and therefore does not warrant a repetition of the analysis presented in Sec. IV, we emphasize that our framework offers a new perspective on this problem when compared to previous literature.

A. Beam displacement estimation

Let us consider a monochromatic aperture field $\hat{E}(x, y) e^{-i\omega t}$ of angular frequency ω in the detection plane $z = 0$, which can be decomposed into spatial plane-wave modes as

$$\hat{E}(x, y) = \frac{1}{2\pi} \iint_{k_x^2 + k_y^2 < \omega^2} dk_x dk_y \hat{A}(k_x, k_y) e^{-i(k_x x + k_y y)}. \quad (72)$$

In the paraxial regime, the mode operators $\hat{E}(x, y)$ and $\hat{A}(k_x, k_y)$ in the spatial and spectral domains satisfy the commutation relations $[\hat{E}(x, y), \hat{E}^\dagger(x', y')] = \delta(x - x')\delta(y - y')$ and $[\hat{A}(k_x, k_y), \hat{A}^\dagger(k'_x, k'_y)] = \delta(k_x - k'_x)\delta(k_y - k'_y)$, and the integration domain in Eq. (72) may be extended to \mathbb{R}^2 . A beam displacement is a transverse displacement d of the beam in the aperture plane, corresponding to $\hat{E}(x, y) \rightarrow \hat{E}(x+d, y)$, which induces the transformation $\hat{A}(k_x, k_y) \rightarrow \hat{A}(k_x, k_y) e^{-ik_x d}$ on the spectral mode operators.

From this, one can readily deduce the unitary operator $\hat{U}_d = e^{-id\hat{G}_d}$ of the beam displacement transformation, with

generator

$$\hat{G}_d = \iint_{\mathbb{R}^2} dk_x dk_y k_x \hat{A}^\dagger(k_x, k_y) \hat{A}(k_x, k_y). \quad (73)$$

This generator is already expressed in diagonal form; in an arbitrary basis, one would require four integrals (or sums in the discrete case) instead of two.

Small tilts of the beam by an angle ϑ in the xz plane about the origin correspond to the transformation $\hat{E}(x, y) \rightarrow \hat{E}(x, y) e^{-i\vartheta \frac{\omega}{c} x}$, from which one deduces the unitary operator $\hat{U}_\vartheta = e^{-i\vartheta \hat{G}_\vartheta}$ of the tilt transformation, with generator

$$\hat{G}_\vartheta = \frac{\omega}{c} \iint_{\mathbb{R}^2} dx dy x \hat{E}^\dagger(x, y) \hat{E}(x, y), \quad (74)$$

which is likewise already expressed in the basis in which it takes diagonal form.

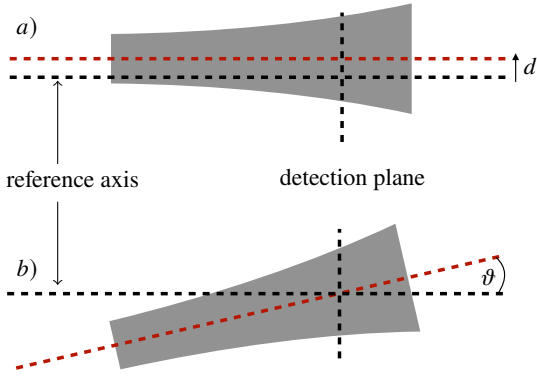


FIG. 5. Two mode transforms are illustrated: *a*) beam displacement, where the beam is shifted by a distance d in direction transverse to the detection plane, and *b*), beam tilt, where the beam is rotated by an angle ϑ around an axis perpendicular to the reference axis. This schematic is widely inspired from [31].

B. Resources and optimal states for beam displacement and tilt estimation

Let us now discuss the resources for beam displacement and tilt estimation. The common resource is the signal photon number

$$N_S = \iint_{\mathbb{R}^2} dk_x dk_y \langle \psi | \hat{A}^\dagger(k_x, k_y) \hat{A}(k_x, k_y) | \psi \rangle \quad (75)$$

$$= \iint_{\mathbb{R}^2} dx dy \langle \psi | \hat{E}^\dagger(x, y) \hat{E}(x, y) | \psi \rangle. \quad (76)$$

We define $I^{\text{spec}}(k_x, k_y) = \langle \psi | \hat{A}^\dagger(k_x, k_y) \hat{A}(k_x, k_y) | \psi \rangle / N_S$ as the normalized spectral photon-number intensity, and $I^{\text{spat}}(x, y) = \langle \psi | \hat{E}^\dagger(x, y) \hat{E}(x, y) | \psi \rangle / N_S$ as the normalized spatial photon-number intensity. The resources for beam dis-

placement estimation are then

$$\bar{k}_x = \iint_{\mathbb{R}^2} dk_x dk_y k_x I^{\text{spec}}(k_x, k_y), \quad (77)$$

$$\Delta k_x^2 = \iint_{\mathbb{R}^2} dk_x dk_y (k_x - \bar{k}_x)^2 I^{\text{spec}}(k_x, k_y), \quad (78)$$

corresponding to the mean and variance of the transverse wave vector in the x direction. The resources for beam tilt estimation are

$$\bar{x} \frac{\omega}{c} = \iint_{\mathbb{R}^2} dx dy x I^{\text{spat}}(x, y), \quad (79)$$

$$\Delta x^2 \frac{\omega^2}{c^2} = \iint_{\mathbb{R}^2} dx dy (x - \bar{x})^2 I^{\text{spat}}(x, y), \quad (80)$$

corresponding to the mean and variance of the spatial intensity distribution in the x direction, each multiplied by the factor ω/c .

Applying the results of Sec. III, the optimal QFI for displacement and tilt estimation is $(8\bar{k}_x^2 + 4\Delta k_x^2)N_S^2 + O(N_S)$ and $(\omega^2/c^2)(8\bar{x}^2 + 4\Delta x^2)N_S^2 + O(N_S)$, respectively. Completely analogously to Sec. IV C 3, an optimal state can be constructed by squeezing two regularized modes of the basis in which the generator is diagonal. For displacement estimation one may, for example, appropriately squeeze regularized versions of $\hat{A}(k_{x_i}, 0)$ and $\hat{A}(k_{x_j}, 0)$, and for tilt estimation, $\hat{E}(x_i, 0)$ and $\hat{E}(x_j, 0)$. The discussion of phase-sensitive and phase-insensitive measurements is entirely analogous to that of Sec. IV D. The phase-insensitive measurements that achieve variance-optimal performance are spatially resolved photon counting for beam displacement estimation, and k_x - k_y -resolved photon counting for beam tilt estimation.

C. Comparison with related work

The recent work of Ref. [41] also considered the problem of beam displacement sensing using a quantum metrology framework. Their approach was to describe the problem in the spatial Hermite-Gaussian (HG) mode basis, compute the generator matrix in this basis, and evaluate the QFI via a formula analogous to Eq. (17) for a general single-mode squeezed state. Because the problem is intrinsically infinite-dimensional, they introduce a mode cutoff and then maximize the QFI subject to a photon-number constraint, without invoking additional resources. They find that the optimal state is related to the basis in which the truncated generator matrix appears diagonal, a result similar to our manuscript. Specifically, their optimal state is a single-mode squeezed state squeezed in the mode belonging to the generator-diagonalizing mode basis corresponding to the largest generator eigenvalue $k_{x,\text{max}}$, achieving a QFI of $8k_{x,\text{max}}^2 N_S^2 + O(N_S)$. This is consistent with our framework, as this state corresponds to the mean-optimal state discussed in Sec. III D 3. The authors have also found that the phase-sensitive homodyne measurement of the populated mode is optimal [41].

Our approach extends this analysis by introducing two additional resources, \bar{k}_x and Δk_x , alongside N_S . Although we likewise truncate the mode space, a key advantage of our framework is that the optimal states we identify are independent of the mode cutoff. More importantly, our analysis reveals that the state found in Ref. [41] is not the only optimal state but belongs to a broader family: any state squeezed in a single arbitrary mode makes optimal use of the mean resource \bar{k}_x , with the prefactor of the mean term in the QFI universally equal to 8. Furthermore, by appropriately squeezing two modes in the generator-diagonalizing basis, one can also saturate the variance resource Δk_x . A particularly attractive special case is the variance-optimal state with $\bar{k}_x = 0$, for which phase-insensitive spatially-resolved photon counting achieves the optimal Fisher information $4\Delta k_x^2 N_S^2 + O(N_S)$, as shown in Sec. IV D. Such a phase-insensitive measurement strategy may be experimentally more accessible than the phase-sensitive homodyne detection proposed in [41]: intensity measurements on HG modes via spatial mode demultiplexing with a multiplane light conversion system [30, 66, 67] already constitute a well-established practical toolbox that could be directly repurposed as a near-optimal platform for beam displacement sensing with non-classical states.

There are various related experimental works [30, 31, 66, 68] on beam displacement and tilt estimation using strong coherent states with squeezing in its derivative mode. These are examples of the general framework in Ref. [38] discussed in Sec. III F. These approaches are practical due to the use of coherent light and homodyne measurements, which are readily available. However, according to our framework, they are suboptimal due to their linear scaling with photon number. However, they can be made variance optimal as shown in Sec. IV C 4 by allocating half of the energy to squeezing.

VI. OUTLOOK AND DISCUSSION

In this paper, we have established that, for pure Gaussian states, the QFI of any mode parameter estimation protocol is upper-bounded by a function of three resource parameters: the mean and variance of the generator intensity distribution over the natural mode basis induced by the transformation, denoted \bar{g} and Δg , and the mean signal photon number N_S . We have shown that an appropriately configured two-mode squeezed vacuum state is optimal, in the sense that its QFI saturates this upper bound for any fixed values of \bar{g} , Δg , and N_S . Crucially, we have further demonstrated that multimode homodyne detection on these two modes constitutes an optimal measurement, in the sense that it achieves the QCRB and thus extracts all the information available in the optimal probe state. This resource formulation applies across estimation tasks: we have demonstrated its optimality explicitly for time delays and frequency shifts, and for tilt and beam displacement. We have summarized the sensitivities that can be reached with different quantum states in Table I, that provide a complete characterization of optimal quantum strategies for mode parameter estimation.

As perspectives, performing mode estimation protocol, at

State	QFI $\mathcal{F}(\psi_\lambda\rangle)$
Coherent state $[\otimes_n \hat{D}_{\hat{a}_n}(\alpha_n)] 0\rangle$	$(4\bar{g}^2 + 4\Delta g^2)N_S$
Single-mode squeezed state $\hat{S}_{\hat{e}_i} 0\rangle$	$(8\bar{g}^2 + 0\Delta g^2)N_S^2 + O(N_S)$
Derivative mode state Eq. (69)	$(2\bar{g}^2 + 4\Delta g^2)N_S^2 + O(N_S)$
Variance-optimal state Eq. (40)	$(4\bar{g}^2 + 4\Delta g^2)N_S^2 + O(N_S)$
Optimal state in Eq. (34)	$(8\bar{g}^2 + 4\Delta g^2)N_S^2 + O(N_S)$

TABLE I. Quantum Fisher Information (QFI) for mode parameter estimation with various quantum states. The definition of the various types of optimality are given in Sec. III.2.

constant level resources, for non-Gaussian states, is a natural step as investigated in [9, 69]. The difficulty that seems to arise however, is that for such a state, the modal and particle-number statistics can be intertwined [9], which renders more difficult the resource comparison. On the other hand, from a foundational perspective, an important question would concern the role of superselection rules in setting the ultimate limits of precision [70]. Besides, the QCR bounds may not be adapted for non-Gaussian statistics in the non-asymptotic regime [71], and other bounds were developed [72]. Then, the other perspectives are to determine the optimal strategies for the loss and noise regime encountered in realistic lidar and radar scenarios [24–29, 49, 73], where thermal noise is expected to degrade mode parameter estimation below the Heisenberg limit while potentially preserving a constant-factor quantum advantage over the shot-noise scaling. Finally, our formalism can be applied across a wide range of experimental scenarios, from estimating parameter-shift mode transformations like time and frequency shifts to analyzing nonlinear phase effects that arise in dispersive propagation, diffraction, or even reflection from accelerating or time-varying surfaces.

ACKNOWLEDGMENT

M. R. acknowledges insightful discussions with Francesco Albarelli. M. R. acknowledges support from UPV/EHU Ph.D. Grant No. PIF21/289. M. S. and M. R. acknowledge support from HORIZON-CL4-2022-QUANTUM01-SGA project 101113946 OpenSuperQ-Plus100 of the EU Flagship on Quantum Technologies, the Spanish Ramon y Cajal Grant RYC-2020-030503-I, and the ‘‘Generaci3n de Conocimiento’’ project Grant No. PID2024-156808NB-I00 funded by MICIU/AEI/10.13039/501100011033, by ‘‘ERDF Invest in your Future’’ and by FEDER EU. We also acknowledge support from the Basque Government through Grants No. IT1470-22, the Elkartek project KUBIBIT -kuantikaren berrikuntzarako ibilbide teknologikoak (ELKARTEK25/79) and from the IKUR Strategy under the collaboration agreement between Ikerbasque Foundation and BCAM on behalf of the Department of Education of the Basque Government. This work has also been partially supported by the Ministry for Digital Transformation and the Civil Service of the Spanish Government through the QUANTUM ENIA project call – Quantum Spain project, and by the European Union through the Recovery, Transformation

Appendix A: Mode transformation

1. The mode transform and different bases

Let us summarize the different mode bases used in this manuscript and the most important relations for the calculations that follow.

Throughout the manuscript, $\{\hat{a}_n\}_n$ denotes an arbitrary mode basis. The mode basis $\{\hat{c}_n\}_n$, defined by $\hat{c}_n = \hat{V}\hat{a}_n\hat{V}^\dagger$, is the special basis in which the squeezing matrix — and correspondingly the covariance matrix (Appendix A3) — is diagonal. Equivalently, a multimode squeezed vacuum state expressed in this basis factorizes as a tensor product of single-mode squeezed vacuum states.

The action of \hat{V} on $\{\hat{a}_n\}_n$ is given by the transformation rules:

$$\hat{V}^\dagger \hat{a}_n \hat{V} = \sum_{i=1}^M V_{ni} \hat{a}_i, \quad (\text{A1})$$

$$\hat{V}^\dagger \hat{a}_n^\dagger \hat{V} = \sum_{i=1}^M V_{ni}^* \hat{a}_i^\dagger, \quad (\text{A2})$$

$$\hat{V} \hat{a}_j \hat{V}^\dagger = \sum_{n=1}^M (V^\dagger)_{jn} \hat{a}_n = \sum_{n=1}^M V_{nj}^* \hat{a}_n, \quad (\text{A3})$$

$$\hat{V} \hat{a}_j^\dagger \hat{V}^\dagger = \sum_{n=1}^M (V^\dagger)_{jn}^* \hat{a}_n^\dagger = \sum_{n=1}^M V_{nj} \hat{a}_n^\dagger, \quad (\text{A4})$$

where V_{nm} are the elements of the corresponding $M \times M$ unitary matrix V . Analogous relations hold for \hat{U}_λ : $\hat{U}_\lambda^\dagger \hat{a}_n \hat{U}_\lambda = \sum_{i=1}^M U_{ni}(\lambda) \hat{a}_i$. We also define $\hat{a}_n(\lambda) := \hat{U}_\lambda \hat{a}_n \hat{U}_\lambda^\dagger$.

The generator \hat{G} of the unitary mode transformation $\hat{U}_\lambda = e^{-i\lambda\hat{G}}$ can be expressed in any mode basis. In the bases $\{\hat{a}_n\}_n$ and $\{\hat{c}_n\}_n$ it reads

$$\hat{G} = \sum_{n,m=1}^M G_{nm} \hat{a}_n^\dagger \hat{a}_m = \sum_{i,j=1}^M \tilde{G}_{ij} \hat{c}_i^\dagger \hat{c}_j, \quad (\text{A5})$$

where $\tilde{G}_{ij} = (V^\dagger G V)_{ij}$, obtained by applying Eqs. (A1)–(A2) together with $\hat{c}_n = \hat{V}\hat{a}_n\hat{V}^\dagger$. The generator matrix G is Hermitian and therefore diagonalizable, so it is always possible to find a mode basis $\{\hat{b}_i\}_i$, defined by $\hat{b}_i = \hat{B}\hat{a}_i\hat{B}^\dagger$, in which the generator takes the diagonal form

$$\hat{G} = \sum_{i=1}^M g_i \hat{b}_i^\dagger \hat{b}_i, \quad (\text{A6})$$

where $\{g_1, \dots, g_M\}$ are the real eigenvalues of G , ordered without loss of generality as $g_1 \leq g_2 \leq \dots \leq g_M$. The mode transformation \hat{B} acts on the basis $\{\hat{a}_n\}_n$ as

$$\hat{B} \hat{a}_n \hat{B}^\dagger = \sum_{i=1}^M (B^\dagger)_{ni} \hat{a}_i, \quad (\text{A7})$$

where B_{ij} are the elements of a $M \times M$ unitary matrix B , and one has $G = B \text{diag}(g_1, \dots, g_M) B^\dagger$.

2. Bringing Gaussian states into disentangled form

We stated in the main text that any pure Gaussian state can be written in the product form of Eq. (6), that we will now show. A singular value decomposition of the complex symmetric squeezing matrix f appearing in Eq. (5) takes the general form

$$f = V_L D V_R^\dagger, \quad (\text{A8})$$

Basis	Notation	Property	Relation
Arbitrary mode basis	$\{\hat{a}_n\}_n$	-	-
Generator Diagonalizing basis	$\{\hat{b}_n\}_n$	$\hat{G} = \sum_{n=1}^M g_n \hat{b}_n^\dagger \hat{b}_n$	$\hat{b}_n = \hat{B} \hat{a}_n \hat{B}^\dagger$
Schmidt/Takagi basis	$\{\hat{c}_n\}_n$	$\hat{S} = [\otimes_{n=1}^M \hat{S}_{\hat{c}_n}(r_n)]$	$\hat{c}_n = \hat{V} \hat{a}_n \hat{V}^\dagger$

TABLE II. The three mode bases that are used in this manuscript in the discrete and finite mode setting.

where D is a diagonal matrix with non-negative entries and V_L, V_R are unitary matrices. Since f is symmetric, i.e., $f = f^T$, the decomposition specializes to

$$f = V D V^T, \quad (\text{A9})$$

known as the Takagi factorization, with components $f_{nm} = \sum_{j=1}^M V_{nj} r_j V_{mj}$.

Consider the multimode squeezing operator. Substituting the Takagi factorization and regrouping terms gives

$$\begin{aligned} & \exp\left(\frac{1}{2} \sum_{n,m=1}^M f_{nm} \hat{a}_n^\dagger \hat{a}_m^\dagger + \text{h.c.}\right) \\ &= \exp\left(\frac{1}{2} \sum_{n,m=1}^M \sum_{j=1}^M V_{nj} r_j V_{mj} \hat{a}_n^\dagger \hat{a}_m^\dagger + \text{h.c.}\right) \end{aligned} \quad (\text{A10})$$

$$= \exp\left(\frac{1}{2} \sum_{j=1}^M r_j \left(\sum_{n=1}^M V_{nj} \hat{a}_n^\dagger\right) \left(\sum_{m=1}^M V_{mj} \hat{a}_m^\dagger\right) + \text{h.c.}\right) \quad (\text{A11})$$

$$= \exp\left(\frac{1}{2} \sum_{j=1}^M r_j (\hat{c}_j^\dagger)^2 + \text{h.c.}\right), \quad (\text{A12})$$

where we defined $\hat{c}_j := \hat{V} \hat{a}_j \hat{V}^\dagger$ as the new mode basis, and used $\sum_{n=1}^M V_{nj} \hat{a}_n^\dagger = \hat{V} \hat{a}_j^\dagger \hat{V}^\dagger = \hat{c}_j^\dagger$.

The displacement operator can likewise be rewritten in the $\{\hat{c}_j\}_j$ basis. Using $\hat{a}_n^\dagger = \sum_{j=1}^M V_{nj}^* \hat{c}_j^\dagger$, which follows from Eq. (A2), one obtains

$$\exp\left(\sum_{n=1}^M \beta_n \hat{a}_n^\dagger - \text{h.c.}\right) = \exp\left(\sum_{n=1}^M \beta_n \sum_{j=1}^M V_{nj}^* \hat{c}_j^\dagger - \text{h.c.}\right) \quad (\text{A13})$$

$$= \exp\left(\sum_{j=1}^M \alpha_j \hat{c}_j^\dagger - \text{h.c.}\right), \quad (\text{A14})$$

with $\alpha_j = \sum_{n=1}^M (V^\dagger)_{jn} \beta_n$.

Combining these results, the state in Eq. (5) becomes

$$|\psi\rangle = \exp\left(\sum_{j=1}^M \alpha_j \hat{c}_j^\dagger - \text{h.c.}\right) \exp\left(\frac{1}{2} \sum_{j=1}^M r_j (\hat{c}_j^\dagger)^2 - \text{h.c.}\right) |0\rangle = \bigotimes_{j=1}^M \hat{D}_{\hat{c}_j}(\alpha_j) \hat{S}_{\hat{c}_j}(r_j) |0\rangle, \quad (\text{A15})$$

which, expressed back in the original mode basis $\{\hat{a}_n\}_n$, reads

$$|\psi\rangle = \hat{V} \left[\bigotimes_{j=1}^M \hat{D}_{\hat{a}_j}(\alpha_j) \hat{S}_{\hat{a}_j}(r_j) \right] |0\rangle. \quad (\text{A16})$$

3. Relating the squeezing matrix to the covariance matrix

Here, we will relate the squeezing matrix f to the more common covariance matrix Σ that one encounters when working with quadrature operators

$$\hat{q}_n = \frac{\hat{c}_n + \hat{c}_n^\dagger}{\sqrt{2}}, \quad \hat{p}_n = \frac{\hat{c}_n^\dagger - \hat{c}_n}{\sqrt{2}i} \quad (\text{A17})$$

instead of annihilation \hat{c}_n and creation \hat{c}_n^\dagger operators. Note that here we work with $\{\hat{c}_n\}_n$ (with $\hat{c}_n = \hat{V}\hat{a}_n\hat{V}^\dagger$) as in this basis the covariance takes on a simple diagonal form. The quadrature operators satisfy the commutation relation $[\hat{x}_n, \hat{p}_m] = \hbar i\delta_{nm}$. Let us introduce

$$\hat{\mathbf{r}} = (\hat{x}_1, \hat{p}_1, \hat{x}_2, \hat{p}_2, \dots, \hat{x}_M, \hat{p}_M)^T. \quad (\text{A18})$$

The components of the $2M \times 2M$ covariance matrix are defined as

$$\Sigma_{kl} = \text{tr}[|\psi\rangle\langle\psi|\{(\hat{r}_k - \langle\hat{r}_k\rangle), (\hat{r}_l - \langle\hat{r}_l\rangle)\}] \quad (\text{A19})$$

where $\{\hat{A}, \hat{B}\} = AB + BA$.

Now, consider a general pure Gaussian state

$$|\psi\rangle = \hat{V} \left[\otimes_{n=1}^M \hat{D}_{\hat{a}_n}(\alpha_n) \hat{S}_{\hat{a}_n}(r_n) \right] |0\rangle \quad (\text{A20})$$

$$= \left[\otimes_{n=1}^M \hat{D}_{\hat{V}\hat{a}_n\hat{V}^\dagger}(\alpha_n) \hat{S}_{\hat{V}\hat{a}_n\hat{V}^\dagger}(r_n) \right] |0\rangle \quad (\text{A21})$$

$$= \left[\otimes_{n=1}^M \hat{D}_{\hat{c}_n}(\alpha_n) \hat{S}_{\hat{c}_n}(r_n) \right] |0\rangle. \quad (\text{A22})$$

The associated $M \times M$ squeezing matrix expressed in the $\{\hat{c}_n\}_n$ mode basis is

$$f = \text{diag}(r_1, r_2, \dots, r_M) \quad (\text{A23})$$

The $2M \times 2M$ covariance matrix expressed in the $\{\hat{c}_n\}_n$ mode basis

$$\Sigma = \bigoplus_{n=1}^M \begin{pmatrix} e^{+2r_n} & 0 \\ 0 & e^{-2r_n} \end{pmatrix}. \quad (\text{A24})$$

Note that our squeezing operators and the mode basis $\{\hat{c}_n\}_n$ are defined in such a way that the p quadratures are squeezed while the q quadratures are anti-squeezed.

Appendix B: QFI of a multi-mode Gaussian quantum state subject to a mode transform

In what follows and generally throughout all the manuscript, all sums run from 1 to M if not explicitly indicated otherwise.

1. The general case

The derivative of a mode transform is given by

$$\partial_\lambda \hat{U}_\lambda = \partial_\lambda e^{-i\lambda\hat{G}} = -i\hat{U}_\lambda \hat{G}. \quad (\text{B1})$$

Let us continue examining the derivative of the state and simplify it

$$i|\partial_\lambda\psi_\lambda\rangle = \hat{U}_\lambda\hat{G}|\psi\rangle = \hat{U}_\lambda\hat{G}\hat{V}\hat{D}\hat{S}|0\rangle = \hat{U}_\lambda\hat{V}\hat{V}^\dagger\hat{G}\hat{V}\hat{D}\hat{S}|0\rangle \quad (\text{B2})$$

$$= \hat{U}_\lambda\hat{V}\sum_{nm}G_{nm}\hat{V}^\dagger\hat{a}_n^\dagger\hat{V}\hat{V}^\dagger\hat{a}_m\hat{V}\hat{D}\hat{S}|0\rangle \quad (\text{B3})$$

$$= \hat{U}_\lambda\hat{V}\sum_{ij}\sum_{nm}V_{ni}^*G_{nm}(\lambda)V_{mj}\hat{a}_i^\dagger\hat{a}_j\hat{D}\hat{S}|0\rangle \quad (\text{B4})$$

$$= \hat{U}_\lambda\hat{V}\sum_{ij}\tilde{G}_{ij}\hat{a}_i^\dagger\hat{a}_j\hat{D}\hat{S}|0\rangle \quad (\text{B5})$$

$$= \hat{U}_\lambda\hat{V}\hat{D}\sum_{ij}\tilde{G}_{ij}\hat{D}^\dagger\hat{a}_i^\dagger\hat{D}\hat{D}^\dagger\hat{a}_j\hat{D}\hat{S}|0\rangle \quad (\text{B6})$$

$$= \hat{U}_\lambda\hat{V}\hat{D}\sum_{ij}\tilde{G}_{ij}(\hat{a}_i^\dagger + \alpha_i^*)(\hat{a}_j + \alpha_j)\hat{S}|0\rangle \quad (\text{B7})$$

$$= \hat{U}_\lambda\hat{V}\hat{D}\sum_{ij}\tilde{G}_{ij}(\hat{a}_i^\dagger\hat{a}_j + \hat{a}_j\alpha_i^* + \hat{a}_i^\dagger\alpha_j + \alpha_i^*\alpha_j)\hat{S}|0\rangle \quad (\text{B8})$$

$$= \hat{U}_\lambda\hat{V}\hat{D}\hat{S}\sum_{ij}\tilde{G}_{ij}(\hat{S}^\dagger\hat{a}_i^\dagger\hat{S}\hat{S}^\dagger\hat{a}_j\hat{S} + \hat{S}^\dagger\hat{a}_j\hat{S}\alpha_i^* + \hat{S}^\dagger\hat{a}_i^\dagger\hat{S}\alpha_j + \alpha_i^*\alpha_j)|0\rangle \quad (\text{B9})$$

$$= \hat{U}_\lambda\hat{V}\hat{D}\hat{S}\sum_{ij}\tilde{G}_{ij}\left([c_i\hat{a}_i^\dagger + s_i\hat{a}_i][c_j\hat{a}_j + s_j\hat{a}_j^\dagger] \right. \quad (\text{B10})$$

$$\left. + [c_j\hat{a}_j + s_j\hat{a}_j^\dagger]\alpha_i^* + [c_i\hat{a}_i^\dagger + s_i\hat{a}_i]\alpha_j + \alpha_i^*\alpha_j\right)|0\rangle, \quad (\text{B11})$$

where we have used $\hat{V}^\dagger a_m \hat{V} = \sum_j V_{mj} \hat{a}_j$ in the third line, in the fourth line we denoted the Hermitian matrix $\tilde{G}_{ij} = \sum_{nm} V_{ni}^* G_{nm} V_{mj} = (V^\dagger G V)_{ij}$, in the sixth line we used $\hat{D}^\dagger \hat{a}_j \hat{D} = \hat{a}_j + \alpha_j$, and in the 9th and 10th lines we used $\hat{S}^\dagger \hat{a}_j \hat{S} = c_j \hat{a}_j + s_j \hat{a}_j^\dagger$, where we used the shorthand notation $c_j := \cosh(r_j)$ and $s_j := \sinh(r_j)$. Now we can further simplify this by using $\hat{a}_i|0\rangle = 0$ and $\hat{a}_i \hat{a}_j^\dagger|0\rangle = \delta_{ij}|0\rangle$, and we obtain

$$|\partial_\lambda\psi\rangle = -i\hat{U}_\lambda\hat{V}\hat{D}\hat{S}\sum_{ij}\tilde{G}_{ij}\left[c_i s_j \hat{a}_i^\dagger \hat{a}_j^\dagger|0\rangle + (s_j \alpha_i^* \hat{a}_j^\dagger + c_i \alpha_j \hat{a}_i^\dagger)|0\rangle + (s_i s_j \delta_{ij} + \alpha_i^* \alpha_j)|0\rangle\right] \quad (\text{B12})$$

$$=: |\partial_\lambda\psi\rangle_2 + |\partial_\lambda\psi\rangle_1 + |\partial_\lambda\psi\rangle_0. \quad (\text{B13})$$

The derivative state is now in a form such that all Gaussian operators are on the left side. We see that the derivative states split up into three different components, a two-photon, one-photon, and zero-photon component. We can examine these individually due to $\langle\partial_\lambda\psi|\partial_\lambda\psi_\lambda\rangle = {}_2\langle\partial_\lambda\psi|\partial_\lambda\psi_\lambda\rangle_2 + {}_1\langle\partial_\lambda\psi|\partial_\lambda\psi_\lambda\rangle_1 + {}_0\langle\partial_\lambda\psi|\partial_\lambda\psi_\lambda\rangle_0$.

So, let us start with the two-photon term:

$${}_2\langle\partial_\lambda\psi|\partial_\lambda\psi_\lambda\rangle_2 = \sum_{i',j',i,j}\tilde{G}_{j'i'}^*\tilde{G}_{ij}c_{i'}s_{j'}c_i s_j\langle 0|\hat{a}_{i'}\hat{a}_{j'}\hat{a}_i^\dagger\hat{a}_j^\dagger|0\rangle \quad (\text{B14})$$

$$= \sum_{ij}\tilde{G}_{ji}^*\tilde{G}_{ij}c_j s_i c_i s_j + \sum_{ij}\tilde{G}_{ij}^*\tilde{G}_{ij}c_i s_j c_i s_j \quad (\text{B15})$$

$$= \sum_{ij}s_i\tilde{G}_{ij}c_j s_j\tilde{G}_{ji}^*c_i + \sum_{ij}c_i\tilde{G}_{ij}s_j s_j\tilde{G}_{ji}c_i, \quad (\text{B16})$$

where we used $\langle 0|\hat{a}_{i'}\hat{a}_{j'}\hat{a}_i^\dagger\hat{a}_j^\dagger|0\rangle = \delta_{i',j}\delta_{j',i} + \delta_{i',i}\delta_{j',j}$

Now, we come to the one-photon term

$$|\partial_\lambda\psi_\lambda\rangle_1 = -i\hat{U}_\lambda\hat{V}\hat{D}\hat{S}\sum_{ij}\left[\tilde{G}_{ij}s_j\alpha_i^*\hat{a}_j^\dagger + \tilde{G}_{ij}c_i\alpha_j\hat{a}_i^\dagger\right]|0\rangle \quad (\text{B17})$$

$$= -i\hat{U}_\lambda\hat{V}\hat{D}\hat{S}\sum_{ij}\left[\tilde{G}_{ij}s_j\alpha_i^* + \tilde{G}_{ji}c_j\alpha_i\right]\hat{a}_j^\dagger|0\rangle \quad (\text{B18})$$

$$=: -i\hat{U}_\lambda\hat{V}\hat{D}\hat{S}\sum_{ij}F_{ij}\hat{a}_j^\dagger|0\rangle, \quad (\text{B19})$$

where we defined $F_{ij} = \tilde{G}_{ij}s_j\alpha_i^* + \tilde{G}_{ji}c_j\alpha_i$. With this, we find

$${}_1\langle\partial_\lambda\psi|\partial_\lambda\psi_\lambda\rangle_1 = \sum_{i'j'ij} F_{i'j'}^* F_{ij} \langle 0|\hat{a}_{j'}\hat{a}_j^\dagger|0\rangle \quad (\text{B20})$$

$$= \sum_{i'ij} F_{i'j}^* F_{ij} \quad (\text{B21})$$

$$= \sum_{i'ij} \left(\tilde{G}_{i'j}^* s_j \alpha_{i'} + \tilde{G}_{ji'}^* c_j \alpha_{i'}^* \right) \left(\tilde{G}_{ij} s_j \alpha_i^* + \tilde{G}_{ji} c_j \alpha_i \right) \quad (\text{B22})$$

$$= \sum_{i'ij} \left[\alpha_i^* \tilde{G}_{ij} s_j s_j \tilde{G}_{j'i'} \alpha_{i'} + \alpha_{i'}^* \tilde{G}_{i'j} c_j c_j \tilde{G}_{ji} \alpha_i \right. \quad (\text{B23})$$

$$\left. + \alpha_{i'}^* \tilde{G}_{i'j} c_j s_j \tilde{G}_{ji}^* \alpha_i^* + \alpha_{i'} \tilde{G}_{i'j} s_j c_j \tilde{G}_{ji} \alpha_i \right]. \quad (\text{B24})$$

For the zero-photon term we find

$${}_0\langle\partial_\lambda\psi|\partial_\lambda\psi_\lambda\rangle_0 = \sum_{i'j'} \tilde{G}_{i'j'}^* (s_{i'} s_{j'} \delta_{i'j'} + \alpha_{i'} \alpha_{j'}^*) \sum_{ij} \tilde{G}_{ij} (s_i s_j \delta_{ij} + \alpha_i^* \alpha_j) \quad (\text{B25})$$

$$= |\langle\psi_\lambda|\partial_\lambda\psi_\lambda\rangle|^2. \quad (\text{B26})$$

Now, by adding all of these terms together, we obtain the QFI. We have

$$\mathcal{F}(|\psi_\lambda\rangle) = 4 \left(\langle\partial_\lambda\psi_\lambda|\partial_\lambda\psi_\lambda\rangle - |\langle\psi_\lambda|\partial_\lambda\psi_\lambda\rangle|^2 \right) \quad (\text{B27})$$

$$= 4 \left({}_2\langle\partial_\lambda\psi|\partial_\lambda\psi_\lambda\rangle_2 + {}_1\langle\partial_\lambda\psi|\partial_\lambda\psi_\lambda\rangle_1 + {}_0\langle\partial_\lambda\psi|\partial_\lambda\psi_\lambda\rangle_0 - |\langle\psi_\lambda|\partial_\lambda\psi_\lambda\rangle|^2 \right) \quad (\text{B28})$$

$$= 4 \left({}_2\langle\partial_\lambda\psi|\partial_\lambda\psi_\lambda\rangle_2 + {}_1\langle\partial_\lambda\psi|\partial_\lambda\psi_\lambda\rangle_1 \right). \quad (\text{B29})$$

Plugging in the expressions from above, we obtain Eq. (17) of the main text for the QFI.

$$\mathcal{F}(|\psi_\lambda\rangle) = 4 \sum_{ij} \tilde{G}_{ij} c_j s_j \tilde{G}_{ji}^* c_i s_i + 4 \sum_{ij} \tilde{G}_{ij} s_j s_j \tilde{G}_{ji} c_i c_i \quad (\text{B30})$$

$$+ \sum_{i'ij} 4 \left[\tilde{G}_{ij} s_j s_j \tilde{G}_{j'i'} \alpha_{i'} \alpha_i^* + \tilde{G}_{i'j} c_j c_j \tilde{G}_{ji} \alpha_i \alpha_{i'}^* \right. \quad (\text{B31})$$

$$\left. + \tilde{G}_{i'j} c_j s_j \tilde{G}_{ji}^* \alpha_i^* \alpha_{i'} + \tilde{G}_{i'j} s_j c_j \tilde{G}_{ji} \alpha_i \alpha_{i'} \right]. \quad (\text{B32})$$

The QFI in this form is quite cumbersome, and it is useful to introduce some new notation. We define the matrices $C = \text{diag}(c_1, \dots, c_M)$, $S = \text{diag}(s_1, \dots, s_M)$, and the $M \times M$ matrix \mathcal{A} with components $\mathcal{A}_{ij} = \alpha_i \alpha_j^*$ and $\mathcal{B}_{ij} = \alpha_i \alpha_j$. Also note that $\tilde{G} = V^\dagger G V$. The QFI then takes the form

$$\mathcal{F}(|\psi_\lambda\rangle) = 4 \left(\text{Tr}[\tilde{G} C S \tilde{G}^* C S] + \text{Tr}[\tilde{G} S^2 \tilde{G} C^2] \right. \quad (\text{B33})$$

$$\left. + \text{Tr}[\tilde{G} S^2 \tilde{G} \mathcal{A}] + \text{Tr}[\tilde{G} C^2 \tilde{G} \mathcal{A}] + \text{Tr}[\tilde{G} C S \tilde{G}^* \mathcal{B}^*] + \text{Tr}[\tilde{G}^* S C \tilde{G} \mathcal{B}] \right) \quad (\text{B34})$$

$$= 4 \left(\text{Tr}[\tilde{G} C S \tilde{G}^* C S] + \text{Tr}[\tilde{G} S^2 \tilde{G} C^2] + \text{Tr}[\tilde{G} (S^2 + C^2) \tilde{G} \mathcal{A}] + 2 \text{Re} [\text{Tr}[\tilde{G}^* S C \tilde{G} \mathcal{B}]] \right). \quad (\text{B35})$$

This can be seen by using the following relation

$$\text{tr}[ABCDEF] = \sum_a (ABCDEF)_{aa} = \sum_{a,b,c,d,e,f} A_{ab} B_{bc} C_{cd} D_{de} E_{ef} F_{fa} \quad (\text{B36})$$

for some arbitrary $M \times M$ matrices A, B, C, D, E, F . If B, C, E, F are diagonal, we have

$$\text{tr}[ABCDEF] = \sum_{a,b,c,d,e,f} A_{ab}B_{bc}\delta_{bc}C_{cd}\delta_{cd}D_{de}E_{ef}\delta_{ef}F_{fa}\delta_{fa} \quad (\text{B37})$$

$$= \sum_{a,b,d,e,f} A_{ab}B_{bb}C_{bd}\delta_{bd}D_{de}E_{ef}\delta_{ef}F_{fa}\delta_{fa} \quad (\text{B38})$$

$$= \sum_{a,b,e,f} A_{ab}B_{bb}C_{bb}D_{be}E_{ef}\delta_{ef}F_{fa}\delta_{fa} \quad (\text{B39})$$

$$= \sum_{a,b,e} A_{ab}B_{bb}C_{bb}D_{be}E_{ee}F_{ea}\delta_{ea} \quad (\text{B40})$$

$$= \sum_{a,b} A_{ab}B_{bb}C_{bb}D_{ba}E_{aa}F_{aa}. \quad (\text{B41})$$

With this we confirm the validity of the first two terms in Eq. (B33).

For the last four terms, we consider

$$\text{tr}[ABCDE] = \sum_a (ABCDE)_{aa} = \sum_{a,b,c,d,e} A_{ab}B_{bc}C_{cd}D_{de}E_{ea} \quad (\text{B42})$$

Now, if B, C are diagonal, we have

$$\text{tr}[ABCDE] = \sum_{a,b,c,d,e} A_{ab}B_{bc}\delta_{bc}C_{cd}\delta_{cd}D_{de}E_{ea} \quad (\text{B43})$$

$$= \sum_{a,b,d,e} A_{ab}B_{bb}C_{bd}\delta_{bd}D_{de}E_{ea} \quad (\text{B44})$$

$$= \sum_{a,b,e} A_{ab}B_{bb}C_{bb}D_{be}E_{ea}. \quad (\text{B45})$$

With this, we confirm the four terms in Eq. (B34).

As we will later see, bringing the QFI into this form will be helpful for proving our main result.

2. QFI of a coherent state

As in the main text, the QFI of the coherent state is

$$\mathcal{F}(|\psi^{\text{coh}}\rangle) = 4 \sum_{i'ij} \alpha_{i'}^* \tilde{G}_{i'j} \tilde{G}_{ji} \alpha_i = 4 \alpha^\dagger \tilde{G}^2 \alpha = 4 \alpha^\dagger W^\dagger D^2 W \alpha = 4 \sum_n D_{nn}^2 |(W\alpha)_n|^2. \quad (\text{B46})$$

Now, $W = B^\dagger V$ is the unitary that diagonalizes \tilde{G} (and also \tilde{G}^2). Recall that $G = BDB^\dagger$.

$$|(W\alpha)_n|^2 = \sum_{ij} W_{nj}^* W_{ni} \alpha_j^* \alpha_i = \sum_{ij} W_{nj}^* W_{ni} \langle \psi^{\text{coh}} | \hat{V} \hat{a}_j^\dagger \hat{a}_i \hat{V}^\dagger | \psi^{\text{coh}} \rangle \quad (\text{B47})$$

$$= \sum_{ij} W_{nj}^* W_{ni} \langle \psi^{\text{coh}} | \hat{V} \hat{a}_j^\dagger \hat{V}^\dagger \hat{V} \hat{a}_i \hat{V}^\dagger | \psi^{\text{coh}} \rangle = \sum_{ij} W_{nj}^* W_{ni} \langle \psi^{\text{coh}} | \sum_q V_{qj} \hat{a}_q^\dagger \sum_r V_{ri}^* \hat{a}_r | \psi^{\text{coh}} \rangle \quad (\text{B48})$$

$$= \sum_{ijqr} V_{qj} W_{nj}^* W_{ni} V_{ri}^* \langle \psi^{\text{coh}} | \hat{a}_q^\dagger \hat{a}_r | \psi^{\text{coh}} \rangle = \sum_{qr} \left(\sum_j V_{qj} (W^\dagger)_{jn} \right) \left(\sum_i W_{ni} (V^\dagger)_{ir} \right) \langle \psi^{\text{coh}} | \hat{a}_q^\dagger \hat{a}_r | \psi^{\text{coh}} \rangle \quad (\text{B49})$$

$$= \sum_{qr} (V(B^\dagger V)^\dagger)_{qn} (B^\dagger V V^\dagger)_{nr} \langle \psi^{\text{coh}} | \hat{a}_q^\dagger \hat{a}_r | \psi^{\text{coh}} \rangle = \langle \psi^{\text{coh}} | \left(\sum_q B_{qn} \hat{a}_q^\dagger \right) \left(\sum_r B_{nr}^\dagger \hat{a}_r \right) | \psi^{\text{coh}} \rangle \quad (\text{B50})$$

$$= \langle \psi^{\text{coh}} | \hat{b}_n^\dagger \hat{b}_n | \psi^{\text{coh}} \rangle. \quad (\text{B51})$$

In the first line we used $\alpha_j \alpha_i = \langle \psi^{\text{coh}} | \hat{V} \hat{a}_j^\dagger \hat{a}_i \hat{V}^\dagger | \psi^{\text{coh}} \rangle$, recall that $|\psi^{\text{coh}}\rangle = \hat{V}[\otimes_i \hat{D}_{\hat{a}_i}(\alpha_i)]|0\rangle$. In the second line we used Eq. (A3) and Eq. (A4). In the fourth line we used $W = B^\dagger V$.

From this follows

$$\mathcal{F}(|\psi^{\text{coh}}\rangle) = 4 \sum_n D_{nn}^2 |(W\alpha)_n|^2 \quad (\text{B52})$$

$$= 4 \sum_n g_n^2 \langle \psi^{\text{coh}} | \hat{b}_n^\dagger \hat{b}_n | \psi^{\text{coh}} \rangle. \quad (\text{B53})$$

Appendix C: Resources

In the main text we have given the definition of the resources in terms of the intensity I_n . It will prove useful to express the resources in a basis independent way.

Let us first start with the signal photon number

$$N_S = \sum_{i \in \mathcal{I}_S} \langle \hat{b}_i^\dagger \hat{b}_i \rangle = \sum_{n,m} \sum_{i \in \mathcal{I}_S} (B^\dagger)_{in}^* (B^\dagger)_{im} \langle \hat{a}_n^\dagger \hat{a}_m \rangle \quad (\text{C1})$$

$$= \sum_{n,m} \sum_{i \in \mathcal{I}_S} B_{ni} (B^\dagger)_{im} \langle \hat{a}_n^\dagger \hat{a}_m \rangle \quad (\text{C2})$$

$$= \sum_{n,m} (P_S)_{nm} \langle 0 | \hat{S}^\dagger \hat{D}^\dagger \hat{V}^\dagger \hat{a}_n^\dagger \hat{a}_m \hat{V} \hat{D} \hat{S} | 0 \rangle \quad (\text{C3})$$

$$= \sum_{n,m} (V^\dagger P_S V)_{nm} \langle 0 | \hat{S}^\dagger \hat{D}^\dagger \hat{a}_n^\dagger \hat{a}_m \hat{D} \hat{S} | 0 \rangle \quad (\text{C4})$$

$$= \sum_{n,m} (\tilde{P}_S)_{nm} \left(s_n^2 \delta_{nm} + \alpha_m \alpha_n^* \right) \quad (\text{C5})$$

$$= \text{Tr}[\tilde{P}_S (S^2 + \mathcal{A})] \quad (\text{C6})$$

$$= \text{Tr}[\tilde{P}_S (S^2 + \mathcal{A}) \tilde{P}_S]. \quad (\text{C7})$$

In the third line we defined the projector onto the eigenspace of G with non-zero eigenvalues $P_S = \sum_{i \in \mathcal{I}_S} B_{ni} (B^\dagger)_{im} = \sum_{i,j} B_{ni} \chi_{\mathcal{I}_S}(i) \delta_{ij} (B^\dagger)_{im}$, where $\chi_{\mathcal{I}_S}(i) = 1$ if $i \in \mathcal{I}_S$ and 0 otherwise. That is $P_S G = G P_S = P_S G P_S = G$. In the fourth line, we defined $\tilde{P}_S = V^\dagger P_S V$, which is the projector onto the eigenspace of \tilde{G} with non-zero eigenvalues. We have $\tilde{P}_S \tilde{G} = \tilde{G} \tilde{P}_S = \tilde{P}_S \tilde{G} \tilde{P}_S = \tilde{G}$.

For the mean resource \bar{g} , we have

$$\bar{g} \cdot N_S = \sum_{i \in \mathcal{I}_S} g_i \langle \hat{b}_i^\dagger \hat{b}_i \rangle \quad (\text{C8})$$

$$= \sum_i g_i \langle \hat{b}_i^\dagger \hat{b}_i \rangle \quad (\text{C9})$$

$$= \sum_{n,m} G_{nm} \langle \hat{a}_n^\dagger \hat{a}_m \rangle = \sum_{n,m} G_{nm} \langle 0 | \hat{S}^\dagger \hat{D}^\dagger \hat{V}^\dagger \hat{a}_n^\dagger \hat{a}_m \hat{V} \hat{D} \hat{S} | 0 \rangle \quad (\text{C10})$$

$$= \sum_{nm} (V^\dagger G V)_{nm} \langle 0 | \hat{S}^\dagger \hat{D}^\dagger \hat{a}_n^\dagger \hat{a}_m \hat{D} \hat{S} | 0 \rangle \quad (\text{C11})$$

$$= \sum_{nm} \tilde{G}_{nm} \left(s_n^2 \delta_{nm} + \alpha_n^* \alpha_m \right) \quad (\text{C12})$$

$$= \text{Tr}[\tilde{G} (S^2 + \mathcal{A})] \quad (\text{C13})$$

and thus

$$\bar{g} = \frac{\text{Tr}[\tilde{G} (S^2 + \mathcal{A})]}{N_S}. \quad (\text{C14})$$

We see that this quantity only depends on how the modes are distributed, not on the total number of photons.

And finally, for the variance resource parameter \bar{g} we have

$$\left((\Delta g)^2 + \bar{g}^2\right) N_S = \sum_{i \in \mathcal{I}_S} g_i^2 \langle \hat{b}_i^\dagger \hat{b}_i \rangle \quad (\text{C15})$$

$$= \sum_i g_i^2 \langle \hat{b}_i^\dagger \hat{b}_i \rangle \quad (\text{C16})$$

$$= \sum_{n,m} (G^2)_{nm} \langle \hat{a}_n^\dagger \hat{a}_m \rangle = \sum_{n,m} (G^2)_{nm} \langle 0 | \hat{S}^\dagger \hat{D}^\dagger \hat{V}^\dagger \hat{a}_n^\dagger \hat{a}_m \hat{V} \hat{D} \hat{S} | 0 \rangle \quad (\text{C17})$$

$$= \sum_{nm} (V^\dagger G^2 V)_{nm} \langle 0 | \hat{S}^\dagger \hat{D}^\dagger \hat{a}_n^\dagger \hat{a}_m \hat{D} \hat{S} | 0 \rangle \quad (\text{C18})$$

$$= \sum_{nm} (\tilde{G}^2)_{nm} \left(s_n^2 \delta_{nm} + \alpha_n^* \alpha_m \right) \quad (\text{C19})$$

$$= \text{Tr}[\tilde{G}^2 (S^2 + \mathcal{A})]. \quad (\text{C20})$$

With this, we get

$$(\Delta g)^2 = \frac{\text{Tr}[\tilde{G}^2 (S^2 + \mathcal{A})]}{N_S} - \bar{g}^2. \quad (\text{C21})$$

Appendix D: Proof of Theorem III.1

We now prove Theorem III.1, which requires showing that $\mathcal{F}(|\psi_\lambda\rangle) \leq (8\bar{g}^2 + 4\Delta g^2) N_S^2 + O(N_S)$.

We begin by establishing two lemmas that will enable a concise proof of Theorem III.1.

Lemma D.1. *The QFI given in Eq. (19) is upper bounded by*

$$\mathcal{F}(|\psi_\lambda\rangle) \leq 4 \left(2 \text{Tr}[\tilde{G} S^2 \tilde{G} S^2] + 4 \text{Tr}[\tilde{G} S^2 \tilde{G} \mathcal{A}] \right) + O(N_S). \quad (\text{D1})$$

The proof relies on the Hermiticity of \tilde{G} and, while straightforward, is somewhat lengthy; it is provided in Appendix D 1. The purpose of this intermediate bound is to reduce the expression to one containing only two terms, which simplifies the subsequent analysis.

The second lemma is:

Lemma D.2. *The inequality*

$$0 \leq 4\text{Tr}[HQ]^2 + 4\text{Tr}[H^2Q]\text{Tr}[Q] - 8\text{Tr}[HQHQ] \quad (\text{D2})$$

holds for H Hermitian and Q Hermitian and positive semi-definite.

The proof of this lemma D.2 has been delegated to the Appendix D 2.

We are now ready to complete the proof of Theorem III.1.

Proof. We use the lemma D.2 and set $H = \tilde{G}$ and $Q = \tilde{P}_S (S + \mathcal{A}) \tilde{P}_S := S' + \mathcal{A}'$, where we denote $S' = \tilde{P}_S S \tilde{P}_S$ and $\mathcal{A}' = \tilde{P}_S \mathcal{A} \tilde{P}_S$. With this, we obtain

$$0 \leq 4\text{Tr}[HQ]^2 + 4\text{Tr}[H^2Q]\text{Tr}[Q] - 8\text{Tr}[HQHQ] \quad (\text{D3})$$

$$= 4\text{Tr}[\tilde{G}(S' + \mathcal{A}')]^2 + 4\text{Tr}[\tilde{G}^2(S' + \mathcal{A}')]\text{Tr}[S' + \mathcal{A}'] - 8\text{Tr}[\tilde{G}(S' + \mathcal{A}')\tilde{G}(S' + \mathcal{A}')] \quad (\text{D4})$$

$$= \left(8\bar{g}^2 + 4(\Delta g)^2 \right) N_S^2 - 8\text{Tr}[\tilde{G}S'\tilde{G}S'] - 2 \cdot 8\text{Tr}[\tilde{G}S'\tilde{G}\mathcal{A}'] - 8\text{Tr}[\tilde{G}\mathcal{A}'\tilde{G}\mathcal{A}'] \quad (\text{D5})$$

where in the last line we used $4\text{Tr}[\tilde{G}(S' + \mathcal{A}')]^2 = 4\text{Tr}[\tilde{G}(S + \mathcal{A})]^2 = 4\bar{g}^2 N_S^2$ and $4\text{Tr}[\tilde{G}^2(S' + \mathcal{A}')]\text{Tr}[S' + \mathcal{A}'] = 4\text{Tr}[\tilde{G}^2(S + \mathcal{A})]\text{Tr}[S + \mathcal{A}] = 4(\bar{g}^2 + (\Delta g)^2) N_S^2$, which follows from $\tilde{P}_S \tilde{G} = \tilde{G} \tilde{P}_S = \tilde{G}$. We also used in the last line $\text{Tr}[\tilde{G}(S' + \mathcal{A}')\tilde{G}(S' + \mathcal{A}')] = \text{Tr}[\tilde{G}S'\tilde{G}S'] + 2\text{Tr}[\tilde{G}S'\tilde{G}\mathcal{A}'] + \text{Tr}[\tilde{G}\mathcal{A}'\tilde{G}\mathcal{A}']$ exploiting linearity and the cyclic property of the trace. By now bringing the first two terms with the minus sign to the left side, we obtain:

$$8\text{Tr}[\tilde{G}S'\tilde{G}S'] + 2 \cdot 8\text{Tr}[\tilde{G}S'\tilde{G}\mathcal{A}'] \leq \left(8\bar{g}^2 + 4(\Delta g)^2 \right) N_S^2 - 8\text{Tr}[\tilde{G}\mathcal{A}'\tilde{G}\mathcal{A}']. \quad (\text{D6})$$

We now use the lemma D.1. For this, we add the appropriate terms of order $L := 4 \cdot 3(\bar{g}^2 + \Delta g^2)N_S - 4\text{Tr}[\tilde{G}^2 S^2]$ on both sides of Eq. (D6) and with $\text{Tr}[\tilde{G}\mathcal{A}\tilde{G}\mathcal{A}'] = \text{Tr}[\tilde{G}\mathcal{A}\tilde{G}\mathcal{A}]$, $\text{Tr}[\tilde{G}S'\tilde{G}S'] = \text{Tr}[\tilde{G}S\tilde{G}S]$ and $\text{Tr}[\tilde{G}S'\tilde{G}\mathcal{A}'] = \text{Tr}[\tilde{G}S\tilde{G}\mathcal{A}]$ we obtain:

$$8\text{Tr}[\tilde{G}S\tilde{G}S] + 2 \cdot 8\text{Tr}[\tilde{G}S\tilde{G}\mathcal{A}] + L \leq \left(8\bar{g}^2 + 4(\Delta g)^2\right) N_S^2 - 8\text{Tr}[\tilde{G}\mathcal{A}\tilde{G}\mathcal{A}] + L. \quad (\text{D7})$$

From this and lemma D.1 follows directly:

$$\mathcal{F}(|\psi_\lambda\rangle) \leq \left(8\bar{g}^2 + 4(\Delta g)^2\right) N_S^2 - 8\text{Tr}[\tilde{G}\mathcal{A}\tilde{G}\mathcal{A}] + L \quad (\text{D8})$$

$$\leq \left(8\bar{g}^2 + 4(\Delta g)^2\right) N_S^2 + L \quad (\text{D9})$$

$$= \left(8\bar{g}^2 + 4(\Delta g)^2\right) N_S^2 + 4 \cdot 3(\bar{g}^2 + \Delta g^2)N_S - 4\text{Tr}[\tilde{G}^2 S^2]. \quad (\text{D10})$$

In the last line, we used $\text{Tr}[\tilde{G}\mathcal{A}\tilde{G}\mathcal{A}] \geq 0$. This follows from the fact that \mathcal{A} is Hermitian and positive semi-definite. Therefore, $\mathcal{A}^{1/2}$ exists and is also Hermitian. Thus, we have $\text{Tr}[\mathcal{A}^{1/2}\tilde{G}\mathcal{A}^{1/2}\mathcal{A}^{1/2}\tilde{G}\mathcal{A}^{1/2}] = \text{Tr}[(\mathcal{A}^{1/2}\tilde{G}\mathcal{A}^{1/2})^2] \geq 0$. This follows from the fact that $\mathcal{A}^{1/2}\tilde{G}\mathcal{A}^{1/2}$ is Hermitian, and the trace of the square of a Hermitian matrix is always non-negative. This completes the proof. \square

An important observation is that Eq. (D8) implies that Eq. (D9) can only be attained if $\text{Tr}[\tilde{G}\mathcal{A}\tilde{G}\mathcal{A}] = 0$. While this might suggest that displacement always decreases performance, there may exist special non-zero displacement configurations for which $\text{Tr}[\tilde{G}\mathcal{A}\tilde{G}\mathcal{A}] = 0$, so that the possibility of an optimal state with non-zero displacement cannot be excluded [74]. Indeed, in Sec. E 2 b we identified a variance-optimal state that allocates half of its energy budget to displacement.

In the case of zero displacement, the bound in Eq. (D10) reduces to

$$\mathcal{F}(|\psi_\lambda\rangle) \leq \left(8\bar{g}^2 + 4(\Delta g)^2\right) N_S^2 + 8(\bar{g}^2 + \Delta g^2)N_S, \quad (\text{D11})$$

which is tight even at the level of the linear term in N_S , as can be verified by evaluating the QFI of the optimal state given in Eq. (E83). Finally, in the limit of small squeezing, a multimode squeezed vacuum state reduces to a superposition of the vacuum and a two-photon state, suggesting that the present bound may also be applicable to two-photon states — a direction worth pursuing in future work.

1. Proof of Lemma D.1

Proof. First, recall that the QFI is

$$\mathcal{F}(|\psi_\lambda\rangle) = 4 \left[\text{Tr}[\tilde{G}CS\tilde{G}^*CS] + \text{Tr}[\tilde{G}S^2\tilde{G}C^2] + \text{Tr}[\tilde{G}S^2\tilde{G}A] + \text{Tr}[\tilde{G}C^2\tilde{G}A] + \text{Tr}[\tilde{G}CS\tilde{G}^*B^*] + \text{Tr}[\tilde{G}^*SC\tilde{G}B] \right]. \quad (\text{D12})$$

We have six terms and, by bounding some of them, we derive an upper bound with only two terms quadratic in N_S . Let us start with the terms that are only due to squeezing. We have

$$\text{Tr}[\tilde{G}CS\tilde{G}^*CS] = \sum_{ij} \tilde{G}_{ij}c_j s_j \tilde{G}_{ji}^* c_i s_i = \sum_{ij} \tilde{G}_{ij}^2 c_j s_j c_i s_i \quad (\text{D13})$$

$$= \sum_i \tilde{G}_{ii}^2 a_i a_i + \sum_{i \neq j} \tilde{G}_{ij}^2 a_j a_i \quad (\text{D14})$$

$$= \sum_i \tilde{G}_{ii}^2 a_i a_i + \sum_{i < j} (\tilde{G}_{ij}^2 + \tilde{G}_{ji}^2) a_i a_j \quad (\text{D15})$$

$$= \sum_i \tilde{G}_{ii}^2 a_i a_i + \sum_{i < j} (\tilde{G}_{ij}^2 + (\tilde{G}_{ij}^2)^*) a_i a_j \quad (\text{D16})$$

$$= \sum_i \tilde{G}_{ii}^2 a_i a_i + \sum_{i < j} 2\text{Re}[\tilde{G}_{ij}^2] a_i a_j \quad (\text{D17})$$

$$= \sum_i \tilde{G}_{ii}^2 a_i a_i + \sum_{i \neq j} \text{Re}[\tilde{G}_{ij}^2] a_i a_j \quad (\text{D18})$$

where we introduced $a_i = c_i s_i$ and used $\text{Re}[\tilde{G}_{ij}^2] = \text{Re}[\tilde{G}_{ji}^2]$ in the last line. Note, here a_i does not stand for an annihilation operator. The above clearly shows that $\text{Tr}[\tilde{G}CS\tilde{G}^*CS]$ is real-valued. We continue

$$\text{Tr}[\tilde{G}CS\tilde{G}^*CS] \leq |\text{Tr}[\tilde{G}CS\tilde{G}^*CS]| \leq \left| \sum_i \tilde{G}_{ii}^2 a_i a_i \right| + \left| \sum_{i \neq j} \text{Re}[\tilde{G}_{ij}^2] a_i a_j \right| \quad (\text{D19})$$

$$\leq \sum_i \tilde{G}_{ii}^2 a_i a_i + \sum_{i \neq j} |\text{Re}[\tilde{G}_{ij}^2]| a_i a_j \quad (\text{D20})$$

$$\leq \sum_i \tilde{G}_{ii}^2 a_i a_i + \sum_{i \neq j} |\tilde{G}_{ij}|^2 a_i a_j \quad (\text{D21})$$

$$= \sum_{i,j} |\tilde{G}_{ij}|^2 a_i a_j = \sum_{i,j} |\tilde{G}_{ij}|^2 s_i c_i s_j c_j \quad (\text{D22})$$

$$= \sum_{i,j} |\tilde{G}_{ij}|^2 s_i \sqrt{s_i^2 + 1} s_j \sqrt{s_j^2 + 1} \quad (\text{D23})$$

$$\leq \sum_{ij} |\tilde{G}_{ij}|^2 \left[s_i^2 s_j^2 + \frac{1}{2}(s_i^2 + s_j^2) \right] \quad (\text{D24})$$

$$= \sum_{ij} |\tilde{G}_{ij}|^2 s_i^2 s_j^2 + \frac{1}{2} \sum_{ij} |\tilde{G}_{ij}|^2 (s_i^2 + s_j^2) \quad (\text{D25})$$

$$= \text{Tr}[\tilde{G}S^2\tilde{G}S^2] + 2\frac{1}{2}\text{Tr}[G^2S^2], \quad (\text{D26})$$

where we used $\text{Re}[z^2] \leq |z|^2$ in the third line. In the fifth line we used $c_i = \sqrt{s_i^2 + 1}$. In the sixth line we used $\text{LHS} = s_i \sqrt{s_i^2 + 1} s_j \sqrt{s_j^2 + 1} \leq s_i^2 s_j^2 + \frac{1}{2}(s_i^2 + s_j^2) = \text{RHS}$. This can be seen by squaring both sides (both sides are non-negative), that is, the left hand side squared is $\text{LHS}^2 = s_i^2 (s_i^2 + 1) s_j^2 (s_j^2 + 1) = (s_i^4 + s_i^2)(s_j^4 + s_j^2) = s_i^4 s_j^4 + s_i^4 s_j^2 + s_i^2 s_j^4 + s_i^2 s_j^2$. The right hand side squared is

$$\text{RHS}^2 = [s_i^2 s_j^2 + \frac{1}{2}(s_i^2 + s_j^2)]^2 = s_i^4 s_j^4 + 2\frac{1}{2}s_i^2 s_j^2 (s_i^2 + s_j^2) + \frac{1}{4}(s_i^2 + s_j^2)^2 \quad (\text{D27})$$

$$= s_i^4 s_j^4 + s_i^4 s_j^2 + s_i^2 s_j^4 + \frac{1}{4}(s_i^2 + s_j^2)^2. \quad (\text{D28})$$

Now, let us rewrite $\text{LHS}^2 \leq \text{RHS}^2$ as

$$0 \leq \text{RHS}^2 - \text{LHS}^2 = \frac{1}{4}(s_i^2 + s_j^2)^2 - s_i^2 s_j^2 = \frac{1}{4}(s_i^2 - s_j^2)^2, \quad (\text{D29})$$

which is obviously true as the term after the last equals sign is manifestly non-negative. And thus $\text{LHS} \leq \text{RHS}$ from which Eq. (D26) finally follows.

Now, let us come to the terms that are due to displacement. Note that $\text{Tr}[\tilde{G}CS\tilde{G}^*\mathcal{B}^*] = \text{Tr}[(\tilde{G}CS\tilde{G}^*\mathcal{B}^*)^\dagger] = \text{Tr}[\tilde{G}^*CS\tilde{G}\mathcal{B}]$.

Thus, we have

$$\text{Tr}[\tilde{G}CS\tilde{G}^*\mathcal{B}^*] + \text{Tr}[\tilde{G}^*SC\tilde{G}\mathcal{B}] = 2\text{Re}[\text{Tr}[\tilde{G}CS\tilde{G}^*\mathcal{B}^*]] \quad (\text{D30})$$

$$\leq 2|\text{Tr}[\tilde{G}CS\tilde{G}^*\mathcal{B}^*]| \quad (\text{D31})$$

$$= 2\left|\sum_{ijj'}\alpha_{j'}^*\tilde{G}_{j'j}c_js_j\tilde{G}_{ji}^*\alpha_i^*\right| \quad (\text{D32})$$

$$= 2\left|\sum_jc_js_j\left(\sum_{j'}\tilde{G}_{j'j}\alpha_{j'}^*\right)\left(\sum_i\tilde{G}_{ij}\alpha_i^*\right)\right| \quad (\text{D33})$$

$$= 2\left|\sum_jc_js_j\left(\sum_i\tilde{G}_{ij}\alpha_i^*\right)^2\right| \quad (\text{D34})$$

$$\leq 2\sum_jc_js_j\left|\sum_i\tilde{G}_{ij}\alpha_i^*\right|^2 \quad (\text{D35})$$

$$= 2\sum_jc_js_j\sum_i\tilde{G}_{ij}\alpha_i^*\sum_{j'}\tilde{G}_{j'j}\alpha_{j'} \quad (\text{D36})$$

$$= 2\sum_{ijj'}\tilde{G}_{ij}c_js_j\tilde{G}_{j'j}\alpha_{j'}\alpha_i^* \quad (\text{D37})$$

$$= 2\text{Tr}[\tilde{G}CS\tilde{G}\mathcal{A}] \quad (\text{D38})$$

$$\leq 2\text{Tr}[\tilde{G}C^2\tilde{G}\mathcal{A}] \quad (\text{D39})$$

$$= 2\text{Tr}[\tilde{G}S^2\tilde{G}\mathcal{A}] + 2\text{Tr}[\tilde{G}^2\mathcal{A}]. \quad (\text{D40})$$

With

$$\text{Tr}[\tilde{G}C^2\tilde{G}\mathcal{A}] = \text{Tr}[\tilde{G}(S^2 + 1)\tilde{G}\mathcal{A}] = \text{Tr}[\tilde{G}S^2\tilde{G}\mathcal{A}] + \text{Tr}[\tilde{G}^2\mathcal{A}] \quad (\text{D41})$$

and

$$\text{Tr}[\tilde{G}S^2\tilde{G}C^2] = \text{Tr}[\tilde{G}S^2\tilde{G}S^2] + \text{Tr}[\tilde{G}^2S^2] \quad (\text{D42})$$

we finally obtain with all of the results above

$$\mathcal{F}(|\psi_\lambda\rangle) = 4\left[\text{Tr}[\tilde{G}CS\tilde{G}^*CS] + \text{Tr}[\tilde{G}S^2\tilde{G}C^2]\right] \quad (\text{D43})$$

$$+ \text{Tr}[\tilde{G}S^2\tilde{G}\mathcal{A}] + \text{Tr}[\tilde{G}C^2\tilde{G}\mathcal{A}] + \text{Tr}[\tilde{G}CS\tilde{G}^*\mathcal{B}^*] + \text{Tr}[\tilde{G}^*SC\tilde{G}\mathcal{B}] \quad (\text{D44})$$

$$\leq 4\left[\text{Tr}[\tilde{G}S^2\tilde{G}S^2] + \text{Tr}[G^2S^2] + \text{Tr}[\tilde{G}S^2\tilde{G}S^2] + \text{Tr}[\tilde{G}^2S^2]\right] \quad (\text{D45})$$

$$+ \text{Tr}[\tilde{G}S^2\tilde{G}\mathcal{A}] + \text{Tr}[\tilde{G}S^2\tilde{G}\mathcal{A}] + \text{Tr}[\tilde{G}^2\mathcal{A}] + 2\text{Tr}[\tilde{G}S^2\tilde{G}\mathcal{A}] + 2\text{Tr}[\tilde{G}^2\mathcal{A}] \quad (\text{D46})$$

$$= 4 \cdot \left(2\text{Tr}[\tilde{G}S^2\tilde{G}S^2] + 4\text{Tr}[\tilde{G}S^2\tilde{G}\mathcal{A}] + 3\text{Tr}[\tilde{G}^2(S^2 + \mathcal{A})] - \text{Tr}[\tilde{G}^2S^2]\right) \quad (\text{D47})$$

$$= 4 \cdot \left(2\text{Tr}[\tilde{G}S^2\tilde{G}S^2] + 4\text{Tr}[\tilde{G}S^2\tilde{G}\mathcal{A}]\right) + 4 \cdot 3(\bar{g}^2 + \Delta g^2)N_S - 4\text{Tr}[\tilde{G}^2S^2] \quad (\text{D48})$$

This completes the proof. \square

2. Proof of Lemma D.2

Proof. As Q is Hermitian and positive semi-definite, there is a unitary W , such that $Q = W^\dagger DW$, where $D = \text{diag}(d_1, \dots, d_M)$ is diagonal and we have $d_i \geq 0$. With this, let us consider the right-hand side of the to be proved inequality which we divide by 4 and obtain

$$\text{RHS}/4 = \text{Tr}[HQ]^2 + \text{Tr}[H^2Q]\text{Tr}[Q] - 2\text{Tr}[HQHQ] \quad (\text{D49})$$

$$= \text{Tr}[HW^\dagger DW]^2 + \text{Tr}[H^2W^\dagger DW]\text{Tr}[W^\dagger DW] - 2\text{Tr}[HW^\dagger DWHW^\dagger DW] \quad (\text{D50})$$

$$= \text{Tr}[H'D]^2 + \text{Tr}[H'^2D]\text{Tr}[D] - 2\text{Tr}[H'DH'D], \quad (\text{D51})$$

where we introduced $H' = WHW^\dagger$, which is Hermitian. Let us now continue by rewriting the above in terms of components. For the first term, we have to calculate the square of the following

$$\text{Tr}[H'D] = \sum_k (H'D)_{kk} = \sum_k \sum_i H'_{ki} D_{ik} \delta_{ik} = \sum_i H'_{ii} d_i. \quad (\text{D52})$$

For the second term, we have

$$\text{Tr}[H'^2 D] = \sum_k (H'^2 D)_{kk} = \sum_k \sum_i (H'^2)_{ki} D_{ik} \delta_{ik} = \sum_i (H'^2)_{ii} d_i = \sum_i \sum_n H'_{in} H'_{ni} d_i \quad (\text{D53})$$

$$= \sum_{in} |H'_{in}|^2 d_i. \quad (\text{D54})$$

For the third term, we have

$$\text{Tr}[H'DH'D] = \sum_j (H'DH'D)_{jj} = \sum_j \sum_i (H'D)_{ji} (H'D)_{ij} \quad (\text{D55})$$

$$= \sum_j \sum_i \sum_r H'_{jr} D_{ri} \sum_q H'_{iq} D_{qj} \quad (\text{D56})$$

$$= \sum_{ji} H'_{ji} D_{ii} H'_{ij} D_{jj} \quad (\text{D57})$$

$$= \sum_{ij} |H'_{ij}|^2 d_i d_j \quad (\text{D58})$$

Putting these three terms together, we obtain for the right-hand side

$$\text{RHS}/4 = \sum_i H'_{ii} d_i \sum_j H'_{jj} d_j + \sum_{in} |H'_{in}|^2 d_i \sum_j d_j - 2 \sum_{ij} |H'_{ij}|^2 d_i d_j \quad (\text{D59})$$

$$= \sum_{ij} \left[H'_{ii} H'_{jj} + \sum_n |H'_{in}|^2 - 2 |H'_{ij}|^2 \right] d_i d_j \quad (\text{D60})$$

$$= \sum_i \left[H'_{ii}^2 + \sum_n |H'_{in}|^2 - 2 |H'_{ii}|^2 \right] d_i^2 \quad (\text{D61})$$

$$+ \sum_{i \neq j} \left[H'_{ii} H'_{jj} + \sum_n |H'_{in}|^2 - 2 |H'_{ij}|^2 \right] d_i d_j. \quad (\text{D62})$$

Now, note that we have for the sum over n in the third line

$$\sum_i \sum_n |H'_{in}|^2 d_i^2 = \sum_i \left[|H'_{ii}|^2 + \sum_{n \neq i} |H'_{in}|^2 \right] d_i^2 \quad (\text{D63})$$

and for the sum over n in the fourth line, we have

$$\sum_{i \neq j} \sum_n |H'_{in}|^2 d_i d_j = \sum_{i \neq j} \sum_n \left(\frac{|H'_{in}|^2}{2} + \frac{|H'_{jn}|^2}{2} \right) d_i d_j \quad (\text{D64})$$

$$= \sum_{i \neq j} \left(\frac{|H'_{ii}|^2}{2} + \frac{|H'_{ji}|^2}{2} + \frac{|H'_{ij}|^2}{2} + \frac{|H'_{jj}|^2}{2} \right) d_i d_j + \sum_{i \neq j} \sum_{n \neq i, j} \left(\frac{|H'_{in}|^2}{2} + \frac{|H'_{jn}|^2}{2} \right) d_i d_j \quad (\text{D65})$$

$$= \sum_{i \neq j} \left(\frac{|H'_{ii}|^2}{2} + |H'_{ij}|^2 + \frac{|H'_{jj}|^2}{2} \right) d_i d_j + \sum_{i \neq j} \sum_{n \neq i, j} \left(\frac{|H'_{in}|^2}{2} + \frac{|H'_{jn}|^2}{2} \right) d_i d_j \quad (\text{D66})$$

Plugging these expressions into RHS yields

$$\text{RHS}/4 = \sum_i \underbrace{[H'_{ii}{}^2 + |H'_{ii}|^2 - 2|H'_{ii}|^2]}_{=0} d_i^2 \quad (\text{D67})$$

$$+ \sum_{i \neq j} \left[H'_{ii} H'_{jj} + \frac{|H'_{ii}|^2}{2} + |H'_{ij}|^2 + \frac{|H'_{jj}|^2}{2} - 2|H'_{ij}|^2 \right] d_i d_j \quad (\text{D68})$$

$$+ \sum_i \sum_{\substack{n \\ n \neq i}} |H'_{in}|^2 d_i^2 + \sum_{i \neq j} \sum_{\substack{n \\ n \neq i, j}} \left(\frac{|H'_{in}|^2}{2} + \frac{|H'_{jn}|^2}{2} \right) d_i d_j \quad (\text{D69})$$

$$= \sum_{i \neq j} \left(\frac{H'_{ii}}{2} + \frac{H'_{jj}}{2} \right)^2 d_i d_j + \sum_{i \neq j} -|H'_{ij}|^2 d_i d_j \quad (\text{D70})$$

$$+ \sum_i \sum_{\substack{n \\ n \neq i}} |H'_{in}|^2 d_i^2 + \sum_{i \neq j} \sum_{\substack{n \\ n \neq i, j}} \left(\frac{|H'_{in}|^2}{2} + \frac{|H'_{jn}|^2}{2} \right) d_i d_j \quad (\text{D71})$$

where we used $H'_{ii}{}^2 = |H'_{ii}|^2$ in the first line, which is true to Hermiticity. Now, let us note that

$$\sum_i \sum_{\substack{n \\ n \neq i}} |H'_{in}|^2 d_i^2 = \sum_{i \neq n} |H'_{in}|^2 d_i^2 = \sum_{i \neq j} |H'_{ij}|^2 d_i^2 \quad (\text{D72})$$

$$= \sum_{i \neq j} \frac{|H'_{ij}|^2 d_i^2}{2} + \sum_{i \neq j} \frac{|H'_{ji}|^2 d_j^2}{2} \quad (\text{D73})$$

$$= \sum_{i \neq j} |H'_{ij}|^2 \frac{d_i^2 + d_j^2}{2}. \quad (\text{D74})$$

With this, we finally obtain

$$\text{RHS}/4 = \sum_{i \neq j} \left(\frac{H'_{ii}}{2} + \frac{H'_{jj}}{2} \right)^2 d_i d_j + \sum_{i \neq j} |H'_{ij}|^2 \frac{d_i^2 - 2d_i d_j + d_j^2}{2} \quad (\text{D75})$$

$$+ \sum_{i \neq j} \sum_{\substack{n \\ n \neq i, j}} \left(\frac{|H'_{in}|^2}{2} + \frac{|H'_{jn}|^2}{2} \right) d_i d_j \quad (\text{D76})$$

$$= \sum_{i \neq j} \underbrace{\left(\frac{H'_{ii}}{2} + \frac{H'_{jj}}{2} \right)^2}_{\geq 0} d_i d_j + \sum_{i \neq j} \underbrace{|H'_{ij}|^2 \frac{(d_i - d_j)^2}{2}}_{\geq 0} \quad (\text{D77})$$

$$+ \sum_{i \neq j} \sum_{\substack{n \\ n \neq i, j}} \underbrace{\left(\frac{|H'_{in}|^2}{2} + \frac{|H'_{jn}|^2}{2} \right)}_{\geq 0} d_i d_j \quad (\text{D78})$$

$$\geq 0. \quad (\text{D79})$$

Note that H'_{ii} is real (due to Hermiticity of H), and $d_i \geq 0$ (due to positive semi-definiteness of Q). Thus, the three above terms are in a manifestly non-negative form. Thus, we have $\text{RHS} \geq 0$, which concludes the proof. \square

Appendix E: Optimal states

1. Mean-optimal state

We will now discuss the scenario in which we aim to maximize the prefactor of the term proportional to \bar{g}^2 in the QFI. We refer to such a states as mean optimal.

As an Ansatz, we choose a single-mode squeezed state with zero displacement. Thus, the input state we consider takes the form

$$|\psi\rangle = \hat{V}\hat{S}_{\hat{a}_n}(r_n)|0\rangle = \hat{S}_{\hat{V}\hat{a}_n\hat{V}^\dagger}(r_n)|0\rangle. \quad (\text{E1})$$

Thus, the single mode $\hat{c}_n = \hat{V}\hat{a}_n\hat{V}^\dagger$ is squeezed with squeezing parameter $r_n > 0$. The other modes are in vacuum, i.e., $r_i = 0$ for $i \neq n$. Also note that \hat{V} shall be completely arbitrary.

The calculation of the QFI of such a state is straightforward.

$$\mathcal{F}(|\psi_\lambda\rangle) = 4\text{Tr}[\tilde{G}CS\tilde{G}^*CS] + 4\text{Tr}[\tilde{G}S^2\tilde{G}C^2] \quad (\text{E2})$$

$$= 4 \sum_{ij} s_i \tilde{G}_{ij} c_j s_j \tilde{G}_{ji}^* c_i + 4 \sum_{ij} c_i \tilde{G}_{ij} s_j s_j \tilde{G}_{ji} c_i \quad (\text{E3})$$

$$= 4s_n \tilde{G}_{nn} c_n s_n \tilde{G}_{nn}^* c_n + 4 \sum_i c_i \tilde{G}_{in} s_n s_n \tilde{G}_{ni} c_i \quad (\text{E4})$$

$$= 4|\tilde{G}_{nn}|^2 s_n^2 c_n^2 + 4|\tilde{G}_{nn}|^2 s_n^2 c_n^2 + \sum_{i \neq n} |\tilde{G}_{in}|^2 s_n^2 c_i^2 \quad (\text{E5})$$

$$= 8|\tilde{G}_{nn}|^2 s_n^2 (s_n^2 + 1) + 4 \sum_{i \neq n} |\tilde{G}_{in}|^2 s_n^2 \cdot 1 \quad (\text{E6})$$

$$= 8|\tilde{G}_{nn}|^2 s_n^4 + 4 \sum_i |\tilde{G}_{in}|^2 s_n^2. \quad (\text{E7})$$

In the third line, we used $s_i = 0$ for $i \neq n$, in the fourth line we separated the n term from the sum, in the fifth line we used $c_i^2 = s_i^2 + 1$ for all i and $c_i = 1$ for $i \neq n$.

Now, we want to relate this result for the QFI to the resources N_S , \bar{g} , and Δg . We have

$$N_S = \text{Tr}[\tilde{P}_S S^2] = \sum_i (\tilde{P}_S S^2)_{ii} = \sum_{i,j} (\tilde{P}_S)_{ij} (S^2)_{ji} = \sum_{i,j} (\tilde{P}_S)_{ij} s_i^2 \delta_{ji} = \sum_i (\tilde{P}_S)_{ii} s_i^2 \quad (\text{E8})$$

$$= (\tilde{P}_S)_{nn} s_n^2. \quad (\text{E9})$$

Recall that \tilde{P}_S is the projector onto the subspace spanned by the eigenvectors of \tilde{G} associated to non-zero eigenvalues. In the (common) case where \tilde{G} has only non-zero eigenvalues, \tilde{P}_S is simply the identity.

For the mean resource parameter we have

$$\bar{g} N_S = \text{Tr}[\tilde{G} S^2] = \sum_{ij} \tilde{G}_{ij} s_i^2 \delta_{ij} = \sum_i \tilde{G}_{ii} s_i^2 = \tilde{G}_{nn} s_n^2 \quad (\text{E10})$$

We also have

$$(\Delta g^2 + \bar{g}^2) N_S = \text{Tr}[\tilde{G}^2 S^2] = \sum_{nm} (\tilde{G}^2)_{nm} s_n^2 \delta_{nm} = \sum_n (\tilde{G}^2)_{nn} s_n^2 \quad (\text{E11})$$

$$= \sum_{in} \tilde{G}_{ni} \tilde{G}_{in} s_n^2 = \sum_{in} |\tilde{G}_{in}|^2 s_n^2 \quad (\text{E12})$$

$$= \sum_i |\tilde{G}_{in}|^2 s_n^2. \quad (\text{E13})$$

By examining the QFI in Eq. (E7) and the expressions for $\bar{g} N_S$ and $(\Delta g^2 + \bar{g}^2) N_S$, we recognize that the QFI can be rewritten in terms of the resources parameters:

$$\mathcal{F}(|\psi_\lambda\rangle) = 8\bar{g}^2 N_S^2 + 0 \cdot \Delta g^2 N_S^2 + 4\bar{g}^2 N_S + 4(\Delta g)^2 N_S \quad (\text{E14})$$

$$= 8\bar{g}^2 N_S^2 + 0 \cdot \Delta g^2 N_S^2 + \mathcal{O}(N_S). \quad (\text{E15})$$

Thus, an arbitrary single mode squeezed state attains the best prefactor of 8 in the \bar{g}^2 term, but the worst prefactor of 0 for the $(\Delta g)^2$ term. It is an optimal state if $\Delta g = 0$ or almost optimal in the case of $\bar{g}^2 \gg (\Delta g)^2$.

2. Variance-optimal state

a. Without displacement

Now, let us come to a different state that maximizes the prefactor in front of the variance term Δg^2 . Again, as an Ansatz, we use a state with zero displacement. It takes the form

$$|\psi\rangle = \underbrace{\hat{B}e^{-i\frac{-\phi_n}{2}\hat{a}_i^\dagger\hat{b}_i}e^{-i\frac{-\phi_j}{2}\hat{a}_j^\dagger\hat{b}_j}}_{\hat{V}}\hat{S}_{\hat{a}_i}(r)\hat{S}_{\hat{a}_j}(r)|0\rangle = e^{-i\frac{-\phi_n}{2}\hat{B}\hat{a}_i^\dagger\hat{b}_i\hat{B}^\dagger}e^{-i\frac{-\phi_j}{2}\hat{B}\hat{b}_j^\dagger\hat{b}_j\hat{B}^\dagger}\hat{S}_{\hat{B}\hat{a}_i\hat{B}^\dagger}(r)\hat{S}_{\hat{B}\hat{a}_j\hat{B}^\dagger}(r)|0\rangle \quad (\text{E16})$$

$$= e^{-i\frac{-\phi_n}{2}\hat{b}_i^\dagger\hat{b}_i}e^{-i\frac{-\phi_j}{2}\hat{b}_j^\dagger\hat{b}_j}\hat{S}_{\hat{b}_i}(r)\hat{S}_{\hat{b}_j}(r)|0\rangle \quad (\text{E17})$$

$$= \hat{S}_{e^{-i\phi_i/2}\hat{b}_i}(r)\hat{S}_{e^{-i\phi_j/2}\hat{b}_j}(r)|0\rangle \quad (\text{E18})$$

Thus, we squeeze two mode in the mode basis $\{\hat{b}_n\}_n$ in which the generator \hat{G} appears diagonal. Note that we squeeze both modes i and j equally with squeezing parameters and with squeezing angles ϕ_i, ϕ_j . In the second line we used Eq. (A7). Let us also note we assume $g_i, g_j \neq 0$.

The QFI and the resources of such a state can be calculated quite easily due to the state's simple structure. For the QFI we have

$$\mathcal{F}(|\psi_\lambda\rangle) = 4\text{Tr}[\tilde{G}C\tilde{S}\tilde{G}^*CS] + 4\text{Tr}[\tilde{G}S^2\tilde{G}C^2] \quad (\text{E19})$$

$$= 4\sum_{ij}s_i\tilde{G}_{ij}c_js_j\tilde{G}_{ji}^*c_i + 4\sum_{ij}c_i\tilde{G}_{ij}s_js_j\tilde{G}_{ji}c_i \quad (\text{E20})$$

$$= 8\sum_i g_i^2 s_i^2 c_i^2 = 8g_i^2 s_i^2 c_i^2 + 8g_j^2 s_j^2 c_j^2 \quad (\text{E21})$$

$$= 8\tilde{g}_i^2 s_i^2 (s_i^2 + 1) + 8g_j^2 s_j^2 (s_j^2 + 1). \quad (\text{E22})$$

Note that in the second line we used $V = BT$, where $T_{nm} = e^{-i\frac{-\phi_n}{2}}\delta_{nm}$, where $\phi_n = 0$ for $n \neq i, j$. With this, we find $\tilde{G} = V^\dagger G V = T^\dagger B^\dagger G B T = T^\dagger D T = D = \text{diag}(g_1, \dots, g_M)$.

Now, we want to express the QFI in terms of the resources N_S, \bar{g} , and Δg . We have

$$N_S = \text{Tr}[\tilde{P}_S S^2] = \text{Tr}[S^2] = s_i^2 + s_j^2, \quad (\text{E23})$$

where $\tilde{P}_S S^2 = S^2$ follows from our initial assumption $g_i, g_j \neq 0$. For the mean resource, we have

$$\bar{g}N_S = \text{Tr}[\tilde{G}S^2] = \sum_{nm}\tilde{G}_{nm}s_n^2\delta_{nm} = \sum_n\tilde{G}_{nn}s_n^2 = \tilde{G}_{ii}s_i^2 + \tilde{G}_{jj}s_j^2 \quad (\text{E24})$$

$$= g_i s_i^2 + g_j s_j^2 \quad (\text{E25})$$

and for the variance resource we have

$$(\Delta g^2 + \bar{g}^2)N_S = \text{Tr}[\tilde{G}^2 S^2] = \sum_{nm}(\tilde{G}^2)_{nm}s_n^2\delta_{nm} = \sum_n(\tilde{G}^2)_{nn}s_n^2 \quad (\text{E26})$$

$$= \sum_{rn}\tilde{G}_{nr}\tilde{G}_{rn}s_n^2 = \sum_{rn}|\tilde{G}_{rn}|^2 s_n^2 \quad (\text{E27})$$

$$= \sum_r|\tilde{G}_{ri}|^2 s_i^2 + \sum_r|\tilde{G}_{rj}|^2 s_j^2 \quad (\text{E28})$$

$$= g_i^2 s_i^2 + g_j^2 s_j^2 \quad (\text{E29})$$

Let us now set $s_i^2 = s_j^2 = N_S/2$. From this follows

$$\Delta g^2 + \bar{g}^2 = \frac{g_i^2 + g_j^2}{2} \quad (\text{E30})$$

and

$$\mathcal{F}(|\psi_\lambda\rangle) = 8 \left(g_i^2 + g_j^2 \right) \frac{N_S}{2} \left(\frac{N_S}{2} + 1 \right) \quad (\text{E31})$$

$$= 2 \cdot 2 \frac{g_i^2 + g_j^2}{2} N_S (N_S + 2) \quad (\text{E32})$$

$$= 4 \left(\Delta g^2 + \bar{g}^2 \right) N_S^2 + 8 \left(\Delta g^2 + \bar{g}^2 \right) N_S \quad (\text{E33})$$

$$= 4 \left(\Delta g^2 + \bar{g}^2 \right) N_S^2 + \mathcal{O}(N_S). \quad (\text{E34})$$

We see that the factor 4 in front of the bandwidth term $(\Delta g)^2$ is optimal, while the factor 4 in front of the \bar{g}^2 term is suboptimal, it is only 50% of the optimal factor 8. Thus, the state is variance optimal

We also make an important observation for the $N_S \ll 1$ scenario. In this case, the performance of our state is a factor 2 better than that of the classical coherent state.

b. With displacement

Let us now come to a class of states that makes use of squeezing and displacement and does not rely on the generator-induced mode basis $\{\hat{b}_i\}_i$ in contrast to the previous state in E 2 a. It relies on populating an initial mode and the corresponding derivative mode, and as we show here, under certain conditions this state can be variance optimal. It has been widely discussed in the literature [19, 38].

First recall that in an arbitrary basis $\{\hat{a}_n\}_n$ we have $\partial_\lambda \hat{a}_m^\dagger(\lambda) = \partial_\lambda \hat{U}_\lambda \hat{a}_m^\dagger \hat{U}_\lambda^\dagger = -i \sum_n G_{nm} \hat{a}_n^\dagger(\lambda)$. We see that the derivative mode $\partial_\lambda \hat{a}_m^\dagger$ can be expressed in terms of the initial modes.

Now, let us choose an arbitrary initial mode \hat{u}_0 . It is always possible to find a mode basis $\{\hat{u}_0, \hat{u}_1, \dots\}$ such that the derivative mode of \hat{u}_0 is composed of only two modes

$$\partial_\lambda \hat{u}_0^\dagger(\lambda) = -i [G_{00} \hat{u}_0^\dagger(\lambda) + G_{10} \hat{u}_1^\dagger(\lambda)]. \quad (\text{E35})$$

We refer to \hat{u}_1 as the derivative mode of \hat{u}_0 , as it is the only mode (other than \hat{u}_0 itself) that has overlap with $\partial_\lambda \hat{u}_0(\lambda)$. Now, suppose we displace \hat{u}_0 and squeeze \hat{u}_0 and \hat{u}_1 , that is, we consider the state

$$\hat{V} \hat{D}_{\hat{u}_0}(\alpha_0) \hat{S}_{\hat{u}_0}(r_0) \hat{S}_{\hat{u}_1}(r_1) |0\rangle, \quad (\text{E36})$$

where $\hat{V} = e^{-i\frac{\phi_0}{2} \hat{u}_0^\dagger \hat{u}_0} e^{-i\frac{\phi_1}{2} \hat{u}_1^\dagger \hat{u}_1}$ and we have $V_{ni} = e^{-i(-\phi_n)/2} \delta_{ni}$, where ϕ_n is related to the squeezing angle.

Let us calculate the QFI and the resources of such a state. (assume G is full rank). Recall that $\tilde{G} = V^\dagger G V$. The QFI of the state is then

$$\mathcal{F} = 4 \left[\tilde{G}_{00}^2 \left(|\alpha_0|^2 (c_0^2 + s_0^2) + c_0 s_0 (\alpha_0^2 + \alpha_0^{*2} + 2c_0 s_0) \right) \right. \quad (\text{E37})$$

$$\left. + \tilde{G}_{11}^2 \cdot 2c_1^2 s_1^2 \right] \quad (\text{E38})$$

$$+ |\tilde{G}_{01}|^2 \left((s_1^2 + c_1^2) |\alpha_0|^2 + s_1^2 c_0^2 + c_1^2 s_0^2 \right) \quad (\text{E39})$$

$$\left. + s_1 c_1 (e^{2i\gamma} \{\alpha_0^2 + c_0 s_0\} + e^{-2i\gamma} \{\alpha_0^{*2} + c_0 s_0\}) \right] \quad (\text{E40})$$

where we used $\tilde{G}_{01} = G_{01} e^{i\frac{\phi_1 - \phi_0}{2}}$ and denoted $\gamma = \frac{\phi_1 - \phi_0}{2} + \arg[G_{01}]$ and note that $\tilde{G}_{00} = G_{00}$ and $\tilde{G}_{11} = G_{11}$. Choosing $\gamma = 0$ and $\alpha_0 \in \mathbb{R}$ clearly maximizes the QFI, which is why we will use this parameter setting in the following.

For the resources we have

$$N_S = s_0^2 + s_1^2 + |\alpha_0|^2 \quad (\text{E41})$$

$$\bar{g} N_S = \sum_{n,m} \tilde{G}_{nm} (s_n^2 \delta_{nm} + \alpha_n^* \alpha_m) \quad (\text{E42})$$

$$= \sum_n \tilde{G}_{nn} s_n^2 + \sum_{n,m} \tilde{G}_{nm} \alpha_n^* \alpha_m \quad (\text{E43})$$

$$= \tilde{G}_{00} s_0^2 + \tilde{G}_{11} s_1^2 + \tilde{G}_{00} |\alpha_0|^2 \quad (\text{E44})$$

We also have

$$(\Delta g^2 + \bar{g}^2)N_S = \sum_{n,m} (\tilde{G}^2)_{nm} (s_n^2 \delta_{nm} + \alpha_n^* \alpha_m) \quad (\text{E45})$$

$$= (\tilde{G}^2)_{00} s_0^2 + (\tilde{G}^2)_{11} s_1^2 + (\tilde{G}^2)_{00} |\alpha_0|^2 \quad (\text{E46})$$

$$= \sum_i \tilde{G}_{0i} \tilde{G}_{i0} s_0^2 + \sum_i \tilde{G}_{1i} \tilde{G}_{i1} s_1^2 + \sum_i \tilde{G}_{0i} \tilde{G}_{i0} |\alpha_0|^2 \quad (\text{E47})$$

$$= [|\tilde{G}_{00}|^2 + |\tilde{G}_{01}|^2] (s_0^2 + |\alpha|^2) + [|\tilde{G}_{10}|^2 + |\tilde{G}_{11}|^2] s_1^2 \quad (\text{E48})$$

Now, assuming $s_0^2 = 0$, $|\alpha_0|^2 = s_1^2 = N_S/2$ and considering the limit $N_S \gg 1$, we obtain for the resources $\bar{g} = (\tilde{G}_{00} + \tilde{G}_{11})/2$, $\Delta g^2 = |\tilde{G}_{01}|^2 + (\tilde{G}_{00} - \tilde{G}_{11})^2/4$ and for the QFI

$$\mathcal{F} \approx 2\tilde{G}_{11}^2 N_S^2 + 4 \left(\Delta g^2 - (\tilde{G}_{00} - \tilde{G}_{11})^2 \frac{1}{4} \right) N_S^2 + O(N_S). \quad (\text{E49})$$

We see that if $\tilde{G}_{00} - \tilde{G}_{11} = G_{00} - G_{11} = 0$, then the state is variance optimal with

$$\mathcal{F} \approx 2\bar{g}^2 N_S^2 + 4\Delta g^2 N_S^2 + O(N_S). \quad (\text{E50})$$

The performance associated to the variance term of the QFI can be attained with a homodyne measurement of the mode $\hat{u}_1(\lambda)$.

Also note that this state has been discussed in the parameter setting $|\alpha_0|^2 \gg s_0^2$ and $|\alpha_0|^2 \gg s_1^2$. With the additional assumption of $s_0^2, s_1^2 \gg 1$, we obtain $\mathcal{F} \approx 4 [\bar{g}^2 e^{2r_0} + \Delta g^2 e^{2r_1}] N_S$.

3. Completely optimal state

In Sec. III D 1 of the main text, we identified the optimal state. We now verify that this state is indeed optimal. Recall that it takes the form

$$|\psi\rangle = \hat{S}_{e^{-i\phi_i/2} \hat{b}_i}(r_i) \hat{S}_{e^{-i\phi_j/2} \hat{b}_j}(r_j) |0\rangle, \quad (\text{E51})$$

which generalizes the variance-optimal state of Sec. E 2 by allowing the two squeezing strengths to differ, *i.e.*, $r_i \neq r_j$.

First, recall that we assume $g_i < g_j$ and $g_i \neq 0$ and $g_j \neq 0$. Now, assume that i, j exists such that the corresponding eigenvalues are

$$g_i = \bar{g} - |\Delta g| \sqrt{\frac{s_j^2}{s_i^2}} \quad (\text{E52})$$

$$g_j = \bar{g} + |\Delta g| \sqrt{\frac{s_i^2}{s_j^2}} \quad (\text{E53})$$

and the average photon number of mode i, j are chosen as

$$s_i^2 = \frac{N_S}{2} \left(1 - \frac{\bar{g}}{\sqrt{\bar{g}^2 + (\Delta g)^2}} \right) \quad (\text{E54})$$

$$s_j^2 = \frac{N_S}{2} \left(1 + \frac{\bar{g}}{\sqrt{\bar{g}^2 + (\Delta g)^2}} \right) \quad (\text{E55})$$

where $N_S = s_i^2 + s_j^2$ which follows from $g_i, g_j \neq 0$.

The calculation for the QFI and resources is analogous to the one in the previous Sec. E 2 and we find

$$N_S = \text{Tr}[S^2] = s_i^2 + s_j^2 \quad (\text{E56})$$

$$\bar{g} N_S = g_i s_i^2 + g_j s_j^2 \quad (\text{E57})$$

$$(\Delta g^2 + \bar{g}^2) N_S = g_i^2 s_i^2 + g_j^2 s_j^2 \quad (\text{E58})$$

and

$$\mathcal{F}(|\psi_\lambda\rangle) = 8g_i^2 s_i^2 (s_i^2 + 1) + 8g_j^2 s_j^2 (s_j^2 + 1). \quad (\text{E59})$$

Let us first show that everything is self consistent. We start with the mean resource:

$$\bar{g}N_S = \left(\bar{g} - |\Delta g| \sqrt{\frac{s_j^2}{s_i^2}} \right) s_i^2 + \left(\bar{g} + |\Delta g| \sqrt{\frac{s_i^2}{s_j^2}} \right) s_j^2 \quad (\text{E60})$$

$$= \left(\bar{g} s_i^2 - |\Delta g| \sqrt{s_j^2 s_i^2} \right) + \left(\bar{g} s_j^2 + |\Delta g| \sqrt{s_i^2 s_j^2} \right) \quad (\text{E61})$$

$$= \bar{g} (s_i^2 + s_j^2) \quad (\text{E62})$$

Thus, we have shown self consistence for the mean resource.

Let us continue with the variance resource.

$$(\Delta g^2 + \bar{g}^2) N_S = g_i^2 s_i^2 + g_j^2 s_j^2 = \left(\bar{g} - |\Delta g| \sqrt{\frac{s_j^2}{s_i^2}} \right)^2 s_i^2 + \left(\bar{g} + |\Delta g| \sqrt{\frac{s_i^2}{s_j^2}} \right)^2 s_j^2 \quad (\text{E63})$$

$$= \left(\bar{g}^2 - 2\bar{g}|\Delta g| \sqrt{\frac{s_j^2}{s_i^2}} + \Delta g^2 \frac{s_j^2}{s_i^2} \right) s_i^2 + \left(\bar{g}^2 + 2\bar{g}|\Delta g| \sqrt{\frac{s_i^2}{s_j^2}} + \Delta g^2 \frac{s_i^2}{s_j^2} \right) s_j^2 \quad (\text{E64})$$

$$= \bar{g} (s_i^2 + s_j^2) + \Delta g^2 (s_i^2 + s_j^2). \quad (\text{E65})$$

Thus, we have shown self consistence for the variance resource.

Now, it only remains to show that the QFI reaches its optimal value. We have

$$\mathcal{F} = 8g_i^2 s_i^2 (s_i^2 + 1) + 8g_j^2 s_j^2 (s_j^2 + 1) \quad (\text{E66})$$

$$= 8 \left(\bar{g} - |\Delta g| \sqrt{\frac{s_j^2}{s_i^2}} \right)^2 s_i^2 (s_i^2 + 1) + 8 \left(\bar{g} + |\Delta g| \sqrt{\frac{s_i^2}{s_j^2}} \right)^2 s_j^2 (s_j^2 + 1) \quad (\text{E67})$$

$$= 8 \left(\bar{g}^2 - 2\bar{g}|\Delta g| \sqrt{\frac{s_j^2}{s_i^2}} + \Delta g^2 \frac{s_j^2}{s_i^2} \right) s_i^2 (s_i^2 + 1) + 8 \left(\bar{g}^2 + 2\bar{g}|\Delta g| \sqrt{\frac{s_i^2}{s_j^2}} + \Delta g^2 \frac{s_i^2}{s_j^2} \right) s_j^2 (s_j^2 + 1) \quad (\text{E68})$$

$$= 8\bar{g}^2 \left[s_i^2 (s_i^2 + 1) + s_j^2 (s_j^2 + 1) \right] + 8\Delta g^2 \left[s_j^2 (s_i^2 + 1) + s_i^2 (s_j^2 + 1) \right] + 8 \cdot 2\bar{g}|\Delta g| \sqrt{s_i^2 s_j^2} \left[s_j^2 + 1 - (s_i^2 + 1) \right] \quad (\text{E69})$$

$$= 8\bar{g}^2 \left[s_i^4 + s_j^4 \right] + 8 \cdot 2\Delta g^2 s_i^2 s_j^2 + 8 \cdot 2\bar{g}|\Delta g| \sqrt{s_i^2 s_j^2} \left[s_j^2 - s_i^2 \right] + 8\bar{g}^2 N_S + 8\Delta g^2 N_S + 0. \quad (\text{E70})$$

To make further progress, let us consider the following terms: Let us abbreviate $q = \frac{\bar{g}}{\sqrt{\bar{g}^2 + (\Delta g)^2}}$

$$s_i^4 + s_j^4 = \left(\frac{N_S}{2} \right)^2 (1 - q)^2 + \left(\frac{N_S}{2} \right)^2 (1 + q)^2 \quad (\text{E71})$$

$$= \frac{N_S^2}{2} [1 + q^2] \quad (\text{E72})$$

Next:

$$s_i^2 s_j^2 = \frac{N_S}{2} (1 - q) \frac{N_S}{2} (1 + q) = \left(\frac{N_S}{2} \right)^2 (1 - q^2) \quad (\text{E73})$$

$$= \frac{N_S^2}{4} (1 - q^2) \quad (\text{E74})$$

Lastly, let us consider

$$s_j^2 - s_i^2 = \frac{N_S}{2} (1 + q) - \frac{N_S}{2} (1 - q) = \frac{N_S}{2} (1 + q - 1 + q) = \frac{N_S}{2} 2q \quad (\text{E75})$$

$$= +N_S q \quad (\text{E76})$$

These results can be plugged into the QFI and we obtain:

$$= 8\bar{g}^2 \frac{N_S^2}{2} [1 + q^2] + 8 \cdot 2\Delta g^2 \frac{N_S^2}{4} (1 - q^2) + 8 \cdot 2\bar{g}|\Delta g| \sqrt{\frac{N_S^2}{4} (1 - q^2)} (+) N_S q + 8(\bar{g}^2 + \Delta g^2) N_S \quad (\text{E77})$$

$$= 4\bar{g}^2 N_S^2 [1 + q^2] + 4\Delta g^2 N_S^2 (1 - q^2) + 4 \cdot 2\bar{g}|\Delta g| N_S^2 \sqrt{(1 - q^2)} q + 8(\bar{g}^2 + \Delta g^2) N_S \quad (\text{E78})$$

$$= 4\bar{g}^2 N_S^2 + 4\Delta g^2 N_S^2 + 4\bar{g}^2 N_S^2 q^2 - 4\Delta g^2 N_S^2 q^2 + 4 \cdot 2\bar{g}|\Delta g| N_S^2 \sqrt{(1 - q^2)} q + 8(\bar{g}^2 + \Delta g^2) N_S \quad (\text{E79})$$

$$= 8\bar{g}^2 N_S^2 + 4\Delta g^2 N_S^2 + 4\bar{g}^2 N_S^2 (q^2 - 1) - 4\Delta g^2 N_S^2 q^2 + 4 \cdot 2\bar{g}|\Delta g| N_S^2 \sqrt{(1 - q^2)} q + 8(\bar{g}^2 + \Delta g^2) N_S \quad (\text{E80})$$

Now, the first two terms in the last line above corresponds to optimal QFI for given resources. To prove optimality, we thus have to show that the other terms containing q expressions cancel each other out to zero. So let us consider:

$$4\bar{g}^2 N_S^2 (q^2 - 1) - 4\Delta g^2 N_S^2 q^2 + 4 \cdot 2\bar{g}|\Delta g| N_S^2 \sqrt{(1 - q^2)} q \quad (\text{E81})$$

$$= -4N_S^2 \left[\bar{g} \frac{|\Delta g|}{\sqrt{\bar{g}^2 + \Delta g^2}} - |\Delta g| \frac{\bar{g}}{\sqrt{\bar{g}^2 + (\Delta g)^2}} \right]^2. \quad (\text{E82})$$

With this, we finally arrive at

$$\mathcal{F}(|\psi_\lambda\rangle) = 8\bar{g}^2 N_S^2 + 4\Delta g^2 N_S^2 + 8(\bar{g}^2 + \Delta g^2) N_S. \quad (\text{E83})$$

4. An idler-assisted optimal state

The optimal states we have considered thus far have not made use of an idler beam. So let us now consider states that make use of idler modes. We consider a state with 4 populated initial modes labelled as i, i_I, j, j_I . The state then takes the form

$$|\psi\rangle = \underbrace{\hat{B}\hat{U}_{ii_I}\hat{U}_{jj_I}}_{=\hat{V}} \hat{S}_{\hat{a}_i}(r_i) \hat{S}_{\hat{a}_{i_I}}(r_{i_I}) \hat{S}_{\hat{a}_j}(r_j) \hat{S}_{\hat{a}_{j_I}}(r_{j_I}) |0\rangle. \quad (\text{E84})$$

The unitaries \hat{U}_{nn_I} with $n = i, j$ are beam splitter unitaries that act as

$$\hat{U}_{nn+2}^\dagger \begin{pmatrix} \hat{a}_n \\ \hat{a}_{n_I} \end{pmatrix} \hat{U}_{nn_I} = \underbrace{\begin{pmatrix} \cos \theta_{nn_I} & -\sin \theta_{nn_I} e^{i\phi_{nn_I}} \\ \sin \theta_{nn_I} e^{-i\phi_{nn_I}} & \cos \theta_{nn_I} \end{pmatrix}}_{=U_{nn_I}} \begin{pmatrix} \hat{a}_n \\ \hat{a}_{n_I} \end{pmatrix}, \quad (\text{E85})$$

We recall that the QFI is given by

$$\mathcal{F}(|\psi_\lambda\rangle) = 4\text{Tr}[\tilde{G}CS\tilde{G}^*CS] + 4\text{Tr}[\tilde{G}S^2\tilde{G}C^2]. \quad (\text{E86})$$

In this case, we have

$$\tilde{G} = V^\dagger GV = U_{jj_I}^\dagger U_{ii_I}^\dagger B^\dagger GBU_{ii_I} U_{jj_I}. \quad (\text{E87})$$

With this, we can easily calculate the QFI and the relevant resources. Let us make the parameter choices $r_i = r_{i_I}, r_j = r_{j_I}$, $\theta_{ii_I} = \pi/4, \theta_{jj_I} = \pi/4$. This yields two two-mode squeezed vacuum states between modes i and i_I and modes j and j_I . Let us additionally set $\phi_{ii_I} = 0$ and $\phi_{jj_I} = 0$, this determines the squeezing angles of our two-mode squeezed vacua. With this, we obtain

$$\mathcal{F}(|\psi_\lambda\rangle) = 4 \cdot 2g_i^2 s_i^2 (s_i^2 + 1) + 4 \cdot 2g_j^2 s_j^2 (s_j^2 + 1) \quad (\text{E88})$$

and for the resources

$$N_S = \text{Tr}[\tilde{P}_S S^2 \tilde{P}_S] = s_i^2 + s_j^2 \quad (\text{E89})$$

and

$$\bar{g}N_S = g_i s_i^2 + g_j s_j^2 \quad (\text{E90})$$

$$(\bar{g}^2 + \Delta g^2)N_S = \text{Tr}[\tilde{G}^2 S^2] = g_i^2 s_i^2 + g_j^2 s_j^2. \quad (\text{E91})$$

The structure of the QFI and the resources is exactly the same as for the idler-less optimal state in the previous Subsections E 2 and E 3, compare Eqs. (E22), (E23), (E25) and (E29) with the above four equations.

Due to the fact that the structure of QFI and resources is identical for the idler-less and idler-assisted state, the discussion about optimality for our idler-assisted strategy is completely analogous to the idler-less case in Sections E 2 and E 3. Thus, also the idler-assisted state presented here can be optimal (and also variance optimal) in the sense that

$$\mathcal{F}(|\psi_\lambda\rangle) = \left(8\bar{g}^2 + 4\Delta g^2\right) N_S^2 + O(N_S), \quad (\text{E92})$$

given that we find appropriate modes and populate them according to our findings in E 3.

Appendix F: Optimal measurements

1. Optimal measurement for variance-optimal and completely optimal state

Let us now present an optimal measurement for the variance-optimal and the completely optimal state given in Eq. (40) and Eq. (34), respectively. Recall that the state is of the form $|\psi\rangle = \hat{S}_{e^{-i\phi_i/2}\hat{b}_i}(r_i)\hat{S}_{e^{-i\phi_j/2}\hat{b}_j}(r_j)|0\rangle$. Now, as both modes \hat{b}_i and \hat{b}_j are orthogonal, we can homodyne both of them simultaneously. We measure

$$\hat{x}_{e^{-i(\phi_n/2+\varphi_n)}\hat{b}_n} = \frac{e^{-i(\phi_n/2+\varphi_n)}\hat{b}_n + e^{+i(\phi_n/2+\varphi_n)}\hat{b}_n^\dagger}{\sqrt{2}} \quad (\text{F1})$$

for $n = i, j$ and φ_n is the adjustable phase that determines the quadrature to be measured. We have $\langle\psi_\lambda|\hat{x}_{e^{-i(\phi_n/2+\varphi_n)}\hat{b}_n}|\psi_\lambda\rangle = 0$ and

$$\sigma_{\text{hom},n}^2 := \langle\psi_\lambda|\hat{x}_{e^{-i(\phi_n/2+\varphi_n)}\hat{b}_n}^2|\psi_\lambda\rangle = \langle\psi_\lambda|\frac{\hat{b}_n^2 e^{-i2(\phi_n/2+\varphi_n)} + \hat{b}_n^{\dagger 2} e^{+i2(\phi_n/2+\varphi_n)} + \hat{b}_n \hat{b}_i^\dagger + \hat{b}_n^\dagger \hat{b}_n}{2}|\psi_\lambda\rangle \quad (\text{F2})$$

$$= \langle\psi|\hat{U}_\lambda^\dagger \frac{\hat{b}_n^2 e^{-i2(\phi_n/2+\varphi_n)} + \hat{b}_n^{\dagger 2} e^{+i2(\phi_n/2+\varphi_n)} + \hat{b}_n \hat{b}_i^\dagger + \hat{b}_n^\dagger \hat{b}_n}{2} \hat{U}_\lambda |\psi\rangle \quad (\text{F3})$$

$$= \langle\psi|\frac{\hat{b}_n^2 e^{-i2(\phi_n/2+\varphi_n+\lambda g_n)} + \hat{b}_n^{\dagger 2} e^{+i2(\phi_n/2+\varphi_n+\lambda g_n)} + \hat{b}_n^\dagger \hat{b}_n + \hat{b}_n \hat{b}_n^\dagger}{2}|\psi\rangle \quad (\text{F4})$$

$$= \frac{s_n c_n e^{-i2(\varphi_n+\lambda g_n)} + s_n c_n e^{+i2(\varphi_n+\lambda g_n)} + s_n^2 + s_n^2 + 1}{2} \quad (\text{F5})$$

$$= s_n c_n \cos(2(\varphi_n + \lambda g_n)) + \frac{2s_n^2 + 1}{2} \quad (\text{F6})$$

$$= \frac{\sinh(2r) \cos(2(\varphi_n + \lambda g_n))}{2} + \frac{\cosh(2r)}{2}. \quad (\text{F7})$$

In the third line we used $\hat{U}_\lambda^\dagger \hat{b}_n \hat{U}_\lambda = \hat{b}_n e^{-i\lambda g_n}$.

Note that due to the fact that the state is separable with respect to the measured modes i and j , the corresponding measurement outcomes are independent $x_n \sim \mathcal{N}(0, \sigma_{\text{hom},n}^2)$. The FI of the joint Gaussian probability distributions is the sum of the individual mode FIs. With this, we find

$$F_{\text{hom}}(|\psi_\lambda\rangle) = \sum_{n=\{i,j\}} F_{\text{hom},n}(|\psi_\lambda\rangle) \quad (\text{F8})$$

$$= \sum_{n=\{i,j\}} \frac{1}{2} \frac{(\partial_\lambda \sigma_{\text{hom},n})^2}{\sigma_{\text{hom},n}^2} = \sum_{n=\{i,j\}} \frac{1}{8} \frac{\partial_\lambda (\sigma_{\text{hom},n}^2)}{\sigma_{\text{hom},n}^4} \quad (\text{F9})$$

$$= \sum_{n=\{i,j\}} \frac{2g_n^2 \sinh^2(2r_n) \sin^2(2(g_n \lambda + \varphi_n))}{(\cosh(2r_n) + \sinh(2r_n) \cos(2(g_n \lambda + \varphi_n)))^2}. \quad (\text{F10})$$

Now, the optimal measurement phases φ_n^{opt} can be easily determined [75], and we find

$$\varphi_n^{\text{opt}} = \frac{1}{2} \arccos(\tanh(2r_n)) - g_n \lambda + \frac{\pi}{2} \quad (\text{F11})$$

with which we find the optimal FI

$$\max_{\varphi_i, \varphi_j} F_{\text{hom}}(|\psi_\lambda\rangle) = 8g_i^2 s_i^2 (s_i^2 + 1) + 8g_j^2 s_j^2 (s_j^2 + 1) \quad (\text{F12})$$

which is identical to the QFIs in Eq. (E59) and Eq. (E22) of the optimal state and the variance-optimal state, from which it follows that our proposed homodyne scheme is an optimal measurement for these states.

2. Effect of loss and noise

Let us also consider the effect of photon loss. We model photon loss as a beam splitter of transmissivity η_n right before homodyne detection that mixes the signal mode with a zero-mean environmental mode in a thermal (Gaussian) state. In that case, the mean of the homodyne measurement is still zero and the variance is given by

$$\sigma_{\text{hom},n}^2(\eta_n) = \eta_n \sigma_{\text{hom},n}^2(0) + (1 - \eta_n) \sigma_{\text{env},n}^2, \quad (\text{F13})$$

where $\sigma_{\text{hom},n}^2(0) = \sigma_{\text{hom},n}^2$ is the ideal case.

Now, the calculations for the FI are analogous to above, and we find

$$F_{\text{hom}}(|\psi_\lambda\rangle) = \sum_{n=\{i,j\}} \frac{1}{8} \frac{\partial_\lambda (\eta_n \sigma_{\text{hom},n}^2(0))}{\sigma_{\text{hom},n}^4(\eta)} \quad (\text{F14})$$

$$= \sum_{n=\{i,j\}} \frac{2\eta_n^2 g_n^2 \sinh^2(2r_n) \sin^2(2(g_n \lambda + \varphi_n))}{(\eta_n \sigma_{\text{hom},n}^2(0) + (1 - \eta_n) \sigma_{\text{env},n}^2)^2}. \quad (\text{F15})$$

The optimal phase is given by

$$\varphi_n^{\text{opt}} = \frac{1}{2} \arccos \left(\frac{\eta_n \sinh(2r_n)}{\eta_n \cosh(2r_n) + (1 - \eta_n) \sigma_{\text{env},n}^2} \right) - g_n \lambda + \frac{\pi}{2}. \quad (\text{F16})$$

For the optimal FI under loss and thermal noise, we have

$$\max_{\varphi_i, \varphi_j} F_{\text{hom}}(|\psi_\lambda\rangle) = \sum_{n=\{i,j\}} \frac{2\eta_n^2 g_n^2 \sinh^2(2r_n)}{(\eta_n \cosh(2r_n) + (1 - \eta_n) \sigma_{\text{env},n}^2)^2 + \eta_n^2 \sinh^2(2r_n)^4}. \quad (\text{F17})$$

We thus have obtained a general expression for the FI of an optimal homodyne measurement when loss and noise is present. To gain further insights, let us assume $\eta_i = \eta_j =: \eta$, which is, for example, approximately the case in lidar and radar scenarios.

For the case $\sigma_{\text{env},n} = 1$, which corresponds to an environment in the vacuum state, and the case $\sinh^2(r_n) \gg 1$ for $n = \{i, j\}$, we have

$$\max_{\varphi_i, \varphi_j} F_{\text{hom}}(|\psi_\lambda\rangle) \approx \frac{2\eta}{1 - \eta} \left[g_i^2 \sinh^2(r_i) + g_j^2 \sinh^2(r_j) \right] \quad (\text{F18})$$

$$= \frac{2\eta}{1 - \eta} \left[\bar{g}^2 + \Delta g^2 \right] N_S, \quad (\text{F19})$$

where we used $\sinh^2(2r) \approx 4 \sinh^2(r)$ and $\cosh(2r) \approx 2 \sinh^2(r)$. This should be compared to the performance of a classical coherent state protocol, which achieves $\mathcal{F}(|\psi_\lambda^{\text{coh}}\rangle) = 4\eta \left[\bar{g}^2 + \Delta g^2 \right] N_S$. We have $\max_{\varphi_i, \varphi_j} F_{\text{hom}}(|\psi_\lambda\rangle) \geq \mathcal{F}(|\psi_\lambda^{\text{coh}}\rangle)$, and thus a quantum advantage for transmissivities $\eta \geq 1/2$. Thus, our state that is optimal for $\eta = 1$ and shows good resilience even when photon loss is present.

Let us now also consider the effect of noise. Assume that the environmental modes are in thermal states with average photon number N_B . We then have $\sigma_{\text{env},n} = 2N_B/(1 - \eta) + 1$ (the factor $1/(1 - \eta)$ ensures that we have the same thermal noise photon number for all η). Assume $N_B \gg 1$ to be such that $\sigma_{\text{env},n} \approx 2N_B/(1 - \eta)$. We then find

$$\max_{\varphi_i, \varphi_j} F_{\text{hom}}(\Delta\lambda = 0) = 8\eta^2 \sum_{n=n_0, n_1} \frac{g_n^2 \sinh^2(r_n)}{8\eta \sinh^2(r_n) N_B + 4N_B^2} \quad (\text{F20})$$

$$= \begin{cases} \frac{\eta}{N_B} \left[g_i^2 \sinh^2(r_i) + g_j^2 \sinh^2(r_j) \right] = \frac{\eta N_S}{N_B} \left[\bar{g}^2 + \Delta g^2 \right], & \text{for } \eta \sinh^2(r_n) \gg N_B \\ 2\eta^2 \left[g_i^2 \frac{\sinh^4(r_i)}{N_B^2} + g_j^2 \frac{\sinh^4(r_j)}{N_B^2} \right], & \text{for } \eta \sinh^2(r_n) \ll N_B \end{cases} \quad (\text{F21})$$

with $n = \{i, j\}$.

The upper case is a factor of 2 lower than the classical coherent state performance $\mathcal{F}(|\psi_\lambda\rangle) \approx 2\frac{\eta N_S}{N_B} [\bar{g}^2 + \Delta g^2]$. The performance in the second case is much worse as the FI scales as $\sim (\frac{\eta N_S}{N_B})^2 [\bar{g}^2 + \Delta g^2]$ with $\eta N_S/N_B \ll 1$. Thus, our state that is otherwise optimal for $\eta = 1$ and $N_B = 0$, is inferior in the case of $\eta < 1$ and $N_B \gg 1$ to the classical coherent state.

3. Optimal homodyne measurement for mean-optimal state

Let us now propose an optimal measurement for the mean-optimal single-mode squeezed state $|\psi\rangle = \hat{V}\hat{S}_{\hat{a}_n}(r_n)|0\rangle = \hat{S}_{\hat{V}\hat{a}_n\hat{V}^\dagger}(r_n)|0\rangle$. Let us assume we have a sufficiently good prior guess λ_{prior} of the parameter λ . With out loss of generality, let us assume this prior guess is $\lambda_{\text{prior}} = 0$ and $\lambda \approx 0$. We then have $\hat{U}_\lambda \approx \hat{\mathcal{H}} - i\lambda\hat{G}$.

Now, we propose to homodyne the mode $\hat{c}_n = \hat{V}\hat{a}_n\hat{V}^\dagger$, which corresponds to measuring the operator

$$\hat{x}_{\hat{c}_n} e^{-i\varphi_n} = \frac{\hat{c}_i e^{-i\varphi_n} + \hat{c}_i^\dagger e^{+i\varphi_n}}{\sqrt{2}}. \quad (\text{F22})$$

We find $\langle\psi_\lambda|\hat{x}_{e^{-i(\phi_n/2+\varphi_n)}\hat{c}_n}|\psi_\lambda\rangle = 0$ and

$$\sigma_{\text{hom},n}^2 := \langle\psi_\lambda|\hat{x}_{e^{-i(\phi_n/2+\varphi_n)}\hat{c}_n}^2|\psi_\lambda\rangle \approx \frac{\sinh(2r)\cos(2(\varphi_n + \tilde{G}_{nn}))}{2} + \frac{\cosh(2r)}{2}. \quad (\text{F23})$$

Here, the approximation sign means that we neglect terms of order λ^2 and higher. Analogously to the previous Sec. F 1, we find

$$\max_{\varphi_n} F_{\text{hom}}(|\psi_\lambda\rangle) = 8\tilde{G}_{nn}^2 s_n^2 (s_n^2 + 1) = 8\bar{g}^2 N_S^2 + 8\bar{g}^2 N_S, \quad (\text{F24})$$

where the expression in terms of resources after the last equals sign follows from our results in Sec. E 1. Compare this to the QFI of this state $\mathcal{F}(|\psi_\lambda\rangle) = 8\bar{g}^2 N_S^2 + 8(\bar{g}^2 + \Delta g^2)N_S$. We see that the single homodyne measurement we proposed is only sensitive to the mean resource \bar{g} , and not the the variance resource Δg . In the limit $N_S \gg 1$, the single-mode homodyne measurement is nearly optimal.

Appendix G: Comparison to previous approaches in the literature

In Sec. III F we discussed the approach of Ref. [39] for (optimal) states that maximize the QFI for a parameter imprinting unitary $\hat{U}_\lambda = e^{-i\lambda\hat{G}}$ in a finite dimensional Hilbert space, where \hat{G} is a finite dimensional Hermitian operator. Their results do not apply to our case of mode parameter estimation as in that case we are dealing with an infinite dimensional Hilbert space.

To compare their approach with the one presented here, let us introduce a photon number truncation to turn the infinitely dimensional Hilbert space encountered in mode parameter estimation into a finite one:

$$\hat{G} = \sum_{i=1}^M g_i \hat{b}_i^\dagger \hat{b}_i = \sum_{i=1}^M g_i \sum_{n=0}^{\infty} n |n\rangle_i \langle n| \rightarrow \sum_{i=1}^M g_i \sum_{n=0}^{N_{\text{cut}}} n |n\rangle_i \langle n| \quad (\text{G1})$$

where $|n\rangle_i = \hat{b}_i^{\dagger n}|0\rangle/\sqrt{n!}$ are Fock states of mode i . Without loss of generality, assume that $g_1 = g_{\min}$ and $g_M = g_{\max}$. Thus, the initial infinite Hilbert space has been truncated to a finite dimensional one, which lets us apply the results of Ref. [39]. According to Ref. [39], the (optimal) state that maximizes the QFI takes the form

$$|\psi\rangle = \frac{|N_{\text{cut}}\rangle_1 + |N_{\text{cut}}\rangle_M}{\sqrt{2}} \quad (\text{G2})$$

which is a superposition of the generator's eigenstates corresponding to the minimal and maximal eigenvalues.

Ref. [39] did not introduce the notion of resources, but let us calculate the resources of this state according to our formalism and express the QFI in terms of these. We find $N_S = \sum_i \langle\psi|\hat{b}_i^\dagger \hat{b}_i|\psi\rangle = N_{\text{cut}}$ for the signal photon number and

$$\frac{\langle\psi|\hat{b}_i^\dagger \hat{b}_i|\psi\rangle}{N_S} = \frac{\delta_{i,1} + \delta_{i,M}}{2}. \quad (\text{G3})$$

for the generator intensity. Note that this state has the same generator intensity distribution $\frac{\langle \psi | \hat{b}_i^\dagger \hat{b}_i | \psi \rangle}{N_S}$ as our Gaussian variance-optimal state. We further find

$$\bar{g} = \sum_i g_i^2 \frac{\langle \psi | \hat{b}_i^\dagger \hat{b}_i | \psi \rangle}{N_S} = \frac{g_{\min} + g_{\max}}{2} \quad (\text{G4})$$

$$\Delta g^2 + \bar{g}^2 = \sum_i g_i^2 \frac{\langle \psi | \hat{b}_i^\dagger \hat{b}_i | \psi \rangle}{N_S} = \frac{g_{\min}^2 + g_{\max}^2}{2}. \quad (\text{G5})$$

From this follows $\Delta g^2 = \frac{1}{4}(g_M - g_1)^2$. Now, from Ref. [39] we know that $\mathcal{F}(\hat{U}_\lambda|\psi\rangle) = (g_{\max} - g_{\min})^2 N_{\text{cut}}^2$, from which follows

$$\mathcal{F}(\hat{U}_\lambda|\psi\rangle) = 4\Delta g^2 N_S^2. \quad (\text{G6})$$

Thus, the optimal state proposed in Ref. [39] when applied to truncated mode parameter estimation is variance optimal. There appear no mean contribution $\sim \bar{g}^2 N_S^2$ in the . Thus, their state is suboptimal according to our framework.

Appendix H: Continuous mode bases

In the main text, we encountered continuous mode bases $\hat{D}(z)$ satisfying the commutation relation $[\hat{D}(z), \hat{D}^\dagger(z')] = \delta(z - z')$. We keep the discussion general and do not assign a specific physical meaning to $\hat{D}(z)$: the variable $z \in \mathbb{R}$ may represent time, frequency, a spatial coordinate, momentum k , or any other continuous degree of freedom.

These continuous mode operators can be expanded in terms of discrete ones as

$$\hat{D}(z) = \sum_{n=0}^{\infty} \hat{d}_n \Psi_n(z), \quad (\text{H1})$$

where $\Psi_n(z)$ are the mode functions associated with the discrete basis $\{\hat{d}_n\}_n$ satisfying $[\hat{d}_n, \hat{d}_m^\dagger] = \delta_{nm}$ [33]. The mode functions form a complete orthonormal set, $\int dz \psi_n^*(z) \psi_m(z) = \delta_{nm}$, allowing one to pass freely between a continuous and a discrete mode description. Note, however, that the discrete description still involves countably infinitely many modes.

A second important continuous mode basis is $\hat{F}(p)$, with $p \in \mathbb{R}$, related to $\hat{D}(z)$ by a Fourier transform:

$$\hat{D}(z) = \int dp \hat{F}(p) \frac{e^{-ipz}}{\sqrt{2\pi}}, \quad (\text{H2})$$

$$\hat{F}(p) = \int dz \hat{D}(z) \frac{e^{+ipz}}{\sqrt{2\pi}}. \quad (\text{H3})$$

A multimode squeezed state may be written equivalently in any of these three bases as

$$|\psi\rangle = \exp\left(\iint dz dz' f(z, z') \hat{D}^\dagger(z) \hat{D}^\dagger(z') - \text{h.c.}\right) |0\rangle, \quad (\text{H4})$$

$$= \exp\left(\iint dp dp' \tilde{f}(p, p') \hat{F}^\dagger(p) \hat{F}^\dagger(p') - \text{h.c.}\right) |0\rangle, \quad (\text{H5})$$

$$= \exp\left(\sum_{n,m} f_{nm}^{(\psi)} \hat{d}_n^\dagger \hat{d}_m^\dagger - \text{h.c.}\right) |0\rangle, \quad (\text{H6})$$

with $\tilde{f}(p, p') = \iint dz dz' f(z, z') e^{ipz} e^{ip'z'} / (2\pi)$ and $f_{nm}^{(\psi)} = \iint dz dz' f(z, z') \psi_n^*(z) \psi_m^*(z')$.

The shift transformations are of particular interest and are studied extensively here. The corresponding unitaries are $\hat{U}_{a_z} = e^{-ia_z \hat{G}_{a_z}}$ and $\hat{U}_{a_p} = e^{-ia_p \hat{G}_{a_p}}$, with generators

$$\hat{G}_{a_z} = \int_{-\infty}^{\infty} dp p \hat{F}^\dagger(p) \hat{F}(p), \quad (\text{H7})$$

$$\hat{G}_{a_p} = \int_{-\infty}^{\infty} dz z \hat{D}^\dagger(z) \hat{D}(z). \quad (\text{H8})$$

Let us now examine how states transform under these unitaries. One verifies directly that $\hat{U}_{a_z}^\dagger \hat{F}(p) \hat{U}_{a_z} = \hat{F}(p) e^{-ip a_z}$ and $\hat{U}_{a_p}^\dagger \hat{D}(z) \hat{U}_{a_p} = \hat{D}(z) e^{-iz a_p}$. Combining these with Eqs. (H2)–(H3) yields $\hat{U}_{a_z}^\dagger \hat{D}(z) \hat{U}_{a_z} = \hat{D}(z + a_z)$ and $\hat{U}_{a_p}^\dagger \hat{F}(p) \hat{U}_{a_p} = \hat{F}(p - a_p)$. Using $\hat{U}_{-a_z} = \hat{U}_{a_z}^\dagger$ and $\hat{U}_{-a_p} = \hat{U}_{a_p}^\dagger$, it further follows that $\hat{U}_{a_z} \hat{D}(z) \hat{U}_{a_z}^\dagger = \hat{D}(z - a_z)$ and $\hat{U}_{a_p} \hat{F}(p) \hat{U}_{a_p}^\dagger = \hat{F}(p + a_p)$. Finally, applying these results and performing a change of integration variables, one finds that \hat{U}_{a_z} acting on $|\psi^{\text{sq}}\rangle$ induces $f(z, z') \rightarrow f(z + a_z, z' + a_z)$, while \hat{U}_{a_p} induces $\tilde{f}(p, p') \rightarrow \tilde{f}(p - a_p, p' - a_p)$.

1. Procedure to reduce infinitely many modes to finitely many modes

As discussed in the main text, we frequently encounter situations involving infinitely many modes, whereas our formalism was developed for a finite number of modes. We now demonstrate how the formalism can nevertheless be applied in this setting.

Since experimental constraints confine the relevant range of the variable z to a finite interval $[z_{\min}, z_{\max}]$, we partition this interval into M equally sized bins of width $\delta z := (z_{\max} - z_{\min})/M$ and define the discretized annihilation operators

$$\hat{d}_n := \int_{z_{\min} + \delta z (n-1)}^{z_{\min} + \delta z n} dz \frac{\hat{D}(z)}{\sqrt{\delta z}}, \quad n \in \{1, \dots, M\}, \quad (\text{H9})$$

which satisfy $[\hat{d}_n, \hat{d}_m^\dagger] = \delta_{nm}$, yielding a finite set of M modes with the desired commutation relations.

Discretized versions of $\hat{F}(p)$ are obtained as follows. The p -interval $[p_{\min}, p_{\max}]$ has length $p_{\max} - p_{\min} = 2\pi/\delta z = 2\pi M/(z_{\max} - z_{\min})$, with bin size $\delta p = 2\pi/(z_{\max} - z_{\min})$. Setting $p_k = p_{\min} + (k-1)\delta p$ for $k \in \{1, \dots, M\}$, we define the discrete modes $\{\hat{f}_k\}_k$ via the discrete Fourier relations

$$\hat{d}_n = \sum_{k=1}^M \hat{f}_k \frac{e^{-iz_n p_k}}{\sqrt{M}}, \quad (\text{H10})$$

$$\hat{f}_k = \sum_{n=1}^M \hat{d}_n \frac{e^{+iz_n p_k}}{\sqrt{M}}, \quad (\text{H11})$$

which are the discrete analogues of Eqs. (H2)–(H3), with $z_n = z_{\min} + n\delta z$. The transformation matrix $e^{-iz_n p_k}/\sqrt{M}$ is unitary, as can be seen by writing

$$\frac{e^{-iz_n p_k}}{\sqrt{M}} = \frac{e^{-i\frac{2\pi}{M}(n-1)(k-1)}}{\sqrt{M}} e^{-i(z_{\min} p_{\min} + z_{\min} \delta p (k-1) + p_{\min} \delta z (n-1))}. \quad (\text{H12})$$

The first factor is the standard M -point discrete Fourier transform matrix, which is unitary. The remaining exponential factors depend on at most one index, or are global phases, and therefore correspond to multiplication by diagonal unitary matrices on the rows and columns together with an overall phase — operations that preserve unitarity. It follows that $[\hat{f}_k, \hat{f}_q^\dagger] = \delta_{kq}$.

For the shift transformations studied here, the continuous generators of Eqs. (H7)–(H8) are approximated by

$$\hat{G}_{a_z} \approx \sum_{n=1}^M p_n \hat{f}_n^\dagger \hat{f}_n, \quad (\text{H13})$$

$$\hat{G}_{a_p} \approx \sum_{n=1}^M z_n \hat{d}_n^\dagger \hat{d}_n. \quad (\text{H14})$$

The quality of this approximation improves with increasing M and decreasing bin width, both of which can be adjusted freely. Correspondingly, the multimode squeezed state of Eq. (H4) is well approximated in the discretized basis as

$$|\psi^{\text{sq}}\rangle \approx \exp\left(\sum_{n,m=1}^M f_{nm} \hat{d}_n^\dagger \hat{d}_m^\dagger - \text{h.c.}\right) |0\rangle, \quad (\text{H15})$$

$$\approx \exp\left(\sum_{n,m=1}^M \tilde{f}_{nm} \hat{f}_n^\dagger \hat{f}_m^\dagger - \text{h.c.}\right) |0\rangle, \quad (\text{H16})$$

with $f_{nm} = f(z_n, z_m)$ and $\tilde{f}_{nm} = \tilde{f}(p_n, p_m)$. This procedure reduces an infinite continuous model to a finite discrete one, justifying the application of our formalism to continuous mode settings.

2. Determining the generator matrix

Given only the mode functions $\psi_n(z; \lambda)$, it is not immediately clear how to recover the corresponding unitary mode transformation \hat{U}_λ . However, the generator $\hat{G} = \sum_{n,m=1}^M G_{nm} \hat{c}_n^\dagger \hat{c}_m$ can be computed directly from the mode functions, and this is sufficient to evaluate the QFI.

To this end, we define

$$\hat{d}_n(\lambda) := \hat{U}_\lambda \hat{d}_n \hat{U}_\lambda^\dagger \quad (\text{H17})$$

as the parameter-dependent mode operators in the Schrödinger picture, in contrast to the Heisenberg picture transformation rules of Eq. (3). Following Ref. [37], one has

$$\partial_\lambda |\psi_\lambda\rangle = \sum_{m=1}^M \partial_\lambda \hat{d}_m^\dagger(\lambda) \hat{d}_m(\lambda) |\psi_\lambda\rangle \quad (\text{H18})$$

$$= -i \sum_{n,m=1}^M G_{nm} \hat{d}_n^\dagger(\lambda) \hat{d}_m(\lambda) |\psi_\lambda\rangle, \quad (\text{H19})$$

from which it follows that

$$\partial_\lambda \hat{d}_m^\dagger(\lambda) = -i \sum_{n=1}^M G_{nm} \hat{d}_n^\dagger(\lambda). \quad (\text{H20})$$

Using $\partial_\lambda \hat{d}_n^\dagger(\lambda) = \int dz [\partial_\lambda \Psi_n(z; \lambda)] \hat{D}^\dagger(z)$, this yields the key relation

$$\partial_\lambda \Psi_m(z; \lambda) = -i \sum_{n=1}^M G_{nm} \Psi_n(z; \lambda). \quad (\text{H21})$$

In practice, $\partial_\lambda \Psi_n(z; \lambda)$ often satisfies convenient recurrence relations that allow G_{nm} to be computed straightforwardly. The generator matrix elements can also be obtained directly via

$$-iG_{nm} = \int dz \Psi_n^*(z; \lambda) \partial_\lambda \Psi_m(z; \lambda). \quad (\text{H22})$$

We now apply this framework to the Hermite–Gauss (HG) modes, which form a complete orthonormal basis on $L^2(\mathbb{R})$. They are defined as

$$\Phi_n(z; z_0, p_0, \sigma_z, \theta) = \left(\frac{1}{2\sigma_z^2 \pi} \right)^{1/4} \sqrt{\frac{2^{-n}}{n!}} H_n \left(\frac{z - z_0}{\sqrt{2} \sigma_z} \right) e^{-\frac{1}{2} \left(\frac{z - z_0}{\sqrt{2} \sigma_z} \right)^2} e^{-ip_0(z - z_0)} e^{-i\theta}. \quad (\text{H23})$$

Consider the mode transformation

$$\hat{U}_{a_z} = \exp \left(-ia_z \int dp p \hat{D}^\dagger(p) \hat{D}(p) \right), \quad (\text{H24})$$

which generates a shift in the z domain and acts on the mode operators as

$$\hat{U}_{a_z}^\dagger \hat{D}(p) \hat{U}_{a_z} = \hat{D}(p) e^{-ip a_z}, \quad (\text{H25})$$

from which it follows that $\hat{U}_{a_z}^\dagger \hat{D}(z) \hat{U}_{a_z} = \hat{D}(z + a_z)$. The transformed HG mode operators are then

$$\hat{d}_n(a_z) = \hat{U}_{a_z} \hat{d}_n \hat{U}_{a_z}^\dagger = \int dz \Phi_n^*(z) \hat{U}_{a_z} \hat{D}(z) \hat{U}_{a_z}^\dagger \quad (\text{H26})$$

$$= \int dz \Phi_n^*(z) \hat{D}(z - a_z) \quad (\text{H27})$$

$$= \int dz \Phi_n^*(z + a_z) \hat{D}(z), \quad (\text{H28})$$

and correspondingly $\hat{d}_n^\dagger(a_z) = \int dz \Phi_n(z + a_z) \hat{D}^\dagger(z)$, so that the mode functions transform as $\Phi_n(z) \rightarrow \Phi_n(z + a_z)$, i.e., by a simple shift. Differentiating with respect to a_z and using the recurrence relation for HG modes gives

$$\partial_{a_z} \Phi_m(z + a_z) = \Phi'_m(z + a_z) = \frac{1}{\sqrt{2}\sigma_z} \left(\sqrt{\frac{m}{2}} \Phi_{m-1}(z + a_z) - \sqrt{\frac{m+1}{2}} \Phi_{m+1}(z + a_z) \right) - ip_0 \Phi_m(z + a_z). \quad (\text{H29})$$

Comparing with Eq. (H21), the generator matrix elements are

$$-iG_{nm} = \frac{1}{\sqrt{2}\sigma_z} \left(\sqrt{\frac{m}{2}} \delta_{n,m-1} - \sqrt{\frac{m+1}{2}} \delta_{n,m+1} \right) - ip_0 \delta_{n,m}, \quad (\text{H30})$$

$$\Leftrightarrow G_{nm} = \frac{i}{\sqrt{2}\sigma_z} \left(\sqrt{\frac{m}{2}} \delta_{n,m-1} - \sqrt{\frac{m+1}{2}} \delta_{n,m+1} \right) + p_0 \delta_{n,m}. \quad (\text{H31})$$

3. QFI for a state that appears in product form in the HG mode basis

Let us consider a state that takes on a simple form in the HG mode basis

$$|\psi\rangle = [\otimes_{n=1}^M e^{-i\frac{\phi_n}{2} \hat{c}_n^\dagger \hat{c}_n} \hat{S}_{\hat{c}_n}(r_n)]|0\rangle \quad (\text{H32})$$

with $\hat{c}_n^\dagger = \int dz \Phi_n(z) \hat{D}^\dagger(z)$. The states squeezing matrix is diagonal in the HG mode basis. Note that $\hat{V} = \otimes_n e^{-i\frac{\phi_n}{2} \hat{c}_n^\dagger \hat{c}_n}$, where ϕ_n is related to the squeezing angle of mode n . We can thus rewrite the state in various ways

$$|\psi\rangle = \hat{V} [\otimes_n \hat{S}_{\hat{c}_n}(r_n)]|0\rangle = [\otimes_n \hat{S}_{\hat{V}\hat{c}_n\hat{V}^\dagger}(r_n)]|0\rangle \quad (\text{H33})$$

$$= [\otimes_n \hat{S}_{e^{-i\phi_n/2} \hat{c}_n}(r_n)]|0\rangle, \quad (\text{H34})$$

which follows from $\hat{V} \hat{a}_n \hat{V}^\dagger = \sum_i V_{ni}^* \hat{a}_i$ with $V_{ni} = e^{-i(-\phi_n)/2} \delta_{ni}$.

Let us now calculate the QFI for $\hat{U}_{a_z} |\psi\rangle = |\psi_{a_z}\rangle$. We have

$$\mathcal{F}(|\psi_{a_z}\rangle) = 4 \sum_{ij} s_i \tilde{G}_{ij} c_j s_j \tilde{G}_{ji}^* c_i + 4 \sum_{ij} c_i \tilde{G}_{ij} s_j s_j \tilde{G}_{ji} c_i \quad (\text{H35})$$

For simplicity, we assume that only the first two modes are populated, that is, $s_n = 0$ and $c_n = 1$ for all $n \neq 0, 1$. Using Eq. (H31) and $\tilde{G} = V^\dagger G V$, we find

$$\mathcal{F}(|\psi_{a_z}\rangle) = \frac{8k^2\sigma^2 (c_0^2 s_0^2 + c_1^2 s_1^2) + (c_0^2 + 2) s_1^2 - 2c_0 c_1 s_0 s_1 \cos(\phi_0 - \phi_1) + c_1^2 s_0^2}{\sigma^2}. \quad (\text{H36})$$

Let us also calculate the resource parameters. We have

$$N_S = s_0^2 + s_1^2. \quad (\text{H37})$$

$$\bar{g} = \frac{1}{N_S} \sum_{nm} \tilde{G}_{nm} (s_n^2 \delta_{nm} + \alpha_n^* \alpha_m) = +p_0 \frac{s_0^2 + s_1^2}{s_0^2 + s_1^2} = +p_0 \quad (\text{H38})$$

and

$$(\Delta g^2 + \bar{g}^2) = \frac{1}{N_S} \sum_{nm} (\tilde{G}^2)_{nm} (s_n^2 \delta_{nm} + \alpha_n^* \alpha_m) \quad (\text{H39})$$

$$= \frac{1}{N_S} \sum_{nm} \sum_i \tilde{G}_{ni} \tilde{G}_{im} (s_n^2 \delta_{nm} + \alpha_n^* \alpha_m) \quad (\text{H40})$$

so that

$$\Delta g^2 = \frac{1}{N_S} \sum_{nm} \sum_i \tilde{G}_{ni} \tilde{G}_{im} (s_n^2 \delta_{nm} + \alpha_n^* \alpha_m) - \bar{g}^2 \quad (\text{H41})$$

$$= \frac{s_0^2 + 3s_1^2}{4\sigma_z^2 (s_0^2 + s_1^2)}. \quad (\text{H42})$$

For simplicity, let us assume that $s_0 = s_1$. We then have

$$\bar{g}^2 = p_0^2 \quad (\text{H43})$$

and

$$\Delta g^2 = \frac{1}{2\sigma_z^2}. \quad (\text{H44})$$

For the QFI, we find with $\phi_0 - \phi_1 = \pi$ (these phases clearly maximize the QFI):

$$\mathcal{F}(|\psi_\lambda\rangle) = 2N_S \left(2\bar{g}^2(N_S + 2) + \Delta g^2(N_S + 3) \right) \quad (\text{H45})$$

$$= \left(4\bar{g}^2 + 2\Delta g^2 \right) N_S^2 + \underbrace{\left(8\bar{g}^2 + 6\Delta g^2 \right) N_S}_{=O(N_S)}. \quad (\text{H46})$$

We see that this state is suboptimal. Both prefactors of the mean and variance terms are a factor of 1/2 worse than the maximum possible value.

This example demonstrates how to calculate the QFI and the resource parameters for a generic state. This state is suboptimal as seen by the prefactors 4 and 2 instead of the maximum values 8 and 4.

Appendix I: Analytical calculation of QFI for a regularized optimal state

Let us calculate the QFI of a regularized state. In the main text in Sec. IV C 3 we introduced such a regularized state for time estimation with squeezing matrix given in Eq. (65). In this Appendix, however, we are going to be more general and instead consider the estimation of shifts a_z in the z domain induced by the unitary mode transform $\hat{U}_{a_z} = e^{-a_z i \hat{G}_{a_z}}$. Here, z is a general variable that could stand for time, frequency, space, k space, etc.

Let us consider a squeezing matrix as in Eq. (65) in the z and p domains:

$$f(z, z') = r_- \Phi_{-,0}(z) \Phi_{-,0}(z') + r_+ \Phi_{+,0}(z) \Phi_{+,0}(z') \quad (\text{I1})$$

$$\tilde{f}(p, p') = r_- \tilde{\Phi}_{-,0}(p) \tilde{\Phi}_{-,0}(p') + r_+ \tilde{\Phi}_{+,0}(p) \tilde{\Phi}_{+,0}(p') \quad (\text{I2})$$

where we denote

$$\Phi_{\pm,n}(z) := \Phi_n(z; z_0 \pm \delta_{\pm,z}, p_0 \pm \delta_{\pm,p}, \sigma_z, \theta) \quad (\text{I3})$$

with $\delta_{\pm,k} \geq 0$ and $\delta_{\pm,p} \geq 0$. Thus, the HG mode functions $\Phi_{\pm,n}$ (defined in Eq. (62)) are centered around $z_0 \pm \delta_{\pm,z}$ in z space and centered around $p_0 \pm \delta_{\pm,p}$ in p space. Also, from Eq. (35) and (36) we know that $r_- \leq r_+$ for optimal states. Let us here additionally assume the stricter $r_- < r_+$ so that the case $r_- = r_+$ is excluded.

Now, to compute the QFI given in Eq. (17) of the above state for the mode transform with generator $\hat{G}_{a_z} = \int dp p \hat{F}^\dagger(p) \hat{F}(p)$, we have to determine the components of the generator matrix $\tilde{G} = V^\dagger G V$ in the Schmidt mode basis, that is, the basis in which the state appears disentangled.

So let us first determine the Schmidt decomposition of $f(z, z')$. First we denote

$$\mathcal{S} = \int dz \Phi_{+,0}^*(z) \Phi_{-,0}(z). \quad (\text{I4})$$

Now, let us introduce the orthonormal vectors

$$u_1(z) = \Phi_{+,0}(z) \quad (\text{I5})$$

$$u_2(z) = \frac{\Phi_{-,0}(z) - |\mathcal{S}| \Phi_{+,0}(z)}{\sqrt{1 - |\mathcal{S}|^2}}. \quad (\text{I6})$$

We can invert this and obtain

$$\Phi_{+,0}(z) = u_1(z) \quad (\text{I7})$$

$$\Phi_{-,0}(z) = u_2(z) \sqrt{1 - |\mathcal{S}|^2} + |\mathcal{S}| u_1(z). \quad (\text{I8})$$

We can now rewrite $f(z, z')$ in the orthonormal basis

$$f(z, z') = r_- \left[u_2(z) \sqrt{1 - |\mathcal{S}|^2} + |\mathcal{S}| u_1(z) \right] \left[u_2(z') \sqrt{1 - |\mathcal{S}|^2} + |\mathcal{S}| u_1(z') \right] + r_+ u_1(z) u_1(z') \quad (\text{I9})$$

$$= (r_+ + r_- |\mathcal{S}|^2) u_1(z) u_1(z') + r_- (1 - |\mathcal{S}|^2) u_2(z) u_2(z') \quad (\text{I10})$$

$$+ r_- (|\mathcal{S}| \sqrt{1 - |\mathcal{S}|^2}) u_1(z) u_2(z') + r_- (|\mathcal{S}| \sqrt{1 - |\mathcal{S}|^2}) u_1(z') u_2(z) \quad (\text{I11})$$

$$= \begin{pmatrix} u_1(z') \\ u_2(z') \end{pmatrix}^T \underbrace{\begin{pmatrix} r_+ + r_- |\mathcal{S}|^2 & r_- |\mathcal{S}| \sqrt{1 - |\mathcal{S}|^2} \\ r_- |\mathcal{S}| \sqrt{1 - |\mathcal{S}|^2} & r_- (1 - |\mathcal{S}|^2) \end{pmatrix}}_{=A} \begin{pmatrix} u_1(z) \\ u_2(z) \end{pmatrix}. \quad (\text{I12})$$

It is straightforward to show that the matrix' A eigenvalues are

$$r_1 = \frac{1}{2} \left(r_- + r_+ + \sqrt{4r_- r_+ \mathcal{S}^2 + (r_+ - r_-)^2} \right) \quad (\text{I13})$$

$$r_2 = \frac{1}{2} \left(r_- + r_+ - \sqrt{4r_- r_+ \mathcal{S}^2 + (r_+ - r_-)^2} \right). \quad (\text{I14})$$

Note that in the limit $\mathcal{S} \rightarrow 0$, we have $r_1 \rightarrow r_+$ and $r_2 \rightarrow r_-$ as expected, which follows from our initial assumption $r_+ > r_-$.

Note that A is real symmetric, and thus it can be diagonalized by the orthogonal matrix

$$Q = \begin{pmatrix} \cos \chi & -\sin \chi \\ \sin \chi & \cos \chi \end{pmatrix}, \quad (\text{I15})$$

that is $Q^T A Q = \text{diag}(r_1, r_2)$. For $Q^T A Q$ to be diagonal, we get the following condition:

$$0 \stackrel{\dagger}{=} (Q^T A Q)_{12} = \cos(\chi) \sin(\chi) (A_{22} - A_{11}) + A_{12} (\cos(\chi) - \sin(\chi)) (\cos(\chi) + \sin(\chi)) \quad (\text{I16})$$

$$= \cos(\chi) \sin(\chi) (A_{22} - A_{11}) + A_{12} (\cos^2(\chi) - \sin^2(\chi)) \quad (\text{I17})$$

$$\Leftrightarrow \tan(2\chi) = -2 \frac{A_{12}}{A_{22} - A_{11}} \quad (\text{I18})$$

$$= -2 \frac{r_- |\mathcal{S}| \sqrt{1 - |\mathcal{S}|^2}}{r_- (1 - |\mathcal{S}|^2) - [r_+ + r_- |\mathcal{S}|^2]} \quad (\text{I19})$$

$$= 2 \frac{r_- |\mathcal{S}| \sqrt{1 - |\mathcal{S}|^2}}{r_+ - r_- + 2r_- |\mathcal{S}|^2} \quad (\text{I20})$$

where we used $\cos^2(\chi) - \sin^2(\chi) = \cos(2\chi)$ and $\cos(\chi) \sin(\chi) = \frac{1}{2} \sin(2\chi)$ and assumed $A_{22} - A_{11} \neq 0$.

Now, there are two regimes: 1) $|r_+ - r_-| \ll 2r_- |\mathcal{S}|^2$. If we additionally assume $|\mathcal{S}| \ll 1$, we find $\chi = \pi/2$. 2) $|r_+ - r_-| \gg 2r_- |\mathcal{S}|^2$. If we additionally assume $|\mathcal{S}| \ll 1$, we find $\tan(2\chi) \approx 2 \frac{r_- |\mathcal{S}|}{r_+ - r_-} \approx 0$ from which follows $\chi \approx \frac{r_- |\mathcal{S}|}{r_+ - r_-}$ up to first order in $|\mathcal{S}|$.

It is now evident that the first two Schmidt modes $\Psi_1(z)$ and $\Psi_2(z)$ with non-zero Schmidt coefficients defined as

$$f(z, z') = \sum_{n=1}^2 r_n \Psi_n(z) \Psi_n(z') \quad (\text{I21})$$

are given by

$$\begin{pmatrix} \Psi_1(z) \\ \Psi_2(z) \end{pmatrix} = \begin{pmatrix} \cos \chi & -\sin \chi \\ \sin \chi & \cos \chi \end{pmatrix} \begin{pmatrix} u_1(z) \\ u_2(z) \end{pmatrix}. \quad (\text{I22})$$

We will exclusively consider the regime in which $|\mathcal{S}|$ is sufficiently small so that

$$\Psi_1(z) = \cos(\chi) u_1(z) - \sin(\chi) u_2(z) \approx \cos(\chi) \Phi_{+,0}(z) - \sin(\chi) \Phi_{-,0}(z) \quad (\text{I23})$$

$$\Psi_2(z) = \cos(\chi) u_2(z) + \sin(\chi) u_1(z) \approx \cos(\chi) \Phi_{-,0}(z) + \sin(\chi) \Phi_{+,0}(z) \quad (\text{I24})$$

is a good approximation.

These are just the first two elements of the Schmidt mode basis. The rest of the elements could be constructed via a Gram-Schmidt orthogonalization procedure of the set $\{\Psi_1, \Psi_2, \Phi_{+,1}, \Phi_{-,1}, \Phi_{+,2}, \Phi_{-,2}, \dots\}$. With similar arguments as before, we find for the third and fourth element

$$\Psi_3(z) \approx \Phi_{+,1}(z) \quad (I25)$$

$$\Psi_4(z) \approx \Phi_{-,1}(z) \quad (I26)$$

with negligible corrections of order $|S|$.

The next step is to determine the components of the generator matrix \tilde{G} in the Schmidt mode basis $\{\Psi_n\}_n$. Let us first denote

$$G_{nm}^{\Phi_{\pm}} = +\frac{i}{\sqrt{2}\sigma_z} \left(\sqrt{\frac{m}{2}} \delta_{n,m-1} - \sqrt{\frac{m+1}{2}} \delta_{n,m+1} \right) + (p_0 \pm \delta_{\pm,p}) \delta_{n,m} \quad (I27)$$

as the generator matrix in the mode bases $\{\Phi_{\pm,n}(z)\}_n$.

We then find

$$\partial_{a_z} \Psi_1(z + a_z) \approx \cos(\chi) \partial_{a_z} \Phi_{+,0}(z + a_z) - \sin(\chi) \partial_{a_z} \Phi_{-,0}(z + a_z) \quad (I28)$$

$$= \cos(\chi) \left[-iG_{00}^{\Phi_+} \Phi_{+,0} - iG_{10}^{\Phi_+} \Phi_{+,1} \right] - \sin(\chi) \left[-iG_{00}^{\Phi_-} \Phi_{-,0} - iG_{10}^{\Phi_-} \Phi_{-,1} \right] \quad (I29)$$

$$\approx \cos(\chi) \left[-iG_{00}^{\Phi_+} (\cos(\chi) \Psi_1 + \sin(\chi) \Psi_2) - iG_{10}^{\Phi_+} \Psi_3 \right] - \sin(\chi) \left[-iG_{00}^{\Phi_-} (\cos(\chi) \Psi_2 - \sin(\chi) \Psi_1) - iG_{10}^{\Phi_-} \Psi_4 \right] \quad (I30)$$

$$= -i \underbrace{\left[G_{00}^{\Phi_+} \cos^2(\chi) + G_{00}^{\Phi_-} \sin^2(\chi) \right]}_{\approx \tilde{G}_{11}} \Psi_1 - i \underbrace{\left[G_{00}^{\Phi_+} - G_{00}^{\Phi_-} \right] \cos(\chi) \sin(\chi)}_{\approx \tilde{G}_{21}} \Psi_2 - i \underbrace{G_{10}^{\Phi_+} \cos(\chi)}_{\approx \tilde{G}_{31}} \Psi_3 - i \underbrace{G_{10}^{\Phi_-} (-\sin(\chi))}_{\approx \tilde{G}_{41}} \Psi_4, \quad (I31)$$

where we used $\Phi_{+,0} \approx \cos(\chi) \Psi_1 + \sin(\chi) \Psi_2$ and $\Phi_{-,0} \approx \cos(\chi) \Psi_2 - \sin(\chi) \Psi_1$, which follows from Eqs. (I23) and (I24) by inversion, and Eq. (H21) to determine elements of \tilde{G} . Completely analogously, we find

$$\partial_{a_z} \Psi_2(z + a_z) \approx \cos(\chi) \partial_{a_z} \Phi_{-,0}(z + a_z) + \sin(\chi) \partial_{a_z} \Phi_{+,0}(z + a_z) \quad (I32)$$

$$= \cos(\chi) \left[-iG_{00}^{\Phi_-} \Phi_{-,0} - iG_{10}^{\Phi_-} \Phi_{-,1} \right] + \sin(\chi) \left[-iG_{00}^{\Phi_+} \Phi_{+,0} - iG_{10}^{\Phi_+} \Phi_{+,1} \right] \quad (I33)$$

$$\approx \cos(\chi) \left[-iG_{00}^{\Phi_-} [\cos(\chi) \Psi_2 - \sin(\chi) \Psi_1] - iG_{10}^{\Phi_-} \Psi_4 \right] + \sin(\chi) \left[-iG_{00}^{\Phi_+} [\cos(\chi) \Psi_1 + \sin(\chi) \Psi_2] - iG_{10}^{\Phi_+} \Psi_3 \right] \quad (I34)$$

$$= -i \underbrace{\left[G_{00}^{\Phi_-} \cos^2(\chi) + G_{00}^{\Phi_+} \sin^2(\chi) \right]}_{\approx \tilde{G}_{22}} \Psi_2 - i \underbrace{\left[G_{00}^{\Phi_+} - G_{00}^{\Phi_-} \right] \cos(\chi) \sin(\chi)}_{\approx \tilde{G}_{12}} \Psi_1 - i \underbrace{G_{10}^{\Phi_-} \cos(\chi)}_{\approx \tilde{G}_{42}} \Psi_4 - i \underbrace{G_{10}^{\Phi_+} \sin(\chi)}_{\approx \tilde{G}_{32}} \Psi_3 \quad (I35)$$

From above, we can read off the matrix elements of \tilde{G} .

Now, let us calculate the QFI. We use the fact that only the two modes Ψ_1 and Ψ_2 are populated, and thus $s_n = 0$ and $c_n = 1$ for $n \neq 1, 2$.

$$\mathcal{F}(|\psi_\lambda\rangle) = 4 \sum_{i,j=1}^{\infty} s_i \tilde{G}_{ij} c_j s_j (\tilde{G}_{ji})^* c_i + 4 \sum_{i,j=1}^{\infty} c_i \tilde{G}_{ij} s_j s_j \tilde{G}_{ji} c_i \quad (I36)$$

$$= 4 \left[2|G_{11}|^2 s_1^4 + 2|G_{22}|^2 s_2^4 + 2s_1^2 s_2^2 (|G_{12}|^2 + \text{Re}[G_{12}^2]) \right] + O(N_S) \quad (I37)$$

$$= 8 \left[|G_{11}|^2 s_1^4 + |G_{22}|^2 s_2^4 + s_1^2 s_2^2 (|G_{12}|^2 + \text{Re}[G_{12}^2]) \right] + O(N_S). \quad (I38)$$

Let us now also calculate the resource parameters and then express the QFI in terms of these. We have

$$N_S = s_1^2 + s_2^2 \quad (I39)$$

and

$$\bar{g} = \frac{1}{N_S} \sum_{nm} \tilde{G}_{nm} \left(s_n^2 \delta_{nm} + \alpha_n^* \alpha_m \right) = \frac{\tilde{G}_{11} s_1^2 + \tilde{G}_{22} s_2^2}{s_1^2 + s_2^2}. \quad (I40)$$

For the variance term, we have

$$\left(\Delta g^2 + \bar{g}^2\right) = \frac{1}{N_S} \sum_{nm} (\tilde{G}^2)_{nm} \left(s_n^2 \delta_{nm} + \alpha_n^* \alpha_m\right) \quad (\text{I41})$$

$$= \frac{1}{N_S} \sum_{nm} \sum_i \tilde{G}_{ni} \tilde{G}_{im} \left(s_n^2 \delta_{nm} + \alpha_n^* \alpha_m\right) \quad (\text{I42})$$

$$= \frac{1}{N_S} \sum_{n=1}^2 \sum_{i=1}^{\infty} \tilde{G}_{ni} \tilde{G}_{in} s_n^2 = \frac{1}{N_S} \sum_{n=1}^2 \sum_{i=1}^{\infty} |\tilde{G}_{ni}|^2 s_n^2 \quad (\text{I43})$$

$$= \frac{1}{N_S} \sum_{i=1}^{\infty} \left[|\tilde{G}_{1i}|^2 s_1^2 + |\tilde{G}_{2i}|^2 s_2^2\right] \quad (\text{I44})$$

$$= \frac{1}{N_S} \left[\left(|\tilde{G}_{11}|^2 + |\tilde{G}_{12}|^2 + |\tilde{G}_{13}|^2 + |\tilde{G}_{14}|^2\right) s_1^2 + \left(|\tilde{G}_{21}|^2 + |\tilde{G}_{22}|^2 + |\tilde{G}_{23}|^2 + |\tilde{G}_{24}|^2\right) s_2^2 \right]. \quad (\text{I45})$$

a. QFI of fully optimal regularized state

Above, we have given the calculation of the QFI of state with squeezing matrix as given in Eq. (II).

Let us now evaluate the QFI of a fully optimal state for which we generally have $r_1 \neq r_2$. Let us assume we are in regime 2) with $|r_+ - r_-| \gg 2r_- |\mathcal{S}|^2$. Assuming $|\mathcal{S}|$ is small enough, we may approximate $\sin(\chi) \approx 0$ and $\cos(\chi) \approx 1$.

Inspired by the choice of modes in Eqs. (38) and (39) for the optimal state in with a finite number of modes presented in Sec. E3, we set

$$\delta_{+,p} = \Delta \cdot \sqrt{\frac{s_2^2}{s_1^2}} \quad (\text{I46})$$

$$\delta_{-,p} = \Delta \cdot \sqrt{\frac{s_1^2}{s_2^2}}, \quad (\text{I47})$$

where $\Delta > 0$.

Now, we find

$$\tilde{G}_{11} \approx G_{00}^{\Phi_+} = p_0 + \delta_{+,p} \quad (\text{I48})$$

$$\tilde{G}_{22} \approx G_{00}^{\Phi_-} = p_0 - \delta_{-,p} \quad (\text{I49})$$

$$\tilde{G}_{12} \approx 0 + O(|\mathcal{S}|) \quad (\text{I50})$$

$$\tilde{G}_{23} \approx 0 + O(|\mathcal{S}|) \quad (\text{I51})$$

$$\tilde{G}_{14} \approx 0 + O(|\mathcal{S}|) \quad (\text{I52})$$

$$\tilde{G}_{31} \approx G_{10}^{\Phi_+} = +\frac{i}{\sqrt{2}\sigma} \frac{1}{\sqrt{2}} = +\frac{i}{2\sigma_z} \quad (\text{I53})$$

$$\tilde{G}_{42} \approx G_{10}^{\Phi_-} = +\frac{i}{\sqrt{2}\sigma} \frac{1}{\sqrt{2}} = +\frac{i}{2\sigma_z}. \quad (\text{I54})$$

Completely analogous to the finite case in Sec. E3, we find

$$\bar{g} = +p_0 \quad (\text{I55})$$

and

$$\Delta g^2 + \bar{g}^2 = \frac{1}{N_S} \left[\left((p_0 + \delta_{+,p})^2 + 0 + \frac{1}{4\sigma_z^2} + 0 \right) + \left(0 + (p_0 - \delta_{-,p})^2 + 0 + \frac{1}{4\sigma_z^2} \right) \right] \frac{N_S}{2} \quad (\text{I56})$$

$$= p_0^2 + \Delta^2 + \frac{1}{4\sigma_z^2} \quad (\text{I57})$$

from which follows

$$\Delta g^2 = \Delta^2 + \frac{1}{4\sigma_z^2}. \quad (\text{I58})$$

In contrast to the finite dimensional case in Sec. E3, here the extra term $\frac{1}{4\sigma_z^2}$ appears due to regularization, which we assume to be negligible.

Until now, we have not specified the squeezing parameter. Inspired by Eqs. (35) and (36), we choose r_1, r_2 such that

$$s_i^2 = \frac{N_S}{2} \left(1 - \frac{\bar{g}}{\sqrt{\bar{g}^2 + \Delta^2}} \right) \quad (\text{I59})$$

$$s_j^2 = \frac{N_S}{2} \left(1 + \frac{\bar{g}}{\sqrt{\bar{g}^2 + \Delta^2}} \right). \quad (\text{I60})$$

With this, the calculation for the QFI is equivalent to the one in Sec. E3 and we find

$$\mathcal{F} = (8p_0^2 + 4\Delta^2) N_S^2 + O(N_S) \quad (\text{I61})$$

$$= \left(8p_0^2 + 4 \left[\Delta g^2 - \frac{1}{4\sigma_z^2} \right] \right) N_S^2 + O(N_S), \quad (\text{I62})$$

where again compared to the finite dimensional case in Sec. E3 the extra term $\frac{1}{4\sigma_z^2}$ appears due to regularization.

b. QFI of variance optimal regularized state

Let us consider the regularized variance-optimal state. A variance-optimal state employs equal squeezing in both modes, i.e., $r_+ = r_-$ from which follows $r_1 = r_2$. We also have $\delta_{+,p} = \delta_{-,p} = \delta$. In this regime, we have $\chi \approx \pi/4$ (assuming $|\mathcal{S}|$ sufficiently small) and thus $\cos(\chi) \approx \sin(\chi) \approx 1/\sqrt{2}$. The photon number in both populated Schmidt modes is then

$$s_1^2 = s_2^2 = N_S/2. \quad (\text{I63})$$

Now, we find that $\tilde{G}_{11} = \tilde{G}_{22} = (G_{00}^{\Phi_+} + G_{00}^{\Phi_-})(\frac{1}{\sqrt{2}})^2 = (p_0 + \delta + p_0 - \delta)\frac{1}{2} = p_0$. From this follows

$$\bar{g} \approx +p_0. \quad (\text{I64})$$

Note that we have $\tilde{G}_{12} = \tilde{G}_{21} \approx (G_{00}^{\Phi_+} - G_{00}^{\Phi_-})(\frac{1}{\sqrt{2}})^2 = (p_0 + \delta - (p_0 - \delta))\frac{1}{2} = \delta$. We also have $|\tilde{G}_{13}|^2 \approx |\tilde{G}_{14}|^2 \approx |\tilde{G}_{24}|^2 \approx |\tilde{G}_{23}|^2 \approx |G_{10}^{\Phi_{\pm}}|^2 (\frac{1}{\sqrt{2}})^2 = \frac{1}{2\sigma_z^2} (\sqrt{\frac{1}{2}})^2 (\sqrt{\frac{1}{2}})^2 = \frac{1}{2^3\sigma^2}$

We then find

$$\Delta g^2 + \bar{g}^2 = \frac{1}{N_S} \left[(|\tilde{G}_{11}|^2 + |\tilde{G}_{12}|^2 + |\tilde{G}_{13}|^2 + |\tilde{G}_{14}|^2) s_1^2 + (|\tilde{G}_{21}|^2 + |\tilde{G}_{22}|^2 + |\tilde{G}_{23}|^2 + |\tilde{G}_{24}|^2) s_2^2 \right] \quad (\text{I65})$$

$$= \frac{1}{N_S} \left[\left(p_0^2 + \delta^2 + \frac{1}{2^3\sigma^2} + \frac{1}{2^3\sigma^2} \right) s_1^2 + \left(p_0^2 + \delta^2 + \frac{1}{2^3\sigma^2} + \frac{1}{2^3\sigma^2} \right) s_2^2 \right] \quad (\text{I66})$$

$$= \frac{1}{N_S} \frac{N_S}{2} \left[\left(p_0^2 + \delta^2 + \frac{1}{2^2\sigma^2} \right) + \left(p_0^2 + \delta^2 + \frac{1}{2^2\sigma^2} \right) \right] \quad (\text{I67})$$

$$= p_0^2 + \delta^2 + \frac{1}{2^2\sigma^2} \quad (\text{I68})$$

so that

$$\Delta g^2 = \delta^2 + \frac{1}{4\sigma_z^2} \quad (\text{I69})$$

$$\Leftrightarrow \delta^2 = \Delta g^2 - \frac{1}{4\sigma_z^2}. \quad (\text{I70})$$

Now, the QFI is

$$\mathcal{F}(|\psi_{\lambda}\rangle) \approx 8 \left[|G_{11}|^2 s_1^4 + |G_{22}|^2 s_2^4 + s_1^2 s_2^2 (|G_{12}|^2 + \text{Re}[G_{12}^2]) \right] + O(N_S) \quad (\text{I71})$$

$$= 8 \frac{N_S^2}{4} [p_0^2 + p_0^2 + \delta^2 + \delta^2] + O(N_S) = 4N_S^2 [p_0^2 + \delta^2] + O(N_S) \quad (\text{I72})$$

$$= 4N_S^2 \left[\bar{g}^2 + \Delta g^2 - \frac{1}{4\sigma_z^2} \right] + O(N_S) \quad (\text{I73})$$

In the limit of $\Delta g^2 \gg \frac{1}{4\sigma_z^2}$, the state is variance optimal.

Above we have assumed that $r_1 = r_2$ from which follows $\chi \approx \pi/4$. Due to experimental imperfections, the equality $r_1 = r_2$ may be slightly perturbed so that $|r_1 - r_2| = \epsilon$. If $|\mathcal{S}|$ is small enough so that $\epsilon \gg 2r_- |\mathcal{S}|^2$ we have $\chi \ll 1$ so that $\sin(\chi) \approx 0$ and $\cos(\chi) \approx 1$. In that case, the state is still variance optimal, as can be shown with a similar calculation to the one presented in the previous Section [10a](#).

Appendix J: Optimal homodyne measurement for regularized state

Let us now propose an optimal measurement for the regularized optimal two-mode squeezed state discussed in Appendix [I](#) for the mode transform $\hat{U}_{a_z} = e^{-a_z i \hat{G}_{a_z}}$. The measurement scheme is analogous to the optimal homodyne scheme for the discrete case presented in [F1](#).

The squeezing matrix is $f(z, z') = r_- \Phi_{-,0}(z) \Phi_{-,0}(z') + r_+ \Phi_{+,0}(z) \Phi_{+,0}(z')$ with $\Phi_{\pm,n}(z)$ as defined in Eq. [\(I3\)](#). Recall that the two modes $\Phi_{+,0}(z)$ and $\Phi_{-,0}(z)$ are orthogonal to a very good approximation under our assumptions given in [I](#).

We denote $\hat{c}_{\pm,n}^{\dagger}(a_z) = \int dz \Phi_{\pm,n}(z + a_z) \hat{D}^{\dagger}(z)$ and note that the transformed state is given by $|\psi_{a_z}\rangle \approx \hat{S}_{\hat{c}_{+,0}(a_z)(r_+)} \hat{S}_{\hat{c}_{-,0}(a_z)(r_-)} |0\rangle$, where the approximate sign is due to the fact that the modes are only approximately orthogonal.

Now, let us assume we have a prior guess $a_{z,\text{prior}}$ of a_z . We propose to homodyne the modes $\hat{c}_{+,0}(a_{z,\text{prior}})$ and $\hat{c}_{-,0}(a_{z,\text{prior}})$. We assume that our prior guess $a_{z,\text{prior}} = a_z + \epsilon$ is good enough so that

$$\hat{c}_{\pm,0}(a_{z,\text{prior}}) \approx \hat{c}_{\pm,0}(a_z) + \epsilon \partial_y \hat{c}_{\pm,0}(y) \Big|_{y=a_z} \quad (\text{J1})$$

$$= \hat{c}_{\pm,0}(a_z) + \epsilon (-i)^* \left[G_{00}^{\Phi_{\pm}^*} \hat{c}_{\pm,0}(a_z) + G_{10}^{\Phi_{\pm}^*} \hat{c}_{\pm,1}(a_z) \right] \quad (\text{J2})$$

$$= \hat{c}_{\pm,0}(a_z) + \epsilon (-i)^* \left[(p_0 \pm \delta_{\pm,p}) \hat{c}_{\pm,0}(a_z) + \frac{-i}{\sqrt{2}\sigma_z} \sqrt{\frac{1}{2}} \hat{c}_{\pm,1}(a_z) \right] \quad (\text{J3})$$

$$\approx \hat{c}_{\pm,0}(a_z) e^{+i\epsilon(p_0 \pm \delta_{\pm,p})} + \epsilon \frac{1}{2\sigma_z} \hat{c}_{\pm,1}(a_z), \quad (\text{J4})$$

where we used Eq. [\(I27\)](#) and Eq. [\(H21\)](#).

Now, we propose to measure the two quadratures

$$\hat{x}_{\hat{c}_{\pm,0}(a_{z,\text{prior}})e^{-i\varphi_{\pm}}} := \frac{\hat{c}_{\pm,0}(a_{z,\text{prior}})e^{-i\varphi_{\pm}} + \hat{c}_{\pm,0}^{\dagger}(a_{z,\text{prior}})e^{+i\varphi_{\pm}}}{\sqrt{2}} \quad (\text{J5})$$

Now, from this point on, we neglect all terms of order ϵ^2 , which is legitimate assuming we have a good enough prior. Then, the analysis is completely analogous to the analysis of the finite mode setting discussed in the Appendix [F1](#). This is due to the fact that the expectation of terms like $\hat{c}_{\pm,1}, \hat{c}_{\pm,1} \hat{c}_{\pm,0}, \hat{c}_{\pm,1} \hat{c}_{\mp,0}$ and $\hat{c}_{\pm,1} \hat{c}_{\mp,1}$ is zero, as our squeezed state has no population in $\hat{c}_{\pm,1}$. The expectation of terms quadratic in $\hat{c}_{\pm,1}$ is non zero, however, these terms are always accompanied by a prefactor ϵ^2 , which is why we can neglect them. Thus, the only relevant operators in the analysis become $\hat{c}_{\pm,0}(a_z) e^{+i\epsilon(p_0 \pm \delta_{\pm,p})}$ like in Appendix [F1](#).

Repeating all the steps from Appendix [F1](#) then leads us to

$$\max_{\varphi_+, \varphi_-} F_{\text{hom}}(|\psi_{a_z}\rangle) = 8(p_0 + \delta_{+,p})^2 s_+^2 (s_+^2 + 1) + 8(p_0 - \delta_{-,p})^2 s_-^2 (s_-^2 + 1) \quad (\text{J6})$$

with $s_{\pm} = \sinh(r_{\pm})$.

Now by using the relations between the parameters $p_0, \delta_{\pm,p}$ and the resource parameters $\bar{p}, \Delta p$ given in [10a](#) for the optimal state and given in [10b](#), we can show that the above FI equals its respective QFI. Thus, the homodyne measurement scheme presented here is optimal for the regularized optimal state from [10a](#) and the variance-optimal state from [10b](#).

We can also introduce loss by modeling it as a beam splitter of transmissivity η_{\pm} , and the analysis is completely analogous to the one presented in Appendix [F2](#).

Appendix K: Variance-optimal measurement for shift mode transforms

Recall from Definition III.3 that variance-optimal measurements are measurements whose FI fully attains the variance contribution of the QFI. So, say we have a state $|\psi_\lambda\rangle$ whose QFI is $\mathcal{F}(|\psi_\lambda\rangle) = c_{\bar{g}}\bar{g}^2 N_S^2 + c_{\Delta g}\Delta g^2 N_S^2 + O(N_S)$. A variance-optimal measurement then attains an FI of $c'_{\bar{g}}\bar{g}^2 N_S^2 + c'_{\Delta g}\Delta g^2 N_S^2 + O(N_S)$ with $c'_{\Delta g} = c_{\Delta g}$ and $c'_{\bar{g}} \leq c_{\bar{g}}$.

Let us consider the mode parameter shift transformation in the z domain. The analysis of a shift in the p domain is analogous due to Fourier duality. So we consider

$$\hat{U}_{a_z} = e^{-ia_z \int dp p \hat{F}^\dagger(p) \hat{F}(p)} \quad (\text{K1})$$

which has the effect

$$\hat{U}_{a_z}^\dagger \hat{F}(p) \hat{U}_{a_z} = \hat{F}(p) e^{-ia_z p} \quad (\text{K2})$$

$$\hat{U}_{a_z}^\dagger \hat{D}(z) \hat{U}_{a_z} = \hat{D}(z + a_z). \quad (\text{K3})$$

Also recall the unitary of a shift in the p domain with unitary $\hat{U}_{a_p} = e^{-ia_p \int dz z \hat{D}^\dagger(z) \hat{D}(z)}$ that acts as $\hat{U}_{a_p}^\dagger \hat{D}(z) \hat{U}_{a_p} = \hat{D}(z) e^{-ia_p z}$ and $\hat{U}_{a_p}^\dagger \hat{F}(p) \hat{U}_{a_p} = \hat{F}(p - a_p)$.

Now, any state $|\psi\rangle$ is characterized by mean parameters \bar{z}, \bar{p} , one in z and the other in its Fourier dual p space. We have

$$\bar{z} = \int dz z \frac{\langle \psi | \hat{D}^\dagger(z) \hat{D}(z) | \psi \rangle}{N_S} \quad (\text{K4})$$

$$\bar{p} = \int dp p \frac{\langle \psi | \hat{F}^\dagger(p) \hat{F}(p) | \psi \rangle}{N_S} \quad (\text{K5})$$

So, let us denote

$$|\psi\rangle =: |\psi(\bar{z}, \bar{p})\rangle = \hat{U}_{-\bar{z}} \hat{U}_{+\bar{p}} |\psi(0, 0)\rangle, \quad (\text{K6})$$

explicitly indicating the mean resource parameters of the respective state. Here, $|\psi(0, 0)\rangle$ is a version of the state $|\psi(\bar{z}, \bar{p})\rangle$ whose mean resource parameters are both zero. Note that

$$|\psi(0, 0)\rangle = \hat{U}_{-\bar{p}} \hat{U}_{+\bar{z}} |\psi(\bar{z}, \bar{p})\rangle \quad (\text{K7})$$

Let us show this:

$$\int dz z \langle \psi(0, 0) | \hat{D}^\dagger(z) \hat{D}(z) | \psi(0, 0) \rangle \quad (\text{K8})$$

$$= \int dz z \langle \psi(\bar{z}, \bar{p}) | \hat{U}_{+\bar{z}}^\dagger \hat{U}_{-\bar{p}}^\dagger \hat{D}^\dagger(z) \hat{D}(z) \hat{U}_{-\bar{p}} \hat{U}_{+\bar{z}} | \psi(\bar{z}, \bar{p}) \rangle \quad (\text{K9})$$

$$= \int dz z \langle \psi(\bar{z}, \bar{p}) | \hat{U}_{+\bar{z}}^\dagger \hat{D}^\dagger(z) \hat{D}(z) \hat{U}_{+\bar{z}} | \psi(\bar{z}, \bar{p}) \rangle e^{-i\bar{p}z} e^{+i\bar{p}z} \quad (\text{K10})$$

$$= \int dz z \langle \psi(\bar{z}, \bar{p}) | \hat{U}_{+\bar{z}}^\dagger \hat{D}^\dagger(z) \hat{U}_{+\bar{z}} \hat{U}_{+\bar{z}}^\dagger \hat{D}(z) \hat{U}_{+\bar{z}} | \psi(\bar{z}, \bar{p}) \rangle \quad (\text{K11})$$

$$= \int dz z \langle \psi(\bar{z}, \bar{p}) | \hat{D}^\dagger(z + \bar{z}) \hat{D}(z + \bar{z}) | \psi(\bar{z}, \bar{p}) \rangle \quad (\text{K12})$$

$$= \int dz (z - \bar{z}) \langle \psi(\bar{z}, \bar{p}) | \hat{D}^\dagger(z) \hat{D}(z) | \psi(\bar{z}, \bar{p}) \rangle \quad (\text{K13})$$

$$= (\bar{z} - \bar{z}) N_S \quad (\text{K14})$$

$$= 0 \quad (\text{K15})$$

Similarly, we have

$$\int dp p \langle \psi(0, 0) | \hat{F}^\dagger(p) \hat{F}(p) | \psi(0, 0) \rangle \quad (\text{K16})$$

$$= \int dp p \langle \psi(\bar{z}, \bar{p}) | \hat{U}_{+\bar{z}}^\dagger \hat{U}_{-\bar{p}}^\dagger \hat{F}^\dagger(p) \hat{F}(p) \hat{U}_{-\bar{p}} \hat{U}_{+\bar{z}} | \psi(\bar{z}, \bar{p}) \rangle \quad (\text{K17})$$

$$= \int dp p \langle \psi(\bar{z}, \bar{p}) | \hat{U}_{+\bar{z}}^\dagger \hat{F}^\dagger(p - (-\bar{p})) \hat{F}(p - (-\bar{p})) \hat{U}_{+\bar{z}} | \psi(\bar{z}, \bar{p}) \rangle \quad (\text{K18})$$

$$= \int dp p \langle \psi(\bar{z}, \bar{p}) | \hat{F}^\dagger(p + \bar{p}) \hat{F}(p + \bar{p}) | \psi(\bar{z}, \bar{p}) \rangle e^{-i\bar{z}(p+\bar{p})} e^{+i\bar{z}(p+\bar{p})} \quad (\text{K19})$$

$$= \int dp (p - \bar{p}) \langle \psi(\bar{z}, \bar{p}) | \hat{F}^\dagger(p) \hat{F}(p) | \psi(\bar{z}, \bar{p}) \rangle \quad (\text{K20})$$

$$= (\bar{p} - \bar{p}) N_S \quad (\text{K21})$$

$$= 0. \quad (\text{K22})$$

1. The variance-optimal measurement condition

In the following we want to show that resolved photon counting in the z domain can be optimal if the state satisfies the variance-optimal measurement condition we are about to introduce. Resolved photon counting in the z domain corresponds to projecting the quantum state onto

$$|z\rangle = \frac{1}{\sqrt{K!}} \otimes_{i=1}^K \hat{D}^\dagger(z_i) |0\rangle \quad (\text{K23})$$

where $\mathbf{z} = (z_1, \dots, z_K)^T \in \mathbb{R}^K$ and $K \in \mathbb{N}_0$.

The variance-optimal measurement condition is as follows:

Lemma K.1. *If a quantum state of interest $|\psi(\bar{z}, \bar{p})\rangle$ satisfies*

$$\partial_{a_z} \arg[\langle z | \hat{U}_{a_z} | \psi(\bar{z}, 0) \rangle] = 0 \quad (\text{K24})$$

for all $\mathbf{z} \in \mathbb{R}^K$ and all $K \in \mathbb{N}$, then

$$F(\hat{U}_{a_z} | \psi(\bar{z}, \bar{p})\rangle, \{|z\rangle\langle z|\}) = \mathcal{F}(\hat{U}_{a_z} | \psi(\bar{z}, 0)\rangle). \quad (\text{K25})$$

Let us explain the above lemma. The condition is essentially that the measurement amplitudes' phase is independent of the parameter a_z to be estimated. If a state satisfies this condition, then the corresponding FI of this state $\hat{U}_{a_z} | \psi(\bar{z}, \bar{p})\rangle$ (centered at \bar{p} in the p domain) for the measurement $\{|z\rangle\langle z|\}$ equals the QFI of the state $\hat{U}_{a_z} | \psi(\bar{z}, 0)\rangle$ centered at 0 in the p domain. To clarify what this means, suppose that the state under consideration has a QFI of $\mathcal{F}(\hat{U}_{a_z} | \psi(\bar{z}, 0)\rangle) = c_{\bar{p}} \bar{p}^2 N_S^2 + c_{\Delta p} \Delta p^2 N_S^2 + O(N_S)$ (see Eq. (33)). If this state satisfies our condition, then the FI of this state for the measurement $\{|z\rangle\langle z|\}$ is $F(\hat{U}_{a_z} | \psi(\bar{z}, \bar{p})\rangle, \{|z\rangle\langle z|\}) = c_{\Delta p} \Delta p^2 N_S^2 + O(N_S)$. That is, the FI attains the variance term of the QFI, but does not attain the mean term. Such a measurement is called variance optimal according to our Definition III.3.

Let us now proof lemma K.1.

Proof. Let us consider

$$\langle z|\hat{U}_{a_z}|\psi(\bar{z}, \bar{p})\rangle = \langle z|\hat{U}_{a_z}\hat{U}_{-\bar{z}}\hat{U}_{\bar{p}}|\psi(0, 0)\rangle = \langle z|\hat{U}_{a_z-\bar{z}}\hat{U}_{\bar{p}}|\psi(0, 0)\rangle \quad (\text{K26})$$

$$= \frac{1}{\sqrt{K!}}\langle 0|[\otimes_{i=1}^K \hat{D}(z_i)]\hat{U}_{a_z-\bar{z}}\hat{U}_{\bar{p}}|\psi(0, 0)\rangle = \frac{1}{\sqrt{K!}}\underbrace{\langle 0|\hat{U}_{a_z-\bar{z}}[\otimes_{i=1}^K \hat{U}_{a_z-\bar{z}}^\dagger \hat{D}(z_i)\hat{U}_{a_z-\bar{z}}]\hat{U}_{\bar{p}}|\psi(0, 0)\rangle}_{=|0\rangle} \quad (\text{K27})$$

$$= \frac{1}{\sqrt{K!}}\langle 0|[\otimes_{i=1}^K \hat{D}(z_i + a_z - \bar{z})]\hat{U}_{\bar{p}}|\psi(0, 0)\rangle = \frac{1}{\sqrt{K!}}\underbrace{\langle 0|\hat{U}_{\bar{p}}[\otimes_{i=1}^K \hat{U}_{\bar{p}}^\dagger \hat{D}(z_i + a_z - \bar{z})\hat{U}_{\bar{p}}]|\psi(0, 0)\rangle}_{=|0\rangle} \quad (\text{K28})$$

$$= \frac{1}{\sqrt{K!}}\langle 0|[\otimes_{i=1}^K e^{-i\bar{p}(z_i+a_z-\bar{z})} \hat{D}(z_i + a_z - \bar{z})]|\psi(0, 0)\rangle \quad (\text{K29})$$

$$= \left(\prod_{i=1}^K e^{-i\bar{p}(z_i+a_z-\bar{z})} \right) \frac{1}{\sqrt{K!}}\langle 0|[\otimes_{i=1}^K \hat{D}(z_i)]\hat{U}_{a_z-\bar{z}}|\psi(0, 0)\rangle \quad (\text{K30})$$

$$= \left(\prod_{i=1}^K e^{-i\bar{p}(z_i+a_z-\bar{z})} \right) \langle z|\hat{U}_{a_z}|\psi(\bar{z}, 0)\rangle \quad (\text{K31})$$

From the above, we see that \bar{p} only enter as a phase into the amplitudes, and thus the measurement probabilities will be independent of \bar{p} , i.e.,

$$|\langle z|\hat{U}_{a_z}|\psi(\bar{z}, \bar{p})\rangle|^2 = |\langle z|\hat{U}_{a_z}|\psi(\bar{z}, 0)\rangle|^2 =: p(z|a_z). \quad (\text{K32})$$

Let us denote

$$\langle z|\hat{U}_{a_z}|\psi(\bar{z}, 0)\rangle =: qe^{i\xi}, \quad (\text{K33})$$

where we defined $q = |\langle z|\hat{U}_{a_z}|\psi(\bar{z}, 0)\rangle|$ as the magnitude and $\xi = \arg[\langle z|\hat{U}_{a_z}|\psi(\bar{z}, 0)\rangle]$ as the phase. The argument function is defined as $\arg[z] = \arg[|z|e^{i\phi}] = \phi$.

Next, we want to calculate the FI of the state $\hat{U}_{a_z}|\psi(\bar{z}, \bar{p})\rangle$ using resolved photon counting in the z domain. First note that we have

$$F(\hat{U}_{a_z}|\psi(\bar{z}, \bar{p})\rangle, \{|z\rangle\langle z|\}) = F(\hat{U}_{a_z}|\psi(\bar{z}, 0)\rangle, \{|z\rangle\langle z|\}) \quad (\text{K34})$$

$$= \sum d^k z \frac{(\partial_{a_z} p(z|a_z))^2}{p(z|a_z)} = \sum d^k z \frac{(\partial_{a_z} q^2)^2}{q^2} = \sum d^k z \frac{(2q\partial_{a_z} q)^2}{q^2} = 4 \sum d^k z (\partial_{a_z} q)^2 \quad (\text{K35})$$

$$= 4 \sum d^k z (\partial_{a_z} |\langle z|\hat{U}_{a_z}|\psi(\bar{z}, 0)\rangle|)^2 \quad (\text{K36})$$

$$= 4 \sum d^k z |\langle z|\partial_{a_z} \hat{U}_{a_z}|\psi(\bar{z}, 0)\rangle|^2 = 4 \langle \psi(\bar{z}, 0)|(\partial_{a_z} \hat{U}_{a_z})^\dagger \left[\sum d^k z |z\rangle\langle z| \right] \partial_{a_z} \hat{U}_{a_z}|\psi(\bar{z}, 0)\rangle \quad (\text{K37})$$

$$= 4 \langle \psi(\bar{z}, 0)|(\partial_{a_z} \hat{U}_{a_z})^\dagger \partial_{a_z} \hat{U}_{a_z}|\psi(\bar{z}, 0)\rangle \quad (\text{K38})$$

$$= 4 \langle \psi(\bar{z}, 0)|(\partial_{a_z} \hat{U}_{a_z})^\dagger \partial_{a_z} \hat{U}_{a_z}|\psi(\bar{z}, 0)\rangle - 4 \underbrace{|\langle \psi(\bar{z}, 0)|\hat{U}_{a_z}^\dagger \partial_{a_z} \hat{U}_{a_z}|\psi(\bar{z}, 0)\rangle|^2}_{=0} \quad (\text{K39})$$

$$= \mathcal{F}(\hat{U}_{a_z}|\psi(\bar{z}, 0)\rangle) \quad (\text{K40})$$

where the symbol $\sum d^k z$ means that we sum the integrals over all the photon number subspaces. In the fourth line we used $(\partial_{a_z} |\langle z|\hat{U}_{a_z}|\psi(\bar{z}, 0)\rangle|)^2 = |\langle z|\partial_{a_z} \hat{U}_{a_z}|\psi(\bar{z}, 0)\rangle|^2$. This follows from $\langle z|\partial_{a_z} \hat{U}_{a_z}|\psi(\bar{z}, 0)\rangle = \partial_{a_z} \langle z|\hat{U}_{a_z}|\psi(\bar{z}, 0)\rangle = \partial_{a_z} (qe^{i\xi}) = e^{i\xi} \partial_{a_z} q = e^{i\xi} \partial_{a_z} |\langle z|\hat{U}_{a_z}|\psi(\bar{z}, 0)\rangle|$. Taking the squared modulus $|\cdot|^2$ of this chain of equalities and noting that $|e^{i\xi} \partial_{a_z} |\langle z|\hat{U}_{a_z}|\psi(\bar{z}, 0)\rangle||^2 = |\partial_{a_z} |\langle z|\hat{U}_{a_z}|\psi(\bar{z}, 0)\rangle||^2 = (\partial_{a_z} |\langle z|\hat{U}_{a_z}|\psi(\bar{z}, 0)\rangle|)^2$ proves the used relation. We also used in the fourth line we used $\sum d^k z |z\rangle\langle z| = \hat{\mathbb{I}}$. In the sixth line we used $|\langle \psi(\bar{z}, 0)|\hat{U}_{a_z}^\dagger \partial_{a_z} \hat{U}_{a_z}|\psi(\bar{z}, 0)\rangle|^2 = 0$ which follows from $0 = \partial_{a_z} \sum d^k z p(z|a_z) = \sum d^k z \partial_{a_z} q^2 = \sum d^k z 2q\partial_{a_z} q = \sum d^k z 2qe^{-i\xi} \partial_{a_z} (qe^{i\xi}) = 2 \sum d^k z \langle \psi(\bar{z}, 0)|\hat{U}_{a_z}^\dagger |z\rangle\langle z|\partial_{a_z} \hat{U}_{a_z}|\psi(\bar{z}, 0)\rangle = \langle \psi(\bar{z}, 0)|\hat{U}_{a_z}^\dagger \partial_{a_z} \hat{U}_{a_z}|\psi(\bar{z}, 0)\rangle$, where we used the completeness relation and $\partial_{a_z} \xi = 0$. With this, our proof is complete. \square

2. Determining if a state satisfies the variance-optimal measurement condition

So, let us now check when the condition $\partial_{a_z} \arg[\langle z | \hat{U}_{a_z} | \psi(\bar{z}, 0) \rangle] = 0$ is satisfied for some arbitrary multi-mode squeezed vacuum state. Let us write the state in the Schmidt mode basis $\hat{c}_n^\dagger = \int dz \Psi_n(z) \hat{D}^\dagger(z)$ in which the state appears in product form:

$$|\psi(\bar{z}, \bar{p})\rangle = \bigotimes_n \exp\left(+\frac{r_n e^{i\phi_n}}{2} \hat{c}_n^{\dagger 2} - \frac{r_n e^{-i\phi_n}}{2} \hat{c}_n^2\right) |0\rangle \quad (\text{K41})$$

$$= \bigotimes_n \exp\left(+\frac{\tanh(r_n) e^{i\phi_n}}{2} \hat{c}_n^{\dagger 2}\right) |0\rangle \quad (\text{K42})$$

$$= \bigotimes_n \exp\left(+\frac{\tanh(r_n) e^{i\phi_n}}{2} \int dz \Psi_n(z) \hat{D}^\dagger(z) \int d\bar{z} \Psi_n(\bar{z}) \hat{D}^\dagger(\bar{z})\right) |0\rangle \quad (\text{K43})$$

$$= \exp\left(\int dz \int d\bar{z} \left[\sum_n \frac{\tanh(r_n) e^{i\phi_n}}{2} \Psi_n(z) \Psi_n(\bar{z}) \right] \hat{D}^\dagger(z) \hat{D}^\dagger(\bar{z})\right) |0\rangle \quad (\text{K44})$$

$$= \exp\left(\int dz \int d\bar{z} g(z, \bar{z}) \hat{D}^\dagger(z) \hat{D}^\dagger(\bar{z})\right) |0\rangle \quad (\text{K45})$$

Now, let us gain some insight and first look at a simple two-photon example:

$$\langle (z, \bar{z})^T | \psi(\bar{z}, \bar{p}) \rangle = \frac{1}{\sqrt{2!}} \langle 0 | \hat{D}(z) \hat{D}(\bar{z}) | \psi(\bar{z}, \bar{p}) \rangle \quad (\text{K46})$$

$$= \frac{1}{\sqrt{2!}} \langle 0 | \hat{D}(z) \hat{D}(\bar{z}) \int dz' \int d\bar{z}' g(z', \bar{z}') \hat{D}^\dagger(z') \hat{D}^\dagger(\bar{z}') |0\rangle \quad (\text{K47})$$

$$= \frac{1}{\sqrt{2!}} \int dz' \int d\bar{z}' g(z', \bar{z}') \langle 0 | \hat{D}(z) \hat{D}(\bar{z}) \hat{D}^\dagger(z') \hat{D}^\dagger(\bar{z}') |0\rangle \quad (\text{K48})$$

$$= \frac{1}{\sqrt{2!}} \int dz' \int d\bar{z}' g(z', \bar{z}') [\delta(z - z') \delta(\bar{z} - \bar{z}') + \delta(z - \bar{z}') \delta(\bar{z} - z')] \quad (\text{K49})$$

$$= \frac{1}{\sqrt{2!}} [g(z, \bar{z}) + g(\bar{z}, z)]. \quad (\text{K50})$$

For the parameter imprinted state we have

$$\langle (z, \bar{z})^T | \hat{U}_{a_z} | \psi(\bar{z}, \bar{p}) \rangle = \frac{1}{\sqrt{2!}} [g(z + a_z, \bar{z} + a_z) + g(\bar{z} + a_z, z + a_z)]. \quad (\text{K51})$$

Now, for an arbitrary z -resolving photon counting measurement, we find

$$\langle z | \psi(\bar{z}, \bar{p}) \rangle = \frac{1}{\sqrt{(2K)!}} \langle 0 | [\otimes_{i=1}^{2K} \hat{D}(z_i)] | \psi(\bar{z}, \bar{p}) \rangle \quad (\text{K52})$$

$$= \frac{1}{\sqrt{(2K)!}} \frac{1}{K!} \int dz'_1 \dots \int dz'_{2K} g(z'_1, z'_2) \dots g(z'_{2K-1}, z'_{2K}) \langle 0 | [\otimes_{i=1}^{2K} \hat{D}(z_i)] [\otimes_{i=1}^{2K} \hat{D}^\dagger(z'_i)] |0\rangle \quad (\text{K53})$$

$$= \frac{1}{\sqrt{(2K)!}} \frac{1}{K!} \sum_{\pi \in S_{2K}} \prod_{b=1}^K g(z_{\pi(2b-1)}, z_{\pi(2b)}). \quad (\text{K54})$$

Here, $\sum_{\pi \in S_{2K}}$ means to sum over all permutations π of the indices $\{1, \dots, 2K\}$.

Let us now consider various states and see if they satisfy the condition for a variance-optimal measurement.

a. Phase-insensitive resolved photon counting measurement for product of single-mode squeezed vacua in the HG mode basis

Let us consider

$$|\psi(\bar{z}, \bar{p})\rangle = \bigotimes_n \exp\left(+\frac{r_n e^{i\phi_n}}{2} \hat{c}_n^{\dagger 2} - \frac{r_n e^{-i\phi_n}}{2} \hat{c}_n^2\right) |0\rangle \quad (\text{K55})$$

where

$$\hat{c}_n^\dagger = \int dz \Phi_n(z) \hat{D}^\dagger(z) \quad (\text{K56})$$

is the HG mode basis with

$$\Phi_n(z) = \Phi(z; z_0, p_0, \sigma, \theta) \quad (\text{K57})$$

It is straightforward to show that

$$\bar{z} = z_0 \quad (\text{K58})$$

$$\bar{p} = p_0 \quad (\text{K59})$$

regardless of how the squeezing r_n is distributed among the modes.

Now, it follows that the state $\hat{U}_{a_z} |\psi(\bar{z}, 0)\rangle = \bigotimes_n \exp\left(+\frac{r_n e^{i\phi_n}}{2} \hat{c}_n^{\dagger 2} - \frac{r_n e^{-i\phi_n}}{2} \hat{c}_n^2\right) |0\rangle$ has the same form, but with the mode operators

$$\hat{c}_n^\dagger = \int dz \Phi_n(z + a_z; z_0, 0, \sigma, \theta_n) \hat{D}^\dagger(z) \quad (\text{K60})$$

Now, let us consider:

$$\langle z | \hat{U}_{a_z} |\psi(\bar{z}, 0)\rangle = \frac{1}{\sqrt{(2K)!}} \frac{1}{K!} \sum_{\pi \in S_{2K}} \prod_{b=1}^K g(z_{\pi(2b-1)} + a_z, z_{\pi(2b)} + a_z). \quad (\text{K61})$$

We then find

$$g(z + a_z, \bar{z} + a_z) = \sum_n \frac{\tanh(r_n)}{2} \Phi_n(z + a_z; z_0, 0, \sigma, \theta_n)(z) \Phi_n(\bar{z} + a_z; z_0, 0, \sigma, \theta_n) \quad (\text{K62})$$

Now, for $\theta = 0$, $g(z + a_z, \bar{z} + a_z)$ is real, and thus, $\langle z | \hat{U}_{a_z} |\psi(\bar{z}, 0)\rangle$ is real valued as well. So the condition $\partial_{a_z} \arg[\langle z | \hat{U}_{a_z} |\psi(\bar{z}, 0)\rangle] = 0$ is satisfied.

Similarly, $\theta_n = \theta$ for all n , we have $\arg g(z + a_z, \bar{z} + a_z) = -2\theta$ from which follows $\arg[\langle z | \hat{U}_{a_z} |\psi(\bar{z}, 0)\rangle] = -2K\theta$, and the condition is also satisfied. In addition, one can show that the condition can be satisfied if θ_n differ from one another by integer multiples of π .

For the general case θ_n , the condition is no longer generally satisfied.

b. Phase-insensitive measurement for the optimal state

Let us now consider our optimal state and examine under what conditions phase-insensitive measurements can be variance optimal. Again, the state can be written as

$$|\psi(\bar{z}, \bar{p})\rangle = \bigotimes_{n=\{i,j\}} \exp\left(+\frac{r_n e^{i\phi_n}}{2} \hat{c}_n^{\dagger 2} - \frac{r_n e^{-i\phi_n}}{2} \hat{c}_n^2\right) |0\rangle \quad (\text{K63})$$

with

$$\hat{c}_n^\dagger = \int dz \Psi_n(z) \hat{D}^\dagger(z). \quad (\text{K64})$$

Recall that the optimal states from Sec. I has Schmidt modes fo the form

$$\Psi_1(z) = \Phi_0(z; z_1, p_1, \sigma_z, \theta_1) + O(|S|) \quad (\text{K65})$$

$$\Psi_2(z) = \Phi_0(z; z_2, p_2, \sigma_z, \theta_2) + O(|S|) \quad (\text{K66})$$

$$\Psi_3(z) = \Phi_1(z; z_1, p_1, \sigma_z, \theta_1) + O(|S|) \quad (\text{K67})$$

$$\Psi_4(z) = \Phi_1(z; z_2, p_2, \sigma_z, \theta_2) + O(|S|). \quad (\text{K68})$$

Now assume that like in Sec. I that

$$p_1 = p_0 + \delta_{+,p} \quad (\text{K69})$$

$$p_2 = p_0 - \delta_{-,p}, \quad (\text{K70})$$

and our choice of r_n shall ensure that

$$\bar{p} = p_0. \quad (\text{K71})$$

How to achieve this was discussed in Sections 10a and 10b.

Now again, the state $\hat{U}_{a_z} |\psi(\bar{z}, 0)\rangle = \bigotimes_n \exp\left(+\frac{r_n e^{i\phi_n}}{2} \hat{c}_n^{\dagger 2} - \frac{r_n e^{-i\phi_n}}{2} \hat{c}_n^{\prime 2}\right) |0\rangle$ has the same form, but with the mode operators

$$\hat{c}_n^{\prime \dagger} = \int dz \Psi_n(z + a_z) e^{+i\bar{p}(z+a_z)} \hat{D}^\dagger(z) = \int dz \Psi_n(z + a_z) e^{+ip_0(z+a_z)} \hat{D}^\dagger(z) \quad (\text{K72})$$

and we have

$$\Psi_1(z + a_z) e^{+ip_0(z+a_z)} = \Phi_0(z; z_1, +\delta_{+,p}, \sigma_z, \theta_1) \quad (\text{K73})$$

$$\Psi_2(z + a_z) e^{+ip_0(z+a_z)} = \Phi_0(z; z_2, -\delta_{-,p}, \sigma_z, \theta_2) \quad (\text{K74})$$

$$\Psi_3(z + a_z) e^{+ip_0(z+a_z)} = \Phi_1(z; z_1, +\delta_{+,p}, \sigma_z, \theta_1) \quad (\text{K75})$$

$$\Psi_4(z + a_z) e^{+ip_0(z+a_z)} = \Phi_1(z; z_2, -\delta_{-,p}, \sigma_z, \theta_2). \quad (\text{K76})$$

Now, let us consider:

$$\langle z | \hat{U}_{a_z} |\psi(\bar{z}, 0)\rangle = \frac{1}{\sqrt{(2K)!}} \frac{1}{K!} \sum_{\pi \in S_{2K}} \prod_{b=1}^K g(z_{\pi(2b-1)} + a_z, z_{\pi(2b)} + a_z) \quad (\text{K77})$$

Now, let us assume $z_1 = z_2 = z_0$ (as we will see, this choice ensures that certain terms can be factored out):

$$g(z + a_z, \bar{z} + a_z) = +\frac{\tanh(r_1)}{2} \Psi_1(z + a_z) e^{+ip_0(z+a_z)} \Psi_1(\bar{z} + a_z) e^{+ip_0(\bar{z}+a_z)} \quad (\text{K78})$$

$$+ \frac{\tanh(r_2)}{2} \Psi_2(z + a_z) e^{+ip_0(z+a_z)} \Psi_2(\bar{z} + a_z) e^{+ip_0(\bar{z}+a_z)} \quad (\text{K79})$$

$$= \left(\frac{1}{2\sigma_z^2 \pi}\right)^{2/4} \sqrt{\frac{2^{-n}}{n!}} e^{-\frac{1}{2} \left(\frac{z+a_z-z_0}{\sqrt{2}\sigma_z}\right)^2} e^{-\frac{1}{2} \left(\frac{\bar{z}+a_z-z_0}{\sqrt{2}\sigma_z}\right)^2} \quad (\text{K80})$$

$$\times \left[t_1 e^{-i(p_0+\delta_{+,p})(z+\bar{z}+2a_z-2z_0)} e^{-i2\theta_1} \cdot e^{+ip_0(z+\bar{z}+2a_z)} + t_2 e^{-i(p_0-\delta_{-,p})(z+\bar{z}+2a_z-2z_0)} e^{-i2\theta_2} \cdot e^{+ip_0(z+\bar{z}+2a_z)} \right] \quad (\text{K81})$$

$$= \left(\frac{1}{2\sigma_z^2 \pi}\right)^{2/4} \sqrt{\frac{2^{-n}}{n!}} e^{-\frac{1}{2} \left(\frac{z+a_z-z_0}{\sqrt{2}\sigma_z}\right)^2} e^{-\frac{1}{2} \left(\frac{\bar{z}+a_z-z_0}{\sqrt{2}\sigma_z}\right)^2} \quad (\text{K82})$$

$$\times e^{+2ip_0 z_0} \left[t_1 e^{-i\delta_{+,p}(z+\bar{z}+2a_z-2z_0)} e^{-i2\theta_1} + t_2 e^{+i\delta_{-,p}(z+\bar{z}+2a_z-2z_0)} e^{-i2\theta_2} \right] \quad (\text{K83})$$

where $t_n = \tanh(r_n)$.

Now, if we pick $\delta_{+,p} = \delta_{-,p} = \delta$, $r_1 = r_2$, and also $\theta_1 = \theta_2 = \theta$, it follows that

$$g(z + a_z, \bar{z} + a_z) = \left(\frac{1}{2\sigma_z^2 \pi}\right)^{2/4} \sqrt{\frac{2^{-n}}{n!}} e^{-\frac{1}{2} \left(\frac{z+a_z-z_0}{\sqrt{2}\sigma_z}\right)^2} e^{-\frac{1}{2} \left(\frac{\bar{z}+a_z-z_0}{\sqrt{2}\sigma_z}\right)^2} \tanh(r) \quad (\text{K84})$$

$$\times e^{+i2p_0 z_0} e^{-i2\theta} \left[e^{+i\delta(z+\bar{z}+2a_z-2z_0)} + e^{-i\delta(z+\bar{z}+2a_z-2z_0)} \right] \quad (\text{K85})$$

$$= \left(\frac{1}{2\sigma_z^2 \pi}\right)^{2/4} \sqrt{\frac{2^{-n}}{n!}} e^{-\frac{1}{2} \left(\frac{z+a_z-z_0}{\sqrt{2}\sigma_z}\right)^2} e^{-\frac{1}{2} \left(\frac{\bar{z}+a_z-z_0}{\sqrt{2}\sigma_z}\right)^2} \tanh(r) \quad (\text{K86})$$

$$\times e^{+i2p_0 z_0} e^{-i2\theta} \cdot 2 \cos(\delta(z + \bar{z} + 2a_z - 2z_0)). \quad (\text{K87})$$

We thus find that $\arg[g(z + a_z, \bar{z} + a_z)] = 2(p_0 z_0 - \theta)$, and therefore $\arg[\langle z | \hat{U}_{a_z} | \Psi(\bar{z}, 0) \rangle] = 2K(p_0 z_0 - \theta)$, from which it follows that $\partial_{a_z} \arg[\langle z | \hat{U}_{a_z} | \psi(\bar{z}, 0) \rangle] = 0$. Note that the choice $\theta_1 = \theta$ and $\theta_2 = \theta + \pi$ leads to an analogous result, with a sin dependence replacing the cos.

The conditions for a variance-optimal measurement thus require equal squeezing $r_1 = r_2$, together with $\delta_- = \delta_+$ and $z_1 = z_2$. For $z_1 \neq z_2$, one generally has $\partial_{a_z} \arg[\langle z | \hat{U}_{a_z} | \psi(\bar{z}, 0) \rangle] \neq 0$, and the variance-optimality condition is no longer satisfied.

-
- [1] C. Fabre and N. Treps, Modes and states in quantum optics, *Reviews of Modern Physics* **92**, 035005 (2020).
- [2] C. W. Helstrom, [Quantum Detection and Estimation Theory](#), Mathematics in Science and Engineering, Vol. 123 (Elsevier, 1976) pp. 297–303.
- [3] C. M. Caves, Quantum-mechanical noise in an interferometer, *Phys. Rev. D* **23**, 1693 (1981).
- [4] M. Tse and al., Quantum-enhanced advanced ligo detectors in the era of gravitational-wave astronomy, *Phys. Rev. Lett.* **123**, 231107 (2019).
- [5] F. Acernese and al (Virgo Collaboration), Increasing the astrophysical reach of the advanced virgo detector via the application of squeezed vacuum states of light, *Phys. Rev. Lett.* **123**, 231108 (2019).
- [6] H. Lee, P. Kok, and J. P. Dowling, A quantum rosetta stone for interferometry, *Journal of Modern Optics* **49**, 2325 (2002), <https://doi.org/10.1080/0950034021000011536>.
- [7] J. P. Dowling, Quantum optical metrology – the lowdown on high-n00n states, *Contemporary Physics* **49**, 125 (2008).
- [8] J. Qin, Y.-H. Deng, H.-S. Zhong, L.-C. Peng, H. Su, Y.-H. Luo, J.-M. Xu, D. Wu, S.-Q. Gong, H.-L. Liu, H. Wang, M.-C. Chen, L. Li, N.-L. Liu, C.-Y. Lu, and J.-W. Pan, Unconditional and robust quantum metrological advantage beyond NOON states, *Phys. Rev. Lett.* **130**, 070801 (2023).
- [9] E. Descamps, N. Fabre, A. Keller, and P. Milman, Quantum metrology using time-frequency as quantum continuous variables: Resources, sub-shot-noise precision and phase space representation, *Phys. Rev. Lett.* **131**, 030801 (2023).
- [10] D. Leibfried, M. D. Barrett, T. Schaetz, J. Britton, J. Chiaverini, W. M. Itano, J. D. Jost, C. Langer, and D. J. Wineland, Toward heisenberg-limited spectroscopy with multiparticle entangled states, *Science* **304**, 1476 (2004).
- [11] C. F. Roos, M. Chwalla, K. Kim, M. Riebe, and R. Blatt, ‘designer atoms’ for quantum metrology, *Nature* **443**, 316 (2006).
- [12] D. J. Wineland, J. J. Bollinger, W. M. Itano, F. L. Moore, and D. J. Heinzen, Spin squeezing and reduced quantum noise in spectroscopy, *Phys. Rev. A* **46**, R6797 (1992).
- [13] A. Sinatra, Spin-squeezed states for metrology, *Applied Physics Letters* **120**, 120501 (2022).
- [14] M. A. Taylor and W. P. Bowen, Quantum metrology and its application in biology, *Physics Reports* **615**, 1 (2016).
- [15] A. Lyons, G. C. Knee, E. Bolduc, T. Roger, J. Leach, E. M. Gauger, and D. Faccio, Attosecond-resolution hong-ou-mandel interferometry, *Science Advances* **4**, eaap9416 (2018).
- [16] Y. Chen, M. Fink, F. Steinlechner, J. P. Torres, and R. Ursin, Hong-ou-mandel interferometry on a biphoton beat note, *npj Quantum Inf* **5**, 43 (2019).
- [17] N. Fabre and S. Felicetti, Parameter estimation of time and frequency shifts with generalized HOM interferometry, *Phys. Rev. A* **104**, 022208 (2021).
- [18] B. Ndagano, H. Defienne, D. Branford, Y. D. Shah, A. Lyons, N. Westerberg, E. M. Gauger, and D. Faccio, Quantum microscopy based on Hong-Ou-Mandel interference, *Nature Photonics* **16**, 384 (2022), arXiv:2108.05346 [quant-ph].
- [19] M. Gessner, N. Treps, and C. Fabre, Estimation of a parameter encoded in the modal structure of a light beam: A quantum theory, *Optica* **10**, 996 (2023).
- [20] W. Górecki, F. Albarelli, S. Felicetti, R. Di Candia, and L. Maccone, Interplay between time and energy in bosonic noisy quantum metrology, *PRX Quantum* **6**, 020351 (2025).
- [21] P. WOODWARD, Front matter, in [Probability and Information Theory with Applications to Radar \(Second Edition\)](#), International Series of Monographs on Electronics and Instrumentation (Pergamon, 1953) second edition ed., p. iii.
- [22] C. Helstrom, [Statistical Theory of Signal Detection, by Carl W. Helstrom](#), International Series of Monographs in Electronics and Instrumentation, V. 9 (Pergamon Press, 1968).
- [23] M. Reichert, R. Di Candia, M. Z. Win, and M. Sanz, Quantum-enhanced Doppler lidar, *npj Quantum Information* **8**, 147 (2022).
- [24] V. Giovannetti, S. Lloyd, and L. Maccone, Quantum-enhanced positioning and clock synchronization, *Nature* **412**, 417 (2001).
- [25] V. Giovannetti, S. Lloyd, and L. Maccone, Positioning and clock synchronization through entanglement, *Physical Review A* **65**, 022309 (2002).
- [26] J. H. Shapiro, Quantum pulse compression laser radar, in [Noise and Fluctuations in Photonics, Quantum Optics, and Communications](#), Vol. 6603 (SPIE, 2007) pp. 31–38.
- [27] L. Maccone, Y. Zheng, and C. Ren, Gaussian beam quantum radar protocol, arXiv preprint arXiv:2309.11834 (2023).
- [28] Z. Huang, C. Lupo, and P. Kok, Quantum-limited estimation of range and velocity, *PRX Quantum* **2**, 030303 (2021).
- [29] Q. Zhuang, Z. Zhang, and J. H. Shapiro, Entanglement-enhanced lidars for simultaneous range and velocity measurements, *Physical Review A* **96**, 040304 (2017).
- [30] V. Delaubert, N. Treps, M. Lassen, C. C. Harb, C. Fabre, P. K. Lam, and H. A. Bachor, Tem 10 homodyne detection as an optimal small-displacement and tilt-measurement scheme, *Physical Review A—Atomic, Molecular, and Optical Physics* **74**, 053823 (2006).
- [31] V. Delaubert, N. Treps, C. C. Harb, P. K. Lam, and H.-A. Bachor, Quantum measurements of spatial conjugate variables: displacement and tilt of a gaussian beam, *Optics letters* **31**, 1537 (2006).
- [32] M. Tsang, R. Nair, and X.-M. Lu, Quantum theory of superresolution for two incoherent optical point sources, *Physical Review X* **6**

(2016).

- [33] K. J. Blow, R. Loudon, S. J. D. Phoenix, and T. J. Shepherd, Continuum fields in quantum optics, *Physical Review A* **42**, 4102 (1990).
- [34] M. Walschaers, Non-gaussian quantum states and where to find them, *PRX quantum* **2**, 030204 (2021).
- [35] A. Serafini, *Quantum Continuous Variables: A Primer of Theoretical Methods* (CRC Press, Boca Raton, 2017).
- [36] J. Liu, H. Yuan, X.-M. Lu, and X. Wang, Quantum fisher information matrix and multiparameter estimation, *Journal of Physics A: Mathematical and Theoretical* **53**, 023001 (2020).
- [37] M. Gessner, N. Treps, and C. Fabre, Estimation of a parameter encoded in the modal structure of a light beam: a quantum theory, *Optica* **10**, 996 (2023).
- [38] O. Pinel, J. Fade, D. Braun, P. Jian, N. Treps, and C. Fabre, Ultimate sensitivity of precision measurements with intense gaussian quantum light: A multimodal approach, *Physical Review A—Atomic, Molecular, and Optical Physics* **85**, 010101 (2012).
- [39] V. Giovannetti, S. Lloyd, and L. Maccone, Quantum metrology, *Physical review letters* **96**, 010401 (2006).
- [40] T. Matsubara, P. Facchi, V. Giovannetti, and K. Yuasa, Optimal Gaussian metrology for generic multimode interferometric circuit, *New Journal of Physics* **21**, 033014 (2019).
- [41] W. He, C. N. Gagatsos, D. J. Wilson, and S. Guha, *Optimal single-mode squeezing for beam displacement sensing* (2025), arXiv:2509.11457 [quant-ph].
- [42] A. Boeschoten, G. Sorelli, M. Gessner, C. Fabre, and N. Treps, *Estimation of multiple parameters encoded in the modal structure of light* (2025), arXiv:2505.16435 [quant-ph].
- [43] J. H. Shapiro, The Quantum Theory of Optical Communications, *IEEE Journal of Selected Topics in Quantum Electronics* **15**, 1547 (2009).
- [44] N. Fabre, C. Nous, A. Keller, and P. Milman, Time-frequency as quantum continuous variables, *Physical Review A* **105**, 052429 (2022).
- [45] M. Combes and D. Robert, Coherent states and applications in mathematical physics (Springer, 2012) Chap. 8.
- [46] F. S. Roux and N. Fabre, *Wigner functional theory for quantum optics* (2020), 1901.07782 [physics, physics:quant-ph].
- [47] M. A. Richards, *Fundamentals of Radar Signal Processing* (McGraw-Hill Professional, 2005) p. 528.
- [48] V. Giovannetti, S. Lloyd, and L. Maccone, Quantum-enhanced measurements: beating the standard quantum limit, *Science* **306**, 1330 (2004), quant-ph/0412078.
- [49] Q. Zhuang and J. H. Shapiro, Ultimate accuracy limit of quantum pulse-compression ranging, *Phys. Rev. Lett.* **128**, 010501 (2022).
- [50] L. Lamata and J. Leon, Dealing with entanglement of continuous variables: Schmidt decomposition with discrete sets of orthogonal functions, *J. Opt. B: Quantum Semiclass. Opt.* **7**, 224 (2005).
- [51] B. Lamine, C. Fabre, and N. Treps, Quantum improvement of time transfer between remote clocks, *Physical review letters* **101**, 123601 (2008).
- [52] A. M. Marino, J. C. R. Stroud, V. Wong, R. S. Bennink, and R. W. Boyd, Bichromatic local oscillator for detection of two-mode squeezed states of light, *J. Opt. Soc. Am. B* **24**, 335 (2007).
- [53] G. Ferrini, J. P. Gazeau, T. Coudreau, C. Fabre, and N. Treps, Compact gaussian quantum computation by multi-pixel homodyne detection, *New J. Phys.* **15**, 093015 (2013).
- [54] A. Eldan, O. Gilon, A. Lagemi, E. F. Furman, and A. Pe'er, *Multiplexed processing of quantum information across an ultra-wide optical bandwidth* (2024), 2310.17819 [quant-ph].
- [55] R. M. d. Araújo, J. Roslund, Y. Cai, G. Ferrini, C. Fabre, and N. Treps, Full characterization of a highly multimode entangled state embedded in an optical frequency comb using pulse shaping, *Phys. Rev. A* **89**, 053828 (2014).
- [56] R. Cheng, Y. Zhou, S. Wang, M. Shen, T. Taher, and H. X. Tang, *Unveiling photon statistics with a 100-pixel photon-number-resolving detector* (2022).
- [57] M. Eaton, A. Hossameldin, R. J. Birrittella, P. M. Alsing, C. C. Gerry, H. Dong, C. Cuevas, and O. Pfister, Resolution of 100 photons and quantum generation of unbiased random numbers, *Nature Photonics* **17**, 106 (2023).
- [58] B. Korzh, Q.-Y. Zhao, J. P. Allmaras, S. Frasca, T. M. Autry, E. A. Bersin, A. D. Beyer, R. M. Briggs, B. Bumble, M. Colangelo, G. M. Crouch, A. E. Dane, T. Gerrits, A. E. Lita, F. Marsili, G. Moody, C. Peña, E. Ramirez, J. D. Rezac, N. Sinclair, M. J. Stevens, A. E. Velasco, V. B. Verma, E. E. Wollman, S. Xie, D. Zhu, P. D. Hale, M. Spiropulu, K. L. Silverman, R. P. Mirin, S. W. Nam, A. G. Kozorezov, M. D. Shaw, and K. K. Berggren, Demonstration of sub-3 ps temporal resolution with a superconducting nanowire single-photon detector, *Nature Photonics* **14**, 250 (2020).
- [59] M. B. Nasr, D. P. Goode, N. Nguyen, G. Rong, L. Yang, B. M. Reinhard, B. E. A. Saleh, and M. C. Teich, Quantum optical coherence tomography of a biological sample, *Optics Communications* **282**, 1154 (2009).
- [60] C. K. Hong, Z. Y. Ou, and L. Mandel, Measurement of subpicosecond time intervals between two photons by interference, *Phys. Rev. Lett.* **59**, 2044 (1987).
- [61] M. B. Nasr, B. E. A. Saleh, A. V. Sergienko, and M. C. Teich, Demonstration of dispersion-cancelled quantum-optical coherence tomography, *Phys. Rev. Lett.* **91**, 083601 (2003), quant-ph/0304160.
- [62] E. Descamps, A. Keller, and P. Milman, Time-frequency metrology with two single-photon states: Phase-space picture and the hong-oumandel interferometer, *Phys. Rev. A* **108**, 013707 (2023).
- [63] M. Reichert, Q. Zhuang, and M. Sanz, Heisenberg-limited quantum lidar for joint range and velocity estimation, *Phys. Rev. Lett.* **133**, 130801 (2024).
- [64] Y. Cai, J. Roslund, V. Thiel, C. Fabre, and N. Treps, Quantum enhanced measurement of an optical frequency comb, *npj Quantum Information* **7**, 82 (2021).
- [65] C. Wang, I. W. Primaatmaja, H. J. Ng, J. Y. Haw, R. Ho, J. Zhang, G. Zhang, and C. Lim, Provably-secure quantum randomness expansion with uncharacterised homodyne detection, *Nat Commun* **14**, 316 (2023).
- [66] P. Boucher, C. Fabre, G. Labroille, and N. Treps, Spatial optical mode demultiplexing as a practical tool for optimal transverse distance estimation, *Optica* **7**, 1621 (2020).
- [67] C. Rouvière, D. Barral, A. Grateau, I. Karuseichyk, G. Sorelli, M. Walschaers, and N. Treps, Ultra-sensitive separation estimation of

- optical sources, *Optica* **11**, 166 (2024).
- [68] N. Treps, V. Delaubert, A. Maître, J.-M. Courty, and C. Fabre, Quantum noise in multipixel image processing, *Physical Review A—Atomic, Molecular, and Optical Physics* **71**, 013820 (2005).
- [69] C. E. Lopetegui, M. Isoard, N. Treps, and M. Walschaers, Detection of mode-intrinsic quantum entanglement, *Optica Quantum* **3**, 312 (2025).
- [70] A. Saharyan, E. Descamps, A. Keller, and P. Milman, Resources for bosonic metrology: Quantum-enhanced precision from a superselection rule perspective, *Phys. Rev. A* **113**, 022428 (2026).
- [71] V. Montenegro, C. Mukhopadhyay, R. Yousefjani, S. Sarkar, U. Mishra, M. G. A. Paris, and A. Bayat, Review: Quantum metrology and sensing with many-body systems, *Physics Reports* **1134**, 1 (2025).
- [72] M. Tsang, Ziv-zakai error bounds for quantum parameter estimation, *Phys. Rev. Lett.* **108**, 230401 (2012).
- [73] M. Reichert, Q. Zhuang, J. H. Shapiro, and R. Di Candia, Quantum illumination with a hetero-homodyne receiver and sequential detection, *Physical Review Applied* **20**, 014030 (2023).
- [74] One can show that $\text{Tr}[\tilde{G}\mathcal{A}\tilde{G}\mathcal{A}] = (\alpha^\dagger\tilde{G}\alpha)^2$. When \tilde{G} has both positive and negative eigenvalues, one can find $\alpha \neq 0$ such that $\text{Tr}[\tilde{G}\mathcal{A}\tilde{G}\mathcal{A}] = (\alpha^\dagger\tilde{G}\alpha)^2 = 0$.
- [75] A. Monras, Optimal phase measurements with pure gaussian states, *Physical Review A—Atomic, Molecular, and Optical Physics* **73**, 033821 (2006).